Roman M. Lutchyn

120 Words

Kinetics of Superconducting Quantum Circuits

Superconducting circuits exhibit quantum properties on a macroscopic scale, and are natural candidates for solid state quantum computing. Their low-energy physics can be described in terms of the phase of the order parameter, a single collective degree of freedom associated with billions of coherently paired electrons. In practice, however, on top of the superfluid condensate there are single-particle excitations (quasiparticles) with a continuous energy spectrum; the quasiparticles are coupled to the phase degree of freedom. The presence of quasiparticles in the system sets serious constraints on the performance of superconducting charge qubits. In this thesis, we study the kinetics of superconducting quantum circuits, and discuss the fundamental limitations on the energy and phase relaxation times in the presence of quasiparticles.

UNIVERSITY OF MINNESOTA

This is to certify that I have examined this bound copy of a doctoral thesis by

Roman M. Lutchyn

and have found that it is complete and satisfactory in all respects and that any and all revisions required by the final examining committee have been made.

Leonid I. Glazman
(Faculty Adviser)

GRADUATE SCHOOL

Kinetics of Superconducting Quantum Circuits

A THESIS
SUBMITTED TO THE FACULTY OF THE GRADUATE SCHOOL
OF THE UNIVERSITY OF MINNESOTA
BY

Roman M. Lutchyn

IN PARTIAL FULFILLMENT OF THE REQUIREMENTS
FOR THE DEGREE OF
DOCTOR OF PHILOSOPHY

July, 2007

Acknowledgements

Having finished this thesis, I would like to express my gratitude to all the people who supported me through this long journey. With pleasure and sincere thanks I acknowledge my teachers and colleagues who helped me to conduct research and formulate my thoughts as well as shaped my understanding of theoretical physics.

My first advisor at the University of Minnesota was the late Anatoly Larkin. Anatoly was a great teacher and a very good person. His remarkable intuition and deep understanding of physical phenomena had a strong and positive influence on me.

The majority of my papers are written with my present PhD advisor Leonid Glazman. Leonid has been an inspiration for me in many ways due to his scientific creativity, broad knowledge of physics, and clarity of thought. Under his guidance I have learned not only a great deal of Physics, but also how to teach and communicate effectively. I am grateful to Leonid for taking me as an advisee after the death of Prof. Larkin and supporting me towards the PhD degree.

Many thanks to other faculty and students of the Physics Department, University of Minnesota. I have learnt a lot from the graduate courses of P. Crowell, L. Glazman, A. Larkin, S. Rudaz, B. Shklovskii, A. Vainshtein, and O. T. Valls. I have also benefited from the stimulating discussions with A. Kamenev, A. Goldman, R. Schoelkopf, E. Kolomeitsev, O. Naaman, J. Aumentado, A. Ferguson and A.B. Zorin.

Finally, I want to thank my parents and my wife Yuliya for their encouragement and love. Without their tireless emotional, intellectual and financial support, I could not have come this far.

The research presented in the thesis was supported by NSF Grants DMR 02-37296,

and DMR 04-39026 and by the Anatoly Larkin Fellowship.

Minneapolis, Minnesota Roman M. Lutchyn

June 08, 2007

Dedicated to my late grandparents

Kinetics of Superconducting Quantum Circuits

by Roman M. Lutchyn
Under the supervision of Leonid I. Glazman

ABSTRACT

Superconducting circuits exhibit quantum properties on a macroscopic scale, and are natural candidates for solid state quantum computing. Their low-energy physics can be described in terms of the phase of the order parameter, a single collective degree of freedom associated with billions of coherently paired electrons. In practice, however, on top of the superfluid condensate there are single-particle excitations (quasiparticles) with a continuous energy spectrum; the quasiparticles are coupled to the phase degree of freedom. The presence of quasiparticles in the system sets serious constraints on the performance of superconducting charge qubits. In this thesis, we study the kinetics of superconducting quantum circuits, and discuss the fundamental limitations on the energy and phase relaxation times in the presence of quasiparticles.

Table of Contents

List of Figures

Chapter 1

Introduction

1.1 Superconducting quantum circuits

This section serves as an introduction to mesoscopic quantum phenomena at the interface between micro and macro scales, where quantum coherent effects can be experimentally observed.

Over the last two decades there has been significant progress towards isolating and controlling microscopic systems like atoms, spins of either electrons or nuclei and photons. These controllable microscopic systems obey the laws of quantum mechanics, and may be relevant for future quantum information processing [1]. One of the manifestations of their quantum nature is the coherent superposition of different states. Quantum mechanical effects can be also observed in carefully designed experiments with electrical circuits, in which the relevant degrees of freedom are well isolated from the environment. Superconductors exhibit quantum properties on a macroscopic scale, and are natural candidates for the artificial quantum systems. The interest in quantum effects in superconducting circuits goes back to the discovery of macroscopic quantum tunneling in the 80s [2–5]. Twenty years later the quantum nature of the mesoscopic electrical circuits incorporating Josephson junctions was demonstrated experimentally [6–12], see also

Fig. 1.1. In these Josephson-based devices the quantum dynamics is encoded in the phase of the order parameter, a single collective degree of freedom associated with billions of coherently paired electrons. Currently, it is considered that these Josephson-based electric circuits might serve as solid-state quantum bits (qubits).[4] Superconducting qubits have several advantages over other microscopic two-level systems like nuclear spins, ions or atoms [13]: they are scalable, they can be individually addressed (which permits to perform quantum logic operations by controlling gate voltages, bias currents or magnetic fields [14–16]), and the read out of the qubit states can be performed using quantum non-demolition [5] measurements [17]. However, unlike isolated atoms or nuclear spins, these solid state quantum systems are strongly coupled to the environment with a large number of parasitic degrees of freedom. Thus, the main drawback of superconducting qubits is strong decoherence, *i.e.* relatively short energy and phase relaxation times.

1.2 Basic types of superconducting qubits

All superconducting quantum circuits use Josephson effect, a coherent transfer of electrons across a tunnel junction. The Josephson junction is an important element of the electric circuits which acts as a non-linear non-dissipative inductor [18]. The non-linearity ensures unequal level spacings between energy levels, which permits to separate the lowest qubit states from the higher energy levels, and address them using the external control fields without inducing parasitic transitions. The Josephson element can be characterized by two parameters - effective inductance $L_J = \phi_0/I_c$ with ϕ_0 and I_c being the reduced flux quantum, $\phi_0 = \hbar/2e$,

[4] Quantum bit - the basic element of a quantum computer - is essentially a physical system whose effective Hilbert space is restricted to the lowest two levels.

[5] A quantum non-demolition (QND) measurement is a non-invasive measurement which minimizes the disturbance of a quantum system by the detector. This is achieved by using a particular system-detector interaction $\hat{H}_{\rm det}$, which commutes with the qubit Hamiltonian, $[\hat{H}_{\rm det}, \hat{H}_{\rm qb}] = 0$.

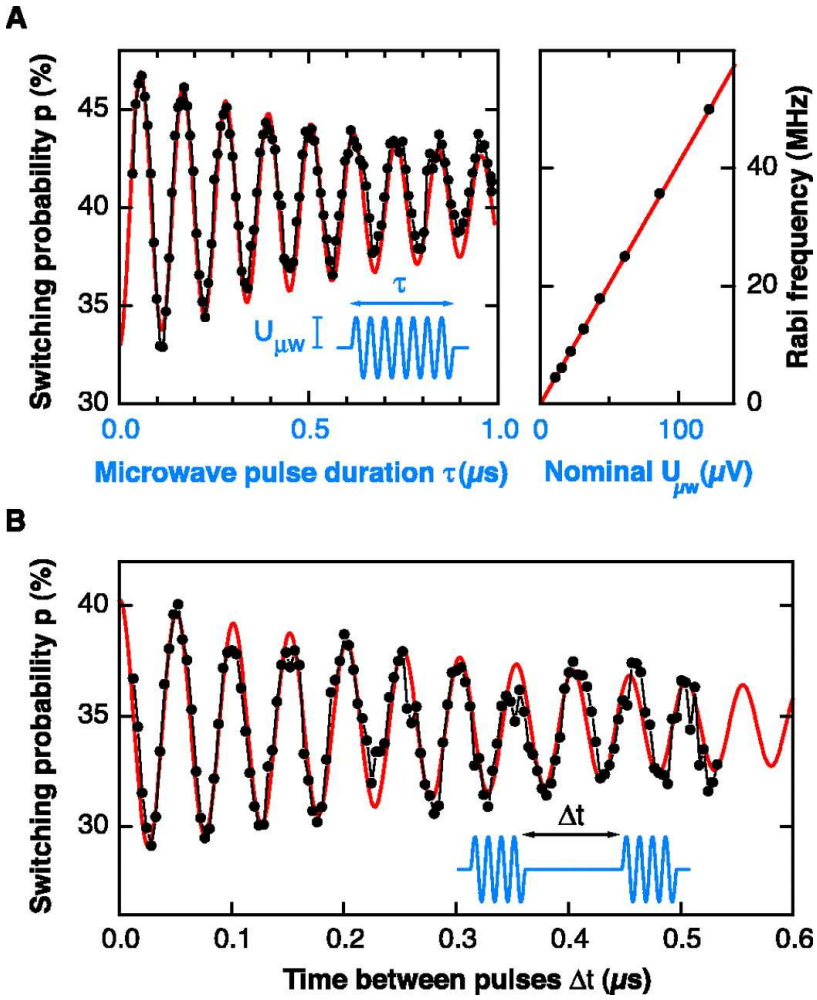

Figure 1.1: Coherent oscillations in superconducting quantum circuits (Saclay experiment). (A) Left: Rabi oscillations of the switching probability measured just after a resonant microwave pulse of duration τ. Right: Measured Rabi frequency (dots) varies linearly with the microwave amplitude $U_{\mu w}$, as expected. (B) Ramsey fringes of the switching probability after two phase-coherent microwave pulses separated by Δt.

and critical current of the junction, respectively; and the capacitance of the junction C_J, which defines the charging energy of the junction $E_{c_J} = e^2/2C_J$. The effective Hamiltonian for the simplest quantum superconducting circuit, a single Josephson junction connected to massive leads, is given by

$$H = \frac{\hat{Q}^2}{2C_J} - E_J \cos(\hat{\varphi}). \tag{1.1}$$

Here $\hat{Q}$ is the charge on the junction capacitor, and $\hat{\varphi}$ is the phase difference across the junction, and $E_J = \phi_0^2/L_J$ is the Josephson coupling. The Hamiltonian (1.1) resembles that of a quantum particle moving in a periodic potential with $\hat{Q}$ and $\hat{\varphi}$ being the "momentum" and "coordinate", respectively. Similar to the momentum-position duality in quantum mechanics, the phase difference $\hat{\varphi}$ and the charge on the capacitor in units of $2e$, $\hat{n} = \hat{Q}/2e$, obey the canonical commutation relation

$$[\hat{\varphi}, \hat{n}] = i. \tag{1.2}$$

The uncertainty relations, which follows from Eq. (1.2), define the range of parameters of the electric circuits when quantum effects are important. When the capacitance of the junction C_J is large (*i.e.* the "mass" of the particle is large), quantum fluctuations are small and the system behaves essentially classically. Thus, superconducting circuits behave quantum-mechanically when the junction capacitances are sufficiently small.

The information can be stored in superconducting quantum circuits by manipulating phase or charge degrees of freedom. There are three basic types of superconducting qubits, which can be classified into two categories depending on the ratio of two characteristic energy scales - charging E_c and Josephson E_J energies. Phase qubits, see Fig. 1.2, exploit the limit of large Josephson energy $E_J \gg E_c$ when the phase φ is well defined and the charge on the junction capacitor fluctuates strongly. Therefore, in these qubits the phase degree of freedom is manipulated. Among phase qubits, the most popular are persistent-current

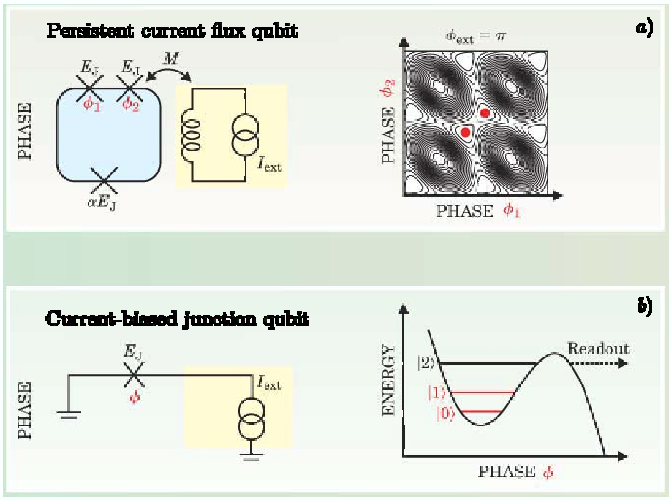

Figure 1.2: Basic types of the phase qubits and their energy diagrams. (a) 3-junction persistent-current qubit. (b) Current-biased junction qubit. Adapted from You *et. al.* [19]

qubits and current-biased-junction qubits, see Fig. 1.2. The former is a modified version of the single junction rf-SQUID qubit, where the information is encoded in clockwise and counterclockwise supercurrent states flowing in the SQUID loop. The Hamiltonian for the RF-SQUID qubit has an additional term compared to Eq. (1.1), which corresponds to the inductive energy of the SQUID,

$$H = \frac{\hat{Q}^2}{2C_J} - E_J \cos(\hat{\varphi}) + E_L(\hat{\varphi} - \varphi_{\text{ext}})^2. \tag{1.3}$$

Here $E_L = \phi_0^2/2L$ with L being the SQUID inductance, and φ_{ext} is external magnetic flux bias, see Fig. 1.2. At $\varphi_{\text{ext}} = \pi$ there is a degeneracy between clockwise and counterclockwise current-carrying states. This degeneracy is lifted by the tunneling between these state, and the lowest two energy levels of the qubit are formed by the symmetric and antisymmetric superposition of the current-carrying states. The other type of the phase qubits is based on a current-biased Josephson junction, see Fig 1.2. The Hamiltonian for this qubit is

$$H = \frac{\hat{Q}^2}{2C_J} - E_J \cos(\hat{\varphi}) + \frac{\hbar}{2e} I_{\text{ext}} \hat{\varphi}. \tag{1.4}$$

Externally applied current I_{ext} provides a slight tilt to the cosine potential, and

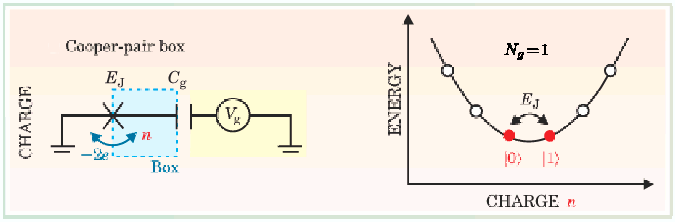

Figure 1.3: Superconducting charge qubit and it's energy diagram. The electrostatic energy of the Cooper-pair box, $E_c(N-N_g)^2$, plotted as a function of excess electrons N for $N_g = 1$.

allows one to control the number of quantum levels within one well, see Fig. 1.2. Logic operations are performed by inducing the transitions within the lowest two levels while the read-out is achieved by selectively exciting the higher levels with microwaves and measuring the average voltage across the junction. The junction switches to the voltage state $\langle\dot{\varphi}\rangle \neq 0$ because the tunneling through the barrier becomes strong for the excited states in the well, *e.g.*, for the state $|2\rangle$ in Fig. 1.2.

The other family of superconducting quantum circuits is called charge or Cooper-pair box qubits. The charge qubit consists of a small mesoscopic island (Cooper-pair box) connected through a Josephson junction to a large superconducting reservoir, see Fig. 1.3. The island is biased with a gate voltage V_g to induce offset charge $Q_g = C_g V_g$. In the case of a large superconducting gap, $\Delta > E_c, E_J \gg T$, the dynamics of the Cooper-pair box qubit can be described by an effective Hamiltonian

$$H = E_c(\hat{N} - N_g)^2 - E_J \cos(\hat{\phi}). \tag{1.5}$$

Here $\hat{N}$ and N_g are the excess charge in the box and induced offset charge in units of $1e$, respectively; E_c is the charging energy, $E_c = e^2/2C_\Sigma$, where $C_\Sigma = C_J + C_g$ is the total capacitance of the island. The Cooper-pair box qubit typically operates in the Coulomb blockade regime, $E_c \gg E_J$[3]. In a slightly modified device, called split-Cooper-pair box qubit, a single Josephson junction is replaced by two in a

[3]There are also experiments with the Cooper-pair box qubit operating in the charge-flux regime [10, 12]

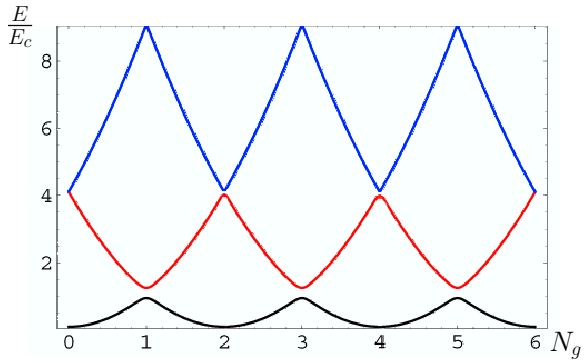

Figure 1.4: The energy spectrum of the Cooper-pair box as a function of the dimensionless gate voltage N_g in the Coulomb blockade regime $E_c \gg E_J$.

loop configuration [20, 21]. This design allows one to vary the effective Josephson energy E_J in Eq. (1.5) by tuning the external magnetic flux Φ_{ext} through the loop. Thus, such a quantum system can be controlled with the gate voltage and magnetic flux penetrating the SQUID, and has only one discrete degree of freedom - the number of Cooper pairs in the box. The energy spectrum of the Cooper-pair box can be found exactly by mapping the Shrödinger equation following from the Hamiltonian (1.5) onto Mathieu equation, see Appendix A. As one can see from Fig. 1.4, the spectrum of the Cooper-pair box is strongly anharmonic. For most values of the gate voltage the energy of the box is well approximated by the charging term in the Hamiltonian (1.5). Only at the special points like $N_g = 1$ does the Josephson term become important as it splits the degeneracy between the adjacent charge states, *e.g.*, N and $N+2$. At $N_g = 1$, a working point for the qubit, the Cooper-pair box can be approximately described as a two-level system. (For $E_c \gg T$, higher energy states of the Cooper-pair box are exponentially suppressed.) In the two-level-system approximation, the Hamiltonian for the qubit can be conveniently written in a spin-1/2 representation

$$H = -\frac{1}{2}B_z\hat{\sigma}_z - \frac{1}{2}B_x\hat{\sigma}_x, \tag{1.6}$$

where $\hat{\sigma}_x$ and $\hat{\sigma}_z$ are Pauli matrices. Here the charge states $|N\rangle$ and $|N+2\rangle$ correspond to the spin states $|\uparrow\rangle$ and $|\downarrow\rangle$, respectively. The spin-1/2 particle is

subject to the fictitious magnetic fields, which can be determined by the gate voltage, $B_z = 4E_c(1 - N_g)$, and external magnetic flux Φ_x, $B_x = E_J(\Phi_x)$. Thus, the Cooper-pair box qubit is a controllable two-level system, where quantum information is encoded in the superposition of the charge states of the island $|N\rangle$ and $|N+2\rangle$, *i.e.*, a presence or absence of an extra Cooper-pair in the box.

1.3 Qubit decoherence

In general, the state of a qubit can be characterized by two parameters θ and ϕ

$$|\psi\rangle = \cos\left(\frac{\theta}{2}\right)|\uparrow\rangle + \sin\left(\frac{\theta}{2}\right)e^{i\phi}|\downarrow\rangle\,. \tag{1.7}$$

These parameters specify a vector on the unit sphere in Euclidean space (Bloch sphere), whose coordinates are $\mathcal{R} = (\sin\theta\cos\phi, \sin\theta\sin\phi, \cos\theta)$, see Fig. 1.5. In this basis, the state $|\uparrow\rangle$ corresponds to a spin pointing along z direction and the state $|\downarrow\rangle$ to a spin pointing along $-z$. By manipulating magnetic fields B_z and B_x, it is possible to make unitary rotations (one-bit operations) and reach any point on the Bloch sphere. However, the quantum information encoded in the state of a qubit can be maintained only for a short period of time due to decoherence. The irreversible interaction of the qubit with its surrounding environment eventually leads to the loss of the quantum information and relaxation of the qubit to its equilibrium value. The process of spin relaxation is well known in the NMR community, and is usually characterized by the longitudinal and transverse relaxation times, T_1 and T_2, respectively. The former describes the energy relaxation of the qubit, *i.e.* the relaxation of the σ_z-component of the spin, while the latter characterizes the decay time of the coherent oscillations, *i.e.* the relaxation of $\sigma_x + i\sigma_y$-component of the spin. In solid-state quantum circuits the problem of decoherence is very complex due to coupling of the qubit dynamical variables to a large number of parasitic environmental modes. It is the subject of this thesis to study the intrinsic limitations on the coherence times

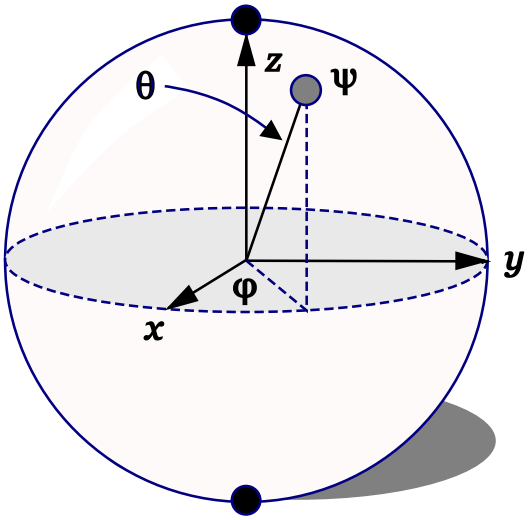

Figure 1.5: The state vector of the qubit on a Bloch sphere.

in superconducting quantum circuits. In particular, we concentrate here on the kinetic problems arising in superconducting quantum circuits due to the interplay between coherent (Cooper pair) tunneling and incoherent processes due to the quasiparticles.

Chapter 2

Decay of coherent oscillations

2.1 Introduction

The main difficulty in technological realization of superconducting qubits is due to the decoherence. The mechanisms of the decoherence in superconducting qubits are not yet well understood and can be attributed to radiative decay of the qubit by photon or phonon emission, fluctuating trapped charges in the substrate of the charge qubits, dielectric losses from insulating materials, *e.g.*, amorphous SiO_2, or the presence of quasiparticles in the superconducting parts of the system. In this thesis we concentrate on the quasiparticle contribution to the decoherence. Quasiparticles having a continuous spectrum are inherently present in any superconducting device and set a fundamental constraint on the coherence time. Quasiparticle "poisoning", first investigated in the context of charge-parity effects in mesoscopic superconductors [22–30], manifests itself also in the experiments with charge qubits [31–40]. It was reported that even at low temperatures ($\sim$10-50mK) quasiparticles are present in these devices. If this is the case, Hilbert space of the Cooper-pair box (CPB) expands, and the qubit is no longer a simple two-level system. The transient presence of a quasiparticle in the CPB detunes the qubit from the resonant state of Cooper pair tunneling and affects coherent

oscillations. In this Chapter we develop a quantitative theory of the effect of quasiparticles on charge qubit oscillations.

We consider two regimes which can be realized experimentally: open system corresponding to fixed chemical potential in the reservoir, and isolated system corresponding to fixed number of electrons in the qubit (see Fig. 2.1). The former case allows for a change of the total number of electrons in the superconducting parts of the system, and is experimentally realized if the reservoir is connected to external leads or a normal-metal quasiparticle trap is included in the circuit. The latter case corresponds to a superconducting qubit isolated from the normal-metal environment. Both cases may be relevant in the context of the cavity quantum electrodynamics experiments where the state of the qubit is determined using photon degrees of freedom [12].

In the charge representation, the Hamiltonian for the superconducting charge qubit of Eq. (1.5) is

$$H_{\rm qb} = E_c(N - N_g)^2 \left|N\right\rangle \left\langle N\right| - \frac{E_J}{2}\left(\left|N{+}2\right\rangle \left\langle N\right| + \left|N\right\rangle \left\langle N{+}2\right|\right). \qquad (2.1)$$

Here E_J is an effective Josephson energy, which can be controlled by external flux Φ_x, *i.e.*, $E_J = E_{J,\max}\cos(\pi\frac{\Phi_x}{\Phi_0})$ with Φ_0 being magnetic flux quantum $\Phi_0 = h/2e$. The amplitude $E_{J,\max}$ is the total Josephson energy of the two junctions. In the case of two identical junctions $E_{J,\max} = 2E_J^0$. (Here E_J^0 is the Josephson energy per junction given by Ambegaokar-Baratoff relation, $E_J^0 = h\Delta/8e^2R_T$ with R_T being the normal-state resistance of the contact.) In the regime where superconducting gap is the largest energy scale in the system $\Delta > E_c > E_J \gg T$, the quasiparticles are usually neglected, and the dynamics of the system is described by the above Hamiltonian, where there is only one discrete degree of freedom - excess number of Cooper pairs in the box. At the operating point, when the dimensionless gate voltage is tuned close to one, only the lowest energy states are important (higher energy levels can be neglected since $E_c \gg T$). In this two-level-system approximation, the energy spectrum of the Hamiltonian (2.1) is

given by

$$E_{|+\rangle}(N_g) = E_c + E_c(1-N_g)^2 + \frac{\sqrt{(4E_c(1-N_g))^2 + E_J^2}}{2},$$
$$E_{|-\rangle}(N_g) = E_c + E_c(1-N_g)^2 - \frac{\sqrt{(4E_c(1-N_g))^2 + E_J^2}}{2}. \tag{2.2}$$

The eigenstates of the qubit are given by the superposition of the charge states

$$\begin{aligned} |+\rangle &= \cos(\theta_+)\,|N\rangle - \sin(\theta_+)\,|N+2\rangle\,, \\ |-\rangle &= \cos(\theta_-)\,|N\rangle + \sin(\theta_-)\,|N+2\rangle \end{aligned} \tag{2.3}$$

with angles $\theta_\pm$ being determined from the following relations:

$$\sin(\theta_\pm) = \frac{\sqrt{(4E_c(1-N_g))^2 + E_J^2} \pm 4E_c(1-N_g)}{\sqrt{\left[4E_c(1-N_g) \pm \sqrt{(4E_c(1-N_g))^2 + E_J^2}\right]^2 + E_J^2}},$$
$$\cos(\theta_\pm) = \frac{E_J}{\sqrt{\left[4E_c(1-N_g) \pm \sqrt{(4E_c(1-N_g))^2 + E_J^2}\right]^2 + E_J^2}}.$$

Exactly at $N_g = 1$ there is degeneracy with respect to charging energy between the states $|N\rangle$ and $|N+2\rangle$, and Eqs. (2.2) and (2.4) can be simplified

$$\omega_+ \equiv E_{|+\rangle}(N_g = 1) = E_c + \frac{E_J}{2}, \text{and}\, |+\rangle = \frac{|N\rangle - |N+2\rangle}{\sqrt{2}},$$
$$\omega_- \equiv E_{|-\rangle}(N_g = 1) = E_c - \frac{E_J}{2}, \text{and}\, |-\rangle = \frac{|N\rangle + |N+2\rangle}{\sqrt{2}}. \tag{2.4}$$

Once a qubit is initialized, quantum oscillations between states $|-\rangle$ and $|+\rangle$ emerge. The frequency of these oscillations is determined by the Josephson energy E_J [20].

The appearance of quasiparticles with a continuous spectrum provides a channel for the relaxation of the qubit. Since quasiparticles are inherently present in any superconducting system, their contribution to the decay rate is intrinsic. The density of equilibrium quasiparticles in the reservoir depends on whether the system(Cooper-pair box and reservoir) is closed or open, *i.e* the total number of electrons is fixed or not (see Fig. 2.1).

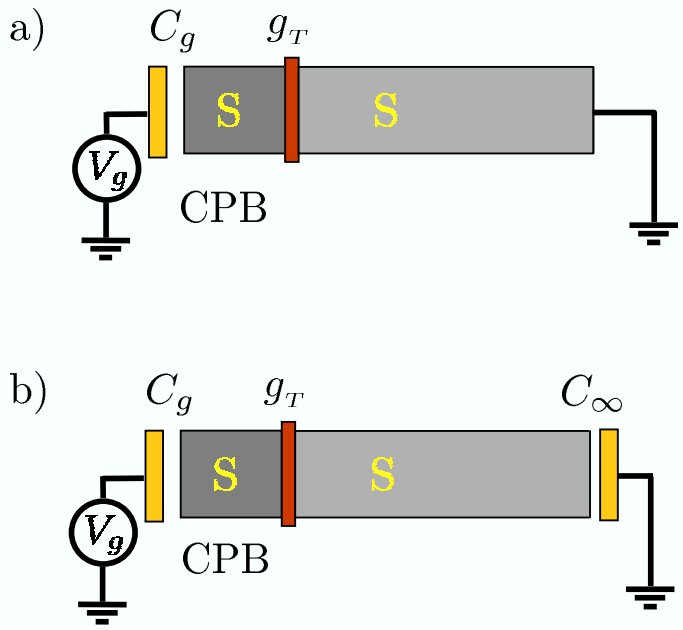

Figure 2.1: Schematic picture of a superconducting charge qubit in different experimental realizations: a) open system, b) isolated system. The left superconducting mesoscopic island is the Cooper-pair box connected via a tunable Josephson junction to the large superconducting reservoir (right). Gate bias is applied through the capacitance C_g (assuming that $C_\infty \gg C_g$).

2.2 Thermodynamic properties of a qubit in an open system

At finite temperature, the density of quasiparticles is exponentially small, $n \propto \exp(-\Delta/T)$, but the number of quasiparticles in a small mesoscopic superconductor can be of the order of one. It is important to point out that even one unpaired electron can affect qubit performance. In order to estimate the number of quasiparticles in the superconducting island, one has to account for the huge statistical weight of the states with a single quasiparticle, proportional to the volume of the box, $N_{\rm qp} = \sqrt{2\pi\Delta_b T}\nu_F V_b \exp(-\Delta_b/T)$, where ν_F is normal density of states at the Fermi level, $\nu_F = mp_F/2\pi^2$, and V_b is the volume of the island. For an isolated island, the characteristic temperature [29] at which quasiparticles appear is ($k_B = 1$)

$$T_b^* = \frac{\Delta_b}{\ln(\Delta_b/\delta_b)}, \tag{2.5}$$

where $\delta_b = 1/\nu_F V_b$ and Δ_b are the mean level spacing and superconducting gap energy in the box, respectively.

The appearance of a quasiparticle in the qubit at $N_g = 1$ occurs at lower temperature $\widetilde{T}_b^*$ due to the finite charging energy of the box:

$$\widetilde{T}_b^* = \frac{\Delta_b - \omega_-}{\log(\Delta_b/\delta_b)} = T_b^*\left(1 - \frac{\omega_-}{\Delta_b}\right). \tag{2.6}$$

If $T \ll \widetilde{T}_b^*$, states with odd number of electrons in the box are statistically rare. The probability of finding the qubit in a "good" state (not poisoned by quasiparticles) is important for qubit preparation and is determined by thermodynamics. However, the qubit coherence time is controlled by the kinetics, which we study in the next section.

2.3 Quasiparticle decay rate in an open system

If an unpaired electron tunnels into the CPB, it tunes the qubit away from the resonant state of Cooper pair tunneling, which leads to the decay of quantum oscillations. At the operating point $N_g = 1$, it is energetically favorable for a quasiparticle to tunnel to the CPB because charging energy is gained in such process. Assuming that initially the qubit was prepared in the state with no quasiparticles in the box, the lifetime of the qubit states is determined by the time of quasiparticle tunneling to the CPB. In order to estimate this time, we use the following Hamiltonian:

$$H = H_0^{'} + H_T, \tag{2.7}$$

$$H_0^{'} = H_{BCS}^L + H_{BCS}^R + E_c(Q/e - N_g)^2,$$

where H_{BCS}^L, H_{BCS}^R are BCS Hamiltonians of the box and superconducting reservoir (see Fig. 2.1), and Q denotes the charge in the box. The tunneling Hamiltonian between two electrodes, H_T, is defined as

$$H_T = \sum_{kp\sigma} (t_{kp} c_{k,\sigma}^\dagger c_{p,\sigma} + t_{kp}^* c_{p,\sigma}^\dagger c_{k,\sigma}), \tag{2.8}$$

where t_{kp} is the tunnelling matrix element [6], $c_{k,\sigma}$ and $c_{p,\sigma}$ are the annihilation operators for an electron in the state k, σ in the CPB and state p, σ in the superconducting reservoir, respectively.

We now consider the lifetime of the qubit states in the open system, assuming that the superconducting reservoir is connected to external leads and the number of electrons in it can change. If the qubit is prepared in the initial state without a quasiparticle in the box, the time of its coherent evolution is limited by the rate of quasiparticle tunneling to the CPB. In order to calculate the lifetime of the qubit states, we have to distinguish between tunneling of Cooper pairs

[6] In the presence of time-reversal symmetry one can choose real wave-functions instead of plane waves as the basis. In this basis the matrix elements t_{pk} are real, *i.e.* $t_{pk} = t_{pk}^*$.

and quasiparticles. To do this, we write the Hamiltonian H in Eq. (2.7) in the following form:

$$H = H_0 + V, \tag{2.9}$$

where $H_0 = H_0^{'} + H_J$, and $V = H_T - H_J$. H_J is second order in tunneling amplitude

$$H_J = |N\rangle \langle N| H_T \frac{1}{E - H_0^{'}} H_T |N+2\rangle \langle N+2| + H.c. \tag{2.10}$$

The matrix element $\langle N| H_T \frac{1}{E-H_0^{'}} H_T |N+2\rangle$ is proportional to the effective Josephson energy E_J, and H_T is defined in Eq. (2.8). Without quasiparticles Hamiltonian H_0 reduces to Eq. (2.1).

The quasiparticle tunneling rate can be found using Fermi's golden rule and averaging over initial configuration with the appropriate density matrix ($\hbar = 1$)

$$\Gamma = 2\pi \sum_{i,f} |\langle f| V |i\rangle|^2 \delta(E_f - E_i) \rho(\beta H_0). \tag{2.11}$$

Here, $\rho(\beta H_0)$ is the density matrix for the initial state of the system. The perturbation Hamiltonian accounts for quasiparticle tunneling only. In the lowest order, we have $\langle f| V |i\rangle = \langle f| H_T |i\rangle$. Thus, Eq. (2.11) takes into account Cooper pair tunneling exactly while treating quasiparticle tunneling perturbatively. At the operating point, $N_g = 1$, the initial state $|i\rangle$ is given by the superposition of 0 and 1 excess Cooper pairs in the box corresponding to the ground $|-\rangle$ or excited state $|+\rangle$ of the qubit; the final state $|f\rangle = |N+1\rangle$ is the state with odd number of electrons in the CPB, corresponding to charge $1e$. There are two mechanisms that contribute to the rate of the process $|\pm\rangle \rightarrow |N+1\rangle$: (1) a quasiparticle tunnels from the superconducting reservoir to the CPB, and (2) a Cooper pair in the box breaks into two quasiparticles, and then one quasiparticle tunnels out into the reservoir. The two corresponding contributions to the total tunneling rate are

$$\Gamma_{\pm} = \Gamma_{1\pm} + \Gamma_{2\pm}, \tag{2.12}$$

with $\Gamma_{1\pm}$ defined as

$$\Gamma_{1\pm} = 2\pi \sum_{n,p_j,k_i} |\langle N{+}1, k, \{p\}_{n-1}| H_T |\pm, \{p\}_n\rangle|^2 \delta(E_k - E_p - \omega_\pm)\rho(\beta H_0), \quad (2.13)$$

$$\Gamma_{2\pm} = 2\pi \sum_{n,p_j,k_i} |\langle N{+}1, p, \{k\}_{2n-1}| H_T |\pm, \{k\}_{2n}\rangle|^2 \delta(E_p - E_k - \omega_\pm)\rho(\beta H_0). \quad (2.14)$$

Here $\Gamma_\pm$ is the decay rate for the excited $|+\rangle$ or ground state $|-\rangle$ of the qubit, and $\omega_\pm$ is defined in Eq. (2.4). State $|+, \{p\}_n\rangle$, for example, denotes the excited state of the qubit with n quasiparticles in the reservoir with energies $E_p = \sqrt{\xi_p^2 + \Delta_r^2}$

$$|+, \{p\}_n\rangle = |+\rangle \otimes |p_1, \ldots, p_j, \ldots, p_n\rangle . \quad (2.15)$$

The state $|+, \{k\}_{2n}\rangle$ denotes the excited state of the qubit with n broken Cooper pairs in the box, leading to the appearance of $2n$ quasiparticles with energies $E_k = \sqrt{\xi_k^2 + \Delta_b^2}$,

$$|+, \{k\}_{2n}\rangle = |+, k_1, \ldots, k_j, \ldots, k_{2n}\rangle . \quad (2.16)$$

In the following, we concentrate on the decay rate of coherent oscillations in an open system, *i.e.*, evaluate $\Gamma_\pm^{\rm op}$. In order to calculate this decay rate, we take into account one-electron processes in the lowest order in the quasiparticle density. The first contribution to $\Gamma_{1\pm}^{\rm op}$, Eq. (2.13), corresponds to the process when all quasiparticles are in the reservoir and one of them is tunneling into an unoccupied state of the CPB; the second contribution, Eq. (2.14), - all quasiparticles are in the box and one of them is tunneling out into an unoccupied state of the reservoir. The density matrix in the former case can be reduced by tracing out irrelevant degrees of freedom: $\rho_{\rm op}(\beta H_0) = Tr_{\{k\}}\rho(\beta H_0)$, and Eq. (2.13) becomes

$$\Gamma_{1\pm}^{\rm op} = 2\pi \sum_{n,p_j,k} |\langle N{+}1, k, \{p\}_{n-1}| H_T |\pm, \{p\}_n\rangle|^2 \delta(E_k - E_p - \omega_\pm)\rho_{\rm op}(\beta H_0). \quad (2.17)$$

Taking into account that only one quasiparticle is transferred through the junction by the action of Hamiltonian H_T, and performing the sum over momenta in

Eq. (2.17), we obtain

$$\Gamma_{1\pm}^{\rm op} = 2\pi \sum_{p_1,k} 2|\left\langle N{+}1, k_\uparrow\right| H_T \left|\pm, p_{1,\uparrow}\right\rangle|^2 \delta(E_k - E_{p_1} - \omega_\pm) \exp\left(-\frac{E_{p_1}}{T}\right). \quad (2.18)$$

Here the exponential factor is the low temperature ($T \ll \Delta_r$) approximation of the Fermi function.

The matrix elements $\left\langle N{+}1, k_\uparrow\right| H_T \left|\pm, p_\uparrow\right\rangle$ can be calculated using the particle conserving Bogoliubov transformation [41, 42]

$$\begin{aligned} c_{p,\sigma}^\dagger &= u_p \gamma_{p,\sigma}^\dagger + \sigma v_p \gamma_{-p,-\sigma} R_r^\dagger \\ c_{p,\sigma} &= u_p \gamma_{p,\sigma} + \sigma v_p \gamma_{-p,-\sigma}^\dagger R_r \end{aligned} \quad (2.19)$$

Here operators $R^\dagger$ and R create and destroy a Cooper pair, *i.e.* $R^\dagger \left|N\right\rangle = \left|N{+}2\right\rangle$ and $R\left|N\right\rangle = \left|N-2\right\rangle$. Using Eq. (2.4) the amplitude for the excited state $\left|+\right\rangle$ is

$$A_{\left|+\right\rangle} = \frac{1}{\sqrt{2}} \left\langle N{+}1, k_\uparrow\right| H_T \left|N, p_\uparrow\right\rangle - \frac{1}{\sqrt{2}} \left\langle N{+}1, k_\uparrow\right| H_T \left|N{+}2, p_\uparrow\right\rangle, \quad (2.20)$$

and for the ground state is

$$A_{\left|-\right\rangle} = \frac{1}{\sqrt{2}} \left\langle N{+}1, k_\uparrow\right| H_T \left|N, p_\uparrow\right\rangle + \frac{1}{\sqrt{2}} \left\langle N{+}1, k_\uparrow\right| H_T \left|N{+}2, p_\uparrow\right\rangle. \quad (2.21)$$

The matrix elements $\left\langle N{+}1, k_\uparrow\right| H_T \left|N, p_\uparrow\right\rangle$ and $\left\langle N{+}1, k_\uparrow\right| H_T \left|N{+}2, p_\uparrow\right\rangle$ can be calculated using Eq. (2.19)

$$\begin{aligned} \left\langle N{+}1, k_\uparrow\right| H_T \left|N, p_\uparrow\right\rangle &= t_{kp} u_k u_p, \\ \left\langle N{+}1, k_\uparrow\right| H_T \left|N{+}2, p_\uparrow\right\rangle &= -t_{kp} v_k v_p. \end{aligned} \quad (2.22)$$

Combining all the terms, we find the amplitudes:

$$\begin{aligned} A_{\left|+\right\rangle} &= \frac{1}{\sqrt{2}} \left(t_{kp} u_k u_p + t_{kp} v_k v_p\right), \\ A_{\left|-\right\rangle} &= \frac{1}{\sqrt{2}} \left(t_{kp} u_k u_p - t_{kp} v_k v_p\right). \end{aligned} \quad (2.23)$$

As one can see from Eq. (2.23), there is an interference between tunneling of a quasiparticle as a quasi-electron and quasi-hole [40]. Different electromagnetic

environment of the states $|+\rangle$ and $|-\rangle$ results in constructive and destructive interference pattern for the amplitudes $A_{|+\rangle}$ and $A_{|-\rangle}$, respectively. Taking into account the expressions for the coherence factors

$$u_p^2 = \frac{1}{2}\left(1+\frac{\xi_p}{E_p}\right), \text{ and } v_p^2 = \frac{1}{2}\left(1-\frac{\xi_p}{E_p}\right), \tag{2.24}$$

we finally obtain squared matrix elements

$$\begin{aligned} |A_{|+\rangle}|^2 &= \frac{1}{4}|t_{kp}|^2\left(1+\frac{\Delta_r\Delta_b}{E_kE_p}\right), \\ |A_{|-\rangle}|^2 &= \frac{1}{4}|t_{kp}|^2\left(1-\frac{\Delta_r\Delta_b}{E_kE_p}\right). \end{aligned} \tag{2.25}$$

Substituting these matrix elements into Eq. (2.18), one obtains

$$\Gamma_{1\pm}^{\rm op} = \pi\sum_{p_1,k}|t_{kp}|^2\left(1\pm\frac{\Delta_r\Delta_b}{E_kE_p}\right)\delta(E_k-E_{p_1}-\omega_\pm)\exp\left(-\frac{E_{p_1}}{T}\right). \tag{2.26}$$

In the thermodynamic limit ($T \gg \delta$), one can change the sums to integrals in Eq. (2.26), and integrate over E_k to get the following expression for $\Gamma_{1\pm}^{\rm op}$:

$$\Gamma_{1\pm}^{\rm op} = \frac{g_{_T}}{2\pi}\int_{\Delta_r}^{\infty} dE_p \frac{\Theta(E_p+\omega_+-\Delta_b)(E_p(E_p+\omega_+)\pm\Delta_r\Delta_b)}{\sqrt{((E_p+\omega_+)^2-\Delta_b^2)(E_p^2-\Delta_r^2)}}\exp\left(-\frac{E_p}{T}\right), \tag{2.27}$$

where $\Theta(x)$ is the step function, $g_{_T}$ is the dimensionless conductance of the junction

$$g_{_T} = \frac{h}{e^2R_{_T}} \text{ and } R_{_T}^{-1} = 4\pi e^2\sum_{p,k}|t_{pk}|^2\delta(\xi_p)\delta(\xi_k). \tag{2.28}$$

Here $R_{_T}$ is the resistance of the tunnel junction in the normal state. Assuming that a mismatch between superconducting gap energies in the box and reservoir is small, $\Delta_r-\Delta_b+\omega_\pm > 0$, which corresponds to most charge qubit experiments, expressions for $\Gamma_1^{\rm op}$ can be evaluated. At low temperature ($\Delta_r-\Delta_b+\omega_\pm \gg T$)

the asymptotic result for $\Gamma^{\rm op}_{1\pm} = W_\pm(\omega_\pm, \Delta_r, \Delta_b)$ is simply given by

$$W_+(\omega_+,\Delta_r,\Delta_b) \approx \frac{g_T\sqrt{\Delta_r T}}{2\sqrt{2\pi}} \sqrt{\frac{\Delta_r+\Delta_b+\omega_+}{\Delta_r-\Delta_b+\omega_+}} \exp\left(-\frac{\Delta_r}{T}\right),$$
$$W_-(\omega_-,\Delta_r,\Delta_b) \approx \frac{g_T\sqrt{\Delta_r T}}{2\sqrt{2\pi}} \sqrt{\frac{\Delta_r-\Delta_b+\omega_-}{\Delta_r+\Delta_b+\omega_-}} \exp\left(-\frac{\Delta_r}{T}\right). \tag{2.29}$$

As expected, the decay rate due to the first mechanism is exponentially suppressed due to the fact that it costs energy Δ to bring a quasiparticle from the normal parts.

It is easy to generalize Eq. (2.29) to the case when the qubit is tuned away from the degeneracy point $N_g = 1$:

$$\begin{aligned}\Gamma^{\rm op}_{1\pm}(N_g) &= \frac{g_T\sqrt{\Delta_r T}}{2\sqrt{2\pi}} \exp\left(-\frac{\Delta_r}{T}\right) \frac{\Delta_r+\omega_\pm \pm \Delta_b \sin(2\theta_\pm)}{\sqrt{(\Delta_r+\omega_\pm)^2-\Delta_b^2}} = \\ &= \frac{g_T n^r_{\rm qp}}{4\pi\nu_F} \frac{\Delta_r+\omega_\pm \pm \Delta_b \sin(2\theta_\pm)}{\sqrt{(\Delta_r+\omega_\pm)^2-\Delta_b^2}}. \end{aligned} \tag{2.30}$$

Here $n^r_{\rm qp}$ is the density of quasiparticles in the reservoir, in the equilibrium $n^r_{\rm qp} = \sqrt{2\pi\Delta_r T}\nu_F \exp(-\Delta_r/T)$. The angle $\theta_\pm$ has been introduced in Eq. (2.4) and is given by

$$\theta_\pm = \arctan\left[\frac{\sqrt{(4E_c(1-N_g))^2+E_J^2} \pm 4E_c(1-N_g)}{E_J}\right] \tag{2.31}$$

At $N_g = 1$, the angles θ_+ and θ_- are equal, $\theta_+ = \theta_- = \pi/4$, and Eq. (2.30) reduces to Eq. (2.29). The different interference pattern for excited and ground states of the qubit is relevant for the gate voltage close to 1, *i.e.* $|1-N_g| \lesssim E_J/4E_c$.

The contribution of the second mechanism to the rate (2.14) depends on the density matrix of the box. The initial state of the qubit corresponds to an even-charge state in the CPB. Statistical weight of the states with an even number of quasiparticles in the dot, $2, 4, 6, ..., 2n$, is determined by the density matrix $\rho_{2n}(\beta H_0)$,

$$\rho_{2n}(\beta H_0)) = Tr_{\{p\}}\rho(\beta H_0) = \frac{\exp\left(-\sum_{j=2}^{2n} \frac{E_{k_j}}{T}\right)}{(2n)! Z_{\rm ev}}. \tag{2.32}$$

Here $Z_{\rm ev} = \cosh\left[z_b(T,\delta_b)\right]$ is the partition function for the dot with an even number of electrons [29] with $z_b(T,\delta_b)$ being

$$z_b(T,\delta_b) = \sum_k \exp\left(-\frac{E_k}{T}\right) = \sqrt{2\pi}\frac{\sqrt{T\Delta_b}}{\delta_b}\exp\left(-\frac{\Delta_b}{T}\right). \tag{2.33}$$

According to Eqs. (2.14) and (2.32), the contribution to the decay rate due to the second mechanism is obtained by summing over the states with an even number of quasiparticles with the appropriate statistical weight

$$\Gamma^{\rm op}_{2\pm} = 2\pi \sum_{n,p,k_j} |\left\langle N+1, p, \{k\}_{2n-1}\right| H_T \left|\pm, \{k\}_{2n}\right\rangle|^2 \delta(E_p - E_{k_1} - \omega_\pm) 2n\rho_{2n}(\beta H_0), \tag{2.34}$$

where, for example, $\langle N+1, p, \{k\}_{2n-1}|$ is a state corresponding to the charge on the box equal to $1e$, $2n-1$ quasiparticles in the box, and 1 quasiparticle in the reservoir

$$|N+1, p, \{k\}_{2n-1}\rangle = |N+1, k_1, \ldots, k_j, \ldots, k_{2n-1}\rangle \otimes |p\rangle. \tag{2.35}$$

The additional factor of $2n$ in Eq. (2.34) is the result of the summation of $2n$ identical terms in Eq. (2.14). The tunneling matrix element in Eq. (2.34) is determined using the particle-conserving Bogoliubov transformation and is dependent only on p and k_1. Therefore, by doing the sum over the other momenta k_j, one gets the following result:

$$\begin{aligned}\Gamma^{\rm op}_{2\pm} &= 2\pi \sum_{p,k_1} |\langle N+1, p|H_T|\pm, k_1\rangle|^2 \delta(E_p - E_{k_1} - \omega_\pm) \exp\left(-\frac{E_{k_1}}{T}\right) \\ &\times \sum_n \frac{\left[z_b(T,\delta_b)\right]^{2n-1}}{(2n-1)! Z_{\rm ev}}.\end{aligned} \tag{2.36}$$

By changing the sum to an integral and integrating over E_p, we obtain

$$\begin{aligned}\Gamma^{\rm op}_{2\pm} &= \frac{g_T}{2\pi}\int_{\Delta_b}^{\infty} dE_k \frac{(E_k(E_k+\omega_\pm) \pm \Delta_r\Delta_b)\Theta(E_k+\omega_\pm-\Delta_r)}{\sqrt{((E_k+\omega_\pm)^2-\Delta_r^2)(E_k^2-\Delta_b^2)}} \exp\left(-\frac{E_k}{T}\right) \\ &\times \tanh[z_b(T,\delta_b)].\end{aligned} \tag{2.37}$$

The integration can be performed assuming that a mismatch between superconducting gap energies in the box and reservoir is small, and $\Delta_b - \Delta_r + \omega_\pm \gg T$. Comparing Eqs. (2.27) and (2.37), one notices that the answer for $\Gamma_2^{\rm op}$ can be expressed via $\Gamma_1^{\rm op}$ by permuting $\Delta_r \leftrightarrow \Delta_b$

$$\Gamma_{2\pm}^{\rm op}(\omega_\pm, \Delta_r, \Delta_b) = \Gamma_{1\pm}^{\rm op}(\omega_\pm, \Delta_b, \Delta_r) \tanh\left[z_b(T, \delta_b)\right]. \tag{2.38}$$

Finally, taking into account Eqs. (2.29) and (2.38), we find the total quasiparticle decay rate for the open system

$$\Gamma_{|N+1\rangle\leftarrow|\pm\rangle}^{\rm op} = W_\pm(\omega_\pm, \Delta_r, \Delta_b) + W_\pm(\omega_\pm, \Delta_b, \Delta_r) \tanh\left[z_b(T, \delta_b)\right]. \tag{2.39}$$

Here the first term corresponds to the first mechanism, and is dominant for the open system. The simplified results for $\Gamma_{|N+1\rangle\leftarrow|\pm\rangle}^{\rm op}$ are discussed in Sec. 2.5.

2.4 States of the qubit in an isolated system

2.4.1 Thermodynamic properties of the qubit with fixed number of electrons

When the number of electrons in the qubit is fixed, parity effects become important at low temperatures, $T < T_r^*, T_b^*$, where T_b^* is defined in Eq. (2.5) and T_r is equal to

$$T_r^* = \frac{\Delta_r}{\ln(\Delta_r/\delta_r)}. \tag{2.40}$$

Here, δ_r is the mean level spacing in the reservoir. The density of quasiparticles in the qubit with an even number of electrons is small, $n \propto \exp(-2\Delta/T)$, because at low temperatures all electrons are paired, and it costs energy 2Δ to break a Cooper pair. In the odd-charge state, an unpaired electron is present in the system even at zero temperature. It is important to estimate the probability of finding a quasiparticle in the CPB since the presence of a quasiparticle in the

CPB degrades the performance of the qubit. To find out whether it is favorable or not for a quasiparticle to reside in the CPB, we calculated the difference in free energy $\Delta F = F_1 - F_0$ between two states: with and without a quasiparticle in the box (F_1 and F_0, respectively). At the operating point, the free energy difference for the qubit with even ($\Delta F_{\rm ev}$) and odd ($\Delta F_{\rm odd}$) total number of electrons is given by the following expressions:

$$\Delta F_{\rm ev} = -\delta E - T\ln[\tanh(z_b(T,\delta_b))] - T\ln[\tanh(z_r(T,\delta_r))], \quad (2.41)$$

$$\Delta F_{\rm odd} = -\delta E - T\ln[\tanh(z_b(T,\delta_b))] - T\ln[\coth(z_r(T,\delta_r))]. \quad (2.42)$$

Here δE is even-odd energy difference. For the charge qubit $\delta E = E_c - E_J/2$. A negative value of ΔF indicates that free energy is lower for a quasiparticle in the CPB. Using these expressions, we can calculate thermodynamic probability $P(T)$ to find an unpaired electron in the box as a function of physical parameters

$$P(T) = \frac{Z_1}{Z_1 + Z_0} = \frac{1}{\exp\left(\frac{\Delta F}{T}\right) + 1}. \quad (2.43)$$

Here $Z_{1(0)} = \exp\left(-\beta F_{1(0)}\right)$ is the partition function with one (zero) unpaired electrons in the box. The expression for the free energy difference ΔF_{op} for an open system (fixed chemical potential regime) can be obtained using $\Delta F_{\rm ev}$ and taking the limit of infinite volume of the reservoir ($\delta_r \to 0$). The temperature dependence of the probability $P(T)$ is plotted in Fig. 2.2.

As shown in Fig. 2.2, at high temperatures $T > T_b^*$ the probability of having an extra electron in the CPB coincides for an open and isolated qubit. At this temperature the number of thermal quasiparticles in the system is large, and parity effects are not important. Parity effects start to manifest themselves below the characteristic temperature T_b^*, when the number of quasiparticles in the box is of the order of unity. As can be seen from Fig. 2.2, at the temperature T_r^* the probability of having a quasiparticle in the CPB is negligible in the even-charge

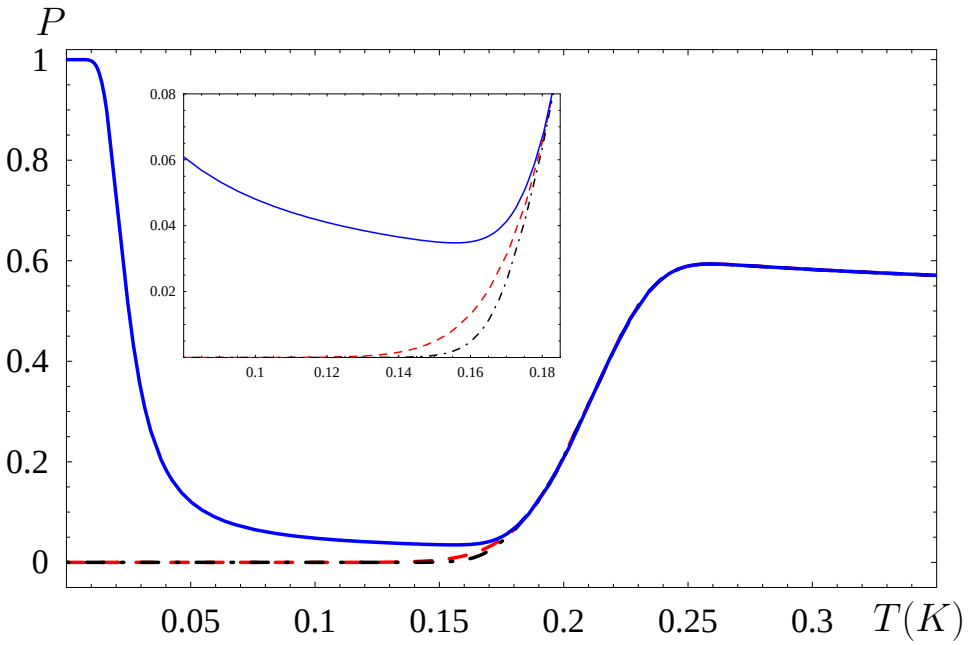

Figure 2.2: Main panel: temperature dependence of the probability of finding a quasiparticle in the island at the operating point ($N_g = 1$). Dash-dot line corresponds to even number of electrons, solid line - odd number of electrons, dashed line - open system. Physical parameters are chosen in correspondence to typical qubit experiments: $\Delta_r = \Delta_b = 2.4$K, $E_c = 0.25$K, $E_J = 0.3$K, $T_b^* = 210$mK, and $T_r^* = 160$mK (see Eqs. (2.5) and (2.40) for definition of T_b^* and T_r^*). Inset: temperature dependence of the number of quasiparticles in the CPB in the vicinity of T_r^*.

state, as well as in the open system. In the case of odd charge state of a qubit, lowering the temperature enhances quasiparticle poisoning. This effect can be explained as a competition of two contributions to the free energy: a charging energy gained by tunneling to the box and entropy contribution proportional to the ratio of the volumes of the reservoir and box, $\sim V_r/V_b$. At the temperature T_s,

$$T_s \simeq \frac{E_c - E_J/2}{\ln\left(\frac{V_r}{V_b}\right)}, \tag{2.44}$$

the entropy contribution becomes smaller, and the quasiparticle resides in the CPB. Thus, for the odd-charge state there is only a certain intermediate temperature range when a qubit can work, *i.e.* can be prepared in the "good" quantum state. For physical parameters used in Fig. 2.2 T_s is approximately equal to 20mK.

The presence of a quasiparticle in the box can be studied experimentally by measuring the periodicity of the Coulomb staircase [31–35, 39, 43]. According to Eq. (2.43), the Coulomb staircase for an open system should be $2e$ periodic below the temperature $\widetilde{T}_b^*$. The qubit with fixed number of electrons should have two distinct types of behavior corresponding to even and odd total number of electrons in the box and reservoir. In the former case the Coulomb staircase is similar to that of the open system, while in the latter case Coulomb staircase is $1e$ periodic for temperatures above T_b^*, then $2e$ periodic from T_b^* to T_s, and again $1e$ periodic for $T < T_s$.

It is possible to reduce the probability of finding a quasiparticle in the CPB, and bring the qubit to the desired quantum state. We discuss several ways of doing that in Sec. 2.5. However, even if the quasiparticle is in the reservoir at the initial moment of time, once the qubit is excited and quantum oscillations emerge, the time of the oscillations is determined by the kinetics, *i.e.*, by the quasiparticle tunneling rate.

2.4.2 Quasiparticle decay rate in an isolated system

Let us turn to the discussion of the lifetime of the qubit states in an isolated system. In order to calculate the quasiparticle decay rate, we proceed in the same manner as for the open system. The decay rate for an even number of electrons is calculated by averaging over initial states with an even parity density matrix $\rho_{2n}(\beta H_0)$. This situation corresponds to having an even number of electrons in the box and reservoir. The appearance of quasiparticles in the system occurs at the expense of breaking Cooper pairs. Using the results of an analogous calculation in Eq. (2.38), we can write the expression for the total decay rate

$$\Gamma^{\rm ev}_{|N+1\rangle\leftarrow|\pm\rangle} = W_{\pm}(\omega_{\pm},\Delta_r,\Delta_b)\tanh\left[z_r(T,\delta_r)\right]+W_{\pm}(\omega_{\pm},\Delta_b,\Delta_r)\tanh\left[z_b(T,\delta_b)\right], \tag{2.45}$$

where $W_{\pm}(\omega_{\pm},\Delta_r,\Delta_b)$ is defined in Eq. (2.29). The first term here corresponds to the first mechanism given by Eq. (2.13) and averaged over the even-parity initial state.

In the odd-charge case the decoherence rate is the largest because a quasiparticle is present in the system even at $T=0$. The initial configuration of the system corresponds to having an odd number of quasiparticles in the reservoir. The reduced density matrix for this initial state $\rho_{2n-1}(\beta H_0)$ is then given by

$$\rho_{2n-1}(\beta H_0) = Tr_{\{k\}}\rho(\beta H_0) = \frac{\exp\left(-\sum\limits_{j=1}^{2n-1}\frac{E_{p_j}}{T}\right)}{(2n-1)!Z_{\rm odd}} \tag{2.46}$$

with $Z_{\rm odd}=\sinh\left[z_r(T,\delta_r)\right]$. Using Eq. (2.13), we write the contribution to the decay rate of the first mechanism

$$\begin{aligned}\Gamma^{\rm odd}_{1\pm} &= 2\pi\sum_{n,p_j,k}|\left\langle N+1,k,\{p\}_{2n-2}\right|H_T\left|\pm,\{p\}_{2n-1}\right\rangle|^2\delta(E_k-E_{p_1}-\omega_{\pm})\\ &\times\ (2n-1)\rho_{2n-1}(\beta H_0).\end{aligned} \tag{2.47}$$

Going through the same arguments as in Eq. (2.36), the expression for $\Gamma_{1\pm}^{\rm odd}$ can be simplified

$$\Gamma_{1\pm}^{\rm odd} = 2\pi \sum_{p_1,k} |\langle N+1,k|H_T|\pm,p_1\rangle|^2 \delta(E_k - E_{p_1} - \omega_\pm) \exp\left(-\frac{E_{p_1}}{T}\right) \times \sum_{n=1}^{\infty} \frac{[z_r(T,\delta_r)]^{2n-2}}{(2n-2)! Z_{\rm odd}}. \quad (2.48)$$

Summing over E_k, we get

$$\Gamma_1^{\rm odd} = \frac{g_T}{2\pi} \int_{\Delta_r}^{\infty} dE_p \frac{(E_p(E_p+\omega_\pm) \pm \Delta_r\Delta_b)\Theta(E_p+\omega_\pm-\Delta_b)}{\sqrt{((E_p+\omega_\pm)^2-\Delta_b^2)(E_p^2-\Delta_r^2)}} \exp\left(-\frac{E_p}{T}\right) \times \coth\left(z_r(T,\delta_r)\right) \quad (2.49)$$

Taking into account Eqs. (2.27), (2.29) and (2.49), $\Gamma_1^{\rm odd}$ is equal to

$$\Gamma_{1\pm}^{\rm odd} = W_\pm(\omega_\pm,\Delta_r,\Delta_b)\coth\left[z_r(T,\delta_r)\right]. \quad (2.50)$$

In order to find the contribution of the second mechanism, one has to average over the initial state of the CPB. The initial configuration of the box corresponds to the even-charge state and is the same for open and isolated qubits. Therefore, contribution of the second mechanism, $\Gamma_2^{\rm odd}$, is given by Eq. (2.38).

Thus, the total decay rate $\Gamma_{|N+1\rangle\leftarrow|\pm\rangle}^{\rm odd}$ with odd number of electrons in the system is the sum of $\Gamma_1^{\rm odd}$ and $\Gamma_2^{\rm odd}$,

$$\Gamma_{|N+1\rangle\leftarrow|\pm\rangle}^{\rm odd} = W_\pm(\omega_\pm,\Delta_r,\Delta_b)\coth\left[z_r(T,\delta_r)\right] + W_\pm(\omega_\pm,\Delta_b,\Delta_r)\tanh\left[z_b(T,\delta_b)\right]. \quad (2.51)$$

At low temperatures, $T < T_r^*, T_b^*$, the first term here is dominant since $z(T,\delta) \ll 1$. The detailed analysis of the low temperature asymptote for different experimental regimes is presented in the next section.

2.5 Discussion of the Results

Temperature dependence of the quasiparticle decay rate for different experimental realizations of the qubit is shown in Fig. 2.3. As it is clear from the figure, at

experimentally relevant temperatures $T \ll T_r^*, T_b^*$, the largest decay rate corresponds to the odd-electron case. In the vicinity of T_r^* defined in Eq. (2.40), the decay rate is growing quickly due to the appearance of a large number of quasiparticles in the reservoir. As we approach the temperature $T = T_b^*$, which corresponds to the appearance of quasiparticles in the Cooper-pair box [see Eq. (2.5)], parity effects become irrelevant and decoherence rates for different cases coincide.

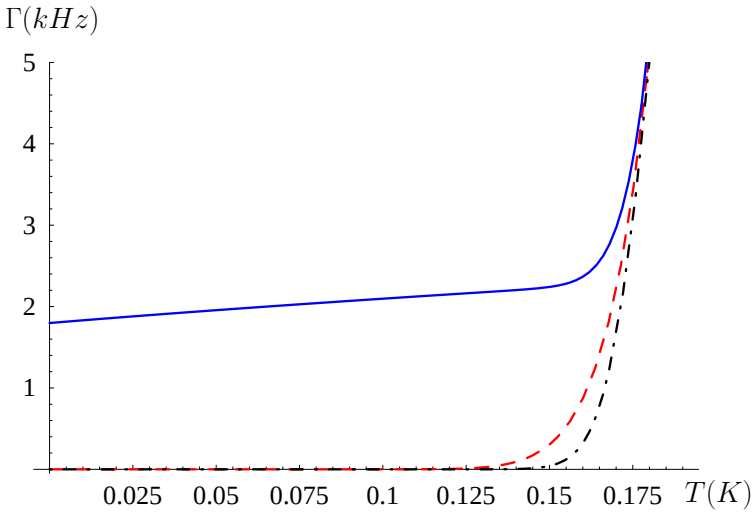

Figure 2.3: Temperature dependence of the quasiparticle decay rate. Dashed line corresponds to the open system, dash-dot - even number of electrons, solid - odd number of electrons. Here, we used the same physical parameters as specified in Fig. 2.2.

Results obtained in Sec. 2.3 and 2.4 allow us to quantitatively estimate the decoherence rate due to the presence of quasiparticles in the system. For simplicity we assume that superconducting gap energies are the same in the box and reservoir, $\Delta_b = \Delta_r = \Delta$, and temperature is low, $T < T_r^*, T_b^* \ll \omega_\pm$, corresponding to typical qubit experiments ($\omega_\pm$ is defined in Eq. (2.4)). In this approximation, the decay rates of the excited and ground states for an "open" qubit are

$$\Gamma^{\rm op}_{|N+1\rangle\leftarrow|+\rangle} \approx \frac{g_T\sqrt{T\Delta}}{2\sqrt{2\pi}}\sqrt{\frac{2\Delta+\omega_+}{\omega_+}}\exp\left(-\frac{\Delta}{T}\right)+\frac{g_T T}{2}\sqrt{\frac{2\Delta+\omega_+}{\omega_+}}\frac{\Delta}{\delta_b}\exp\left(-\frac{2\Delta}{T}\right) \tag{2.52}$$

and

$$\Gamma^{\rm op}_{|N+1\rangle\leftarrow|-\rangle}\approx\frac{g_{_T}\sqrt{T\Delta}}{2\sqrt{2\pi}}\sqrt{\frac{\omega_-}{2\Delta+\omega_-}}\exp\left(-\frac{\Delta}{T}\right)+\frac{g_{_T}T}{2}\sqrt{\frac{\omega_-}{2\Delta+\omega_-}}\frac{\Delta}{\delta_b}\exp\left(-\frac{2\Delta}{T}\right), \tag{2.53}$$

respectively. At low temperature the leading contribution to the decay rate for the open system $\Gamma^{\rm op}_{|N+1\rangle\leftarrow|\pm\rangle}$ is proportional to $\exp(-\Delta/T)$ reflecting the fact that energy equal to Δ is required to bring an electron from the normal parts.

In the even-charge case the leading contribution to $\Gamma^{\rm ev}_{|N+1\rangle\leftarrow|\pm\rangle}$ is also exponentially small, $\propto\exp(-2\Delta/T)$, in accordance with the energy necessary to break a Cooper pair,

$$\Gamma^{\rm ev}_{|N+1\rangle\leftarrow|+\rangle}\approx\frac{g_{_T}T}{2}\sqrt{\frac{2\Delta+\omega_+}{\omega_+}}\frac{\Delta}{\delta_r}\exp\left(-\frac{2\Delta}{T}\right)+\frac{g_{_T}T}{2}\sqrt{\frac{2\Delta+\omega_+}{\omega_+}}\frac{\Delta}{\delta_b}\exp\left(-\frac{2\Delta}{T}\right), \tag{2.54}$$

and

$$\Gamma^{\rm ev}_{|N+1\rangle\leftarrow|-\rangle}\approx\frac{g_{_T}T}{2}\sqrt{\frac{\omega_-}{2\Delta+\omega_-}}\frac{\Delta}{\delta_r}\exp\left(-\frac{2\Delta}{T}\right)+\frac{g_{_T}T}{2}\sqrt{\frac{\omega_-}{2\Delta+\omega_-}}\frac{\Delta}{\delta_b}\exp\left(-\frac{2\Delta}{T}\right). \tag{2.55}$$

Note that Eq. (2.54) and the last term in Eq. (2.52) are essentially the upper bounds for the contributions to the decay rate of the excited state $|+\rangle$ coming from unpaired electrons, which originate in the isolated system and in the Cooper-pair box, respectively. Indeed, we assumed in the derivation of Eqs. (2.52) and (2.54) that the decay rate is limited by the thermodynamic probability of the unpaired state, without discussing the kinetics of pair-breaking leading to such state. It is clear from Fig. 2.3, however, that the above mentioned contributions are negligibly small at low temperatures.

The decay rate of the qubit with an odd number of electrons $\Gamma^{\rm odd}_{|N+1\rangle\leftarrow|\pm\rangle}$ is much larger

$$\Gamma^{\rm odd}_{|N+1\rangle\leftarrow|+\rangle} \approx \frac{g_T\delta_r}{4\pi}\sqrt{\frac{2\Delta+\omega_+}{\omega_+}} + \frac{g_T T}{2}\sqrt{\frac{2\Delta+\omega_+}{\omega_+}}\frac{\Delta}{\delta_b}\exp\left(-\frac{2\Delta}{T}\right), \qquad (2.56)$$

and

$$\Gamma^{\rm odd}_{|N+1\rangle\leftarrow|-\rangle} \approx \frac{g_T\delta_r}{4\pi}\sqrt{\frac{\omega_-}{2\Delta+\omega_-}} + \frac{g_T T}{2}\sqrt{\frac{\omega_-}{2\Delta+\omega_-}}\frac{\Delta}{\delta_b}\exp\left(-\frac{2\Delta}{T}\right). \qquad (2.57)$$

The leading contribution to the decay rate is temperature independent since the number of quasiparticles is finite even at $T = 0$. According to the Eq. (2.56), the lifetime of the qubit excited state is determined by the conductance of the tunnel junction and the mean level spacing in the reservoir. For typical experiments dimensionless conductance g_T is less than one; δ_r depends on the volume of the reservoir and varies between 10^{-10} and 10^{-12} eV. With these parameters, decay rate $\Gamma^{\rm odd}_{|N+1\rangle\leftarrow|+\rangle}$ can be estimated as 10^5-10^3 Hz consequently. This is a substantial contribution to the decoherence of the isolated charge qubits, which limits qubit operation on a fundamental level. However, this decay rate is much smaller than the present estimates for decoherence in charge qubits; see, for example, the recent review by Devoret *et. al* [18].

We assumed so far that in the initial state an unpaired electron resides in the reservoir and finally (after the relaxation) ends up in the box. Then, one can tune the qubit to the charge degeneracy between $1e$ and $3e$ and still have charge oscillations for some time until the quasiparticle escapes into the reservoir. In this case, the quasiparticle escape rate can be calculated in a similar way and is proportional to the conductance of the tunnel junction and level spacing in the Cooper-pair box: $\Gamma^{\rm odd} \propto g_T\delta_b$.

In principle, quasiparticle poisoning can be decreased by tuning proper parameters of the system such as superconducting gap energies $\Delta_{r,b}$, charging and Josephson energies, temperature, and volumes of the box and reservoir. For example, it can be done by adjusting gap energies $\Delta_{r,b}$ with the help of oxygen doping [31], reducing the thickness of the superconductor [38, 39] or magnetic

field [32]. The latter is easy to implement since magnetic field is already used in charge qubits to tune Josephson energy E_J. The question of the relaxation time in a charge qubit with large gap energy mismatch, $\Delta_b \gg \Delta_r$, is considered in Ch. 6.

2.6 Conclusion

We demonstrated that the presence of quasiparticles in the superconducting charge qubit leads to the escape of the qubit outside of its two-level-system Hilbert space, and thus results in the decay of coherent oscillations. Two experimental realizations of the charge qubit are considered here, corresponding to an open and isolated system (in the former, the number of electrons is not fixed). Once the qubit is excited and coherent oscillations emerge, the decay of these oscillations is determined by the quasiparticle tunneling rate to the Cooper-pair box. We calculated temperature dependence of the quasiparticle decay rate in the charge qubit. The quasiparticle decay rate is exponentially suppressed in the open system as well as in the isolated system with an even number of electrons. However, in the case of an odd number of electrons in the system, the quasiparticle decay rate is not exponentially suppressed and is estimated to be $10^5 - 10^3$ Hz depending on the volume of the superconducting reservoir and conductance of the tunnel junction.

Chapter 3

Kinetics of a superconducting charge qubit

3.1 Qualitative Considerations and Main Results

In this Chapter, we consider the kinetics of the qubit due to the presence of a single quasiparticle. This allows us to find qubit energy and phase relaxation times T_1 and T_2, respectively.

In Chapter 2 we evaluated rates of the elementary acts involving quasiparticle tunneling. In particular, we showed that the tunneling rate into the CPB $\Gamma_{\rm in}$ is determined by the dimensionless (in units of e^2/h) conductance $g_{_T}$ of the junction between the CPB and the reservoir, and level spacing in the reservoir: $\Gamma_{\rm in} \sim g_{_T}\delta_r/4\pi$. The tunneling rate out of CPB is $\Gamma_{\rm out} \sim g_{_T}\delta_b/4\pi$ with δ_b being level spacing in the box. Taking into account the difference in the volumes ($V_r \gg V_b$), one can notice that $\Gamma_{\rm out} \gg \Gamma_{\rm in}$. Therefore, for a sufficiently small box the quasiparticle dwell time in the CPB is very short, and the qubit spends most of the time in the "good" part of the Hilbert space. Nevertheless, the evolution of the qubit will be affected by quick "detours" the qubit takes outside that part of the Hilbert space. We demonstrate that even a single detour destroys the

coherence of the qubit. Combined with the phonon-induced relaxation of the non-equilibrium quasiparticle in the reservoir, the detours also lead to the relaxation of the populations of the qubit states. In this Chapter we derive and solve the master equations for the dynamics of the qubit, which describe its relaxation caused by a quasiparticle.

The presence of a quasiparticle with a continuum excitation spectrum provides a channel for the qubit relaxation. If the state $|N\rangle$ is prepared in equilibrium conditions, then the quasiparticle resides in the reservoir part [44] of the qubit. Upon tuning of the qubit from state $|N\rangle$ to the operating point, a charge degeneracy point for the system is passed at $N_g = N + 1/2$, see Fig. 3.1. (Hereafter we assume equal superconducting gap energies in the reservoir and Cooper-pair box.) However, if tuning is performed fast enough, the quasiparticle remains in the reservoir [33].

The coherent charge oscillations at the operating point of the qubit continue until the particle finds its way into the CPB. On average, this occurs on a time scale of the order of $(g_T\delta_r/4\pi)^{-1}$. There are several assumptions that allow for this estimate [44]. First, the mean level spacings δ_b and δ_r in the CPB and reservoir, respectively, must be small compared with the temperature T, which defines the initial width of the energy distribution of the quasiparticle. Second, the fluctuations of the potential between the grains must exceed δ_r, see, *e.g.*, Ref. [45]. Third, we neglected the difference between Δ and E_c when including in the estimate the density of states and tunneling matrix elements of a quasiparticle at energy $\sim E_c$ above the gap in the CPB. Under these conditions, the average time it takes the quasiparticle to leave the reservoir and enter the CPB is of the order of the inverse level width of a state in the reservoir with respect to leaving it through the junction of conductance g_T

$$\Gamma_{\rm in}^{-1} \sim \left(\frac{g_T\delta_r}{4\pi}\right)^{-1}. \tag{3.1}$$

Once the quasiparticle enters the CPB, the charging energy that the qubit has

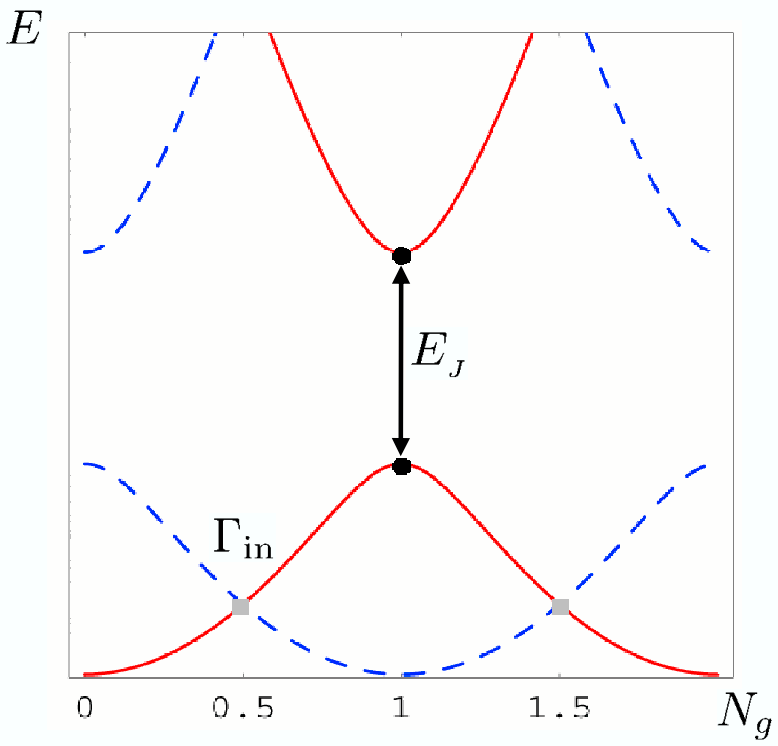

Figure 3.1: Energy of the Cooper-pair box as a function of the dimensionless gate charge N_g in units of e (solid line). Near the degeneracy point ($N_g = 1$) Josephson coupling mixes charge states and modifies the energy of the CPB. The dashed line corresponds to the charging energy of the CPB with an unpaired electron in the box. At $N_g = 0.5$, the tunneling rate $\Gamma_{\rm in}$ lifts the degeneracy between the ground state of the CPB (solid line) and a state with a single quasiparticle in CPB (dashed line). We assume equal superconducting gap energies in the reservoir and CPB.

at operation point is transformed into the kinetic energy of the quasiparticle, see Fig. 3.1. The quasiparticle may escape the CPB leaving the qubit in the excited or ground state, see Fig. 3.2. The rates of the escape into these states are different due to the difference of the kinetic energies available to the quasiparticle upon the escape and due to the energy dependence of the superconducting density of states $\nu(\varepsilon)$. If the qubit ends up in the excited state upon the escape, then only energy $\varepsilon \sim T$ is available for the quasiparticle, and $\nu(T) \sim \delta_r^{-1}(\Delta/T)^{1/2}$ (we used here the condition $\Delta \gg T$). The corresponding escape rate is

$$\Gamma_{\rm out}^{|+\rangle} \sim \frac{g_T \delta_b}{4\pi}\sqrt{\frac{\Delta}{T}}. \tag{3.2}$$

If the qubit arrives in the ground state, then energy $\sim E_J$ is available to the quasiparticle, and its density of states in the final state is $\nu(E_J) \sim \delta_r^{-1}(\Delta/E_J)^{1/2}$; the rate of the escape to this state is

$$\Gamma_{\rm out}^{|-\rangle} \sim \frac{g_T \delta_b}{4\pi}\sqrt{\frac{\Delta}{E_J}}. \tag{3.3}$$

These two rates are much higher than $\Gamma_{\rm in}$ because $\delta_b \gg \delta_r$, so detours of the quasiparticle to the CPB are short compared to the time the quasiparticle spends in the reservoir. Nevertheless, the typical time the quasiparticle spends in the CPB is much greater than the oscillation period of the qubit. Indeed, the ratio

$$\frac{\Gamma_{\rm out}^{|-\rangle}}{E_J} \sim \frac{\delta_b}{\Delta}\sqrt{\frac{\Delta}{E_J}} \tag{3.4}$$

is small: $\delta_b/\Delta \sim 10^{-4} - 10^{-3}$ for any reasonable size of the CPB (we used here the Ambegaokar-Baratoff relation between E_J, g_T and Δ). The times of return of the quasiparticle back to the reservoir are randomly distributed. The probability of the quasiparticle returning to the reservoir during times that are short compared to the oscillation period $2\pi/E_J$ is of the order $\Gamma_{\rm out}/E_J$ and is small (here we do not distinguish between $\Gamma_{\rm out}^{|-\rangle}$ and $\Gamma_{\rm out}^{|+\rangle}$). Therefore, a single detour of the quasiparticle into the CPB destroys coherent oscillations of the qubit with

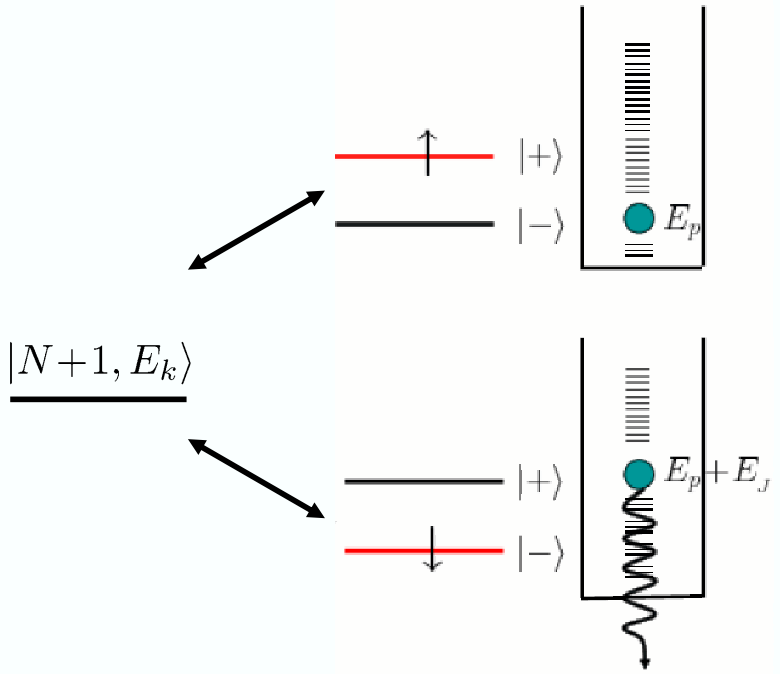

Figure 3.2: Schematic picture of the transitions between the qubit states in the presence of a quasiparticle in the reservoir, *e.g.* $|+, E_p\rangle \leftrightarrow |N+1, E_k\rangle$. Having kinetic energy $\sim E_J$ the quasiparticle can emit a phonon. The corresponding state of the system is $|-, E_p+E_J\rangle$.

overwhelming probability. Taking into account the relation $\Gamma_{\rm in} \ll \Gamma^{\pm}_{\rm out}$, we find that the dephasing rate for the qubit, induced by the quasiparticle, is limited by the rate of quasiparticle tunneling into the CPB

$$\frac{1}{T_2} \sim \Gamma_{\rm in} \tag{3.5}$$

with $\Gamma_{\rm in}$ of Eq. (3.1).

Unlike the phase, the energy stored in the degrees of freedom described by the qubit Hamiltonian (2.1) is not dissipated in the short time scale given by Eq. (3.5). We start analyzing the time evolution of the qubit energy by considering the limit of infinitely slow quasiparticle relaxation (the latter typically is determined by the electron-phonon interaction [46, 47]). If initially the system

was prepared in the $|+\rangle$ state, then upon a single cycle of quasiparticle tunneling, the qubit ends up in the ground state with a small probability defined by the ratio $\Gamma_{\rm out}^{|-\rangle}/\Gamma_{\rm out}^{|+\rangle} \sim \sqrt{T/E_J}$. In other words, the qubit energy will randomly change over time between two values ω_+ and ω_-, see Eq. (2.4). The fraction of the time, the qubit spends in the ground state and the quasiparticle is excited to the energy E_J above the gap, is small $\sim \sqrt{T/E_J}$.

The fraction of time that the quasiparticle spends in an excited state in the reservoir becomes important when we account for the phonon-induced relaxation of the quasiparticle. Having energy E_J, the quasiparticle may emit a phonon at some rate $1/\tau$ and relax to a low-energy state. The relaxation of the quasiparticle prevents further reexcitation of the qubit into $|+\rangle$ state and results in qubit energy relaxation. To find the energy relaxation rate of the qubit, we multiply the fraction of time the quasiparticle spends in the excited state by the relaxation rate $1/\tau$:

$$\frac{1}{T_1} \sim \sqrt{\frac{T}{E_J}}\frac{1}{\tau}. \tag{3.6}$$

This estimate is applicable if $\tau \gg 1/\Gamma_{\rm in}$, and many cycles occur before energy is dissipated into the phonon bath.

In the opposite case of fast relaxation $\tau \ll 1/\Gamma_{\rm in}$, the quasiparticle loses its energy the first time it gets it from the degrees of freedom of the Hamiltonian (2.1). Therefore, in this case the qubit energy relaxation on average occurs on the time scale

$$\frac{1}{\widetilde{T}_1} \sim \sqrt{\frac{T}{E_J}}\Gamma_{\rm in}. \tag{3.7}$$

For aluminum, a typical superconductor used for charge qubits, the quasiparticle relaxation time τ is indeed determined by the inelastic electron-phonon scattering [46, 47], and at low energies ($\varepsilon \leq E_J$) it can be estimated as $\tau \gtrsim 10\,\mu s$. For a small mesoscopic superconductor this time is longer than the typical values of $1/\Gamma_{\rm in}$, and Eq. (3.6) gives an adequate estimate for the qubit energy relaxation

rate.

A comparison of the phase relaxation time (3.5) with even the shortest of the two energy relaxation times (3.7), indicates that the coherence is destroyed much earlier than the populations of the qubit states approach equilibrium. Therefore one may consider the decay of qubit coherence separately from the process of equilibration, which involves the electron-phonon interaction in addition to quasiparticle tunneling. In the rest of the Chapter, we derive and solve the master equations, which yield results discussed qualitatively in this section.

3.2 Derivation of the Master Equations without quasiparticle relaxation

The Hamiltonian of the entire system consists of the qubit Hamiltonian $H_{\rm qb}$, BCS Hamiltonians for the superconducting box and reservoir $H^b_{\rm BCS}$ and $H^r_{\rm BCS}$, respectively, and quasiparticle tunneling Hamiltonian V:

$$H = H_0 + V, \tag{3.8}$$

where $H_0 = H^b_{\rm BCS} + H^r_{\rm BCS} + H_{\rm qb}$ and perturbation Hamiltonian V takes into account only tunneling of quasiparticles $V = H_{_T} - H_{_J}$. The tunneling Hamiltonian $H_{_T}$ is defined as

$$H_{_T} = \sum_{kp\sigma} (t_{kp} c^\dagger_{k,\sigma} c_{p,\sigma} + H.c.), \tag{3.9}$$

where t_{kp} is the tunneling matrix element, $c_{k,\sigma}$, $c_{p,\sigma}$ are the annihilation operators for an electron in the state k,σ in the CPB and state p,σ in the superconducting reservoir, respectively; $H_{_J}$ is of the second order in tunneling amplitude [7]

$$H_{_J} = |N\rangle \langle N| H_{_T} \frac{1}{E - H_0} H_{_T} |N+2\rangle \langle N+2| + H.c. \tag{3.10}$$

[7] The possibility to include the Josephson tunneling term in H_0 while considering the quasiparticle tunneling Hamiltonian V as a perturbation was demonstrated in Ch. 2.

The matrix element $\langle N|\, H_{_T} \frac{1}{E-H_0} H_{_T}\, |N+2\rangle$ is proportional to the effective Josephson energy $E_{_J}$, and $H_{_T}$ is defined in Eq. (3.9). Without quasiparticles, the Hamiltonian H_0 reduces to Eq. (2.1), and qubit dynamics can be described using the states $|+\rangle$ and $|-\rangle$. In the presence of a quasiparticle, the qubit phase space should be extended. Relevant states are now $|+, E_p\rangle$, $|-, E_p\rangle$, and $|N{+}1, E_k\rangle$. The first two states $|\pm, E_p\rangle$ correspond to the qubit being in the excited (ground) state $|\pm\rangle$ and a quasiparticle residing in the reservoir with energy $E_p = \sqrt{\xi_p^2 + \Delta^2}$:

$$|\pm, E_p\rangle \equiv |\pm\rangle \otimes |E_p\rangle\,.$$

The third state $|N{+}1, E_k\rangle$ describes the qubit in the "odd" state with $N+1$ electrons in the box, *i.e.*, the qubit escapes outside of its two-level Hilbert space. Here $E_k = \sqrt{\xi_k^2 + \Delta^2}$ is the energy of the quasiparticle in the box. Perturbation Hamiltonian V causes transitions between the states $|\pm, E_p\rangle$ and $|N{+}1, E_k\rangle$, see Fig. 3.2. Note that V does not induce the transitions between $|+, E_p\rangle$ and $|-, E_p\rangle$.

The evolution of the full density matrix of the system is described by Heisenberg equation of motion ($\hbar = 1$):

$$\dot{\rho}_{_I}(t) = -i[V_{_I}(t), \rho_{_I}(t)], \tag{3.11}$$

where subscript I stands for the interaction representation, *i.e.*, $V_{_I}(t) = e^{iH_0 t} V e^{-iH_0 t}$. The iterative solution of Eq. (3.11) yields for the elements of the density matrix

$$\langle s|\, \dot{\rho}_{_I}(t) |s'\rangle = -i\, \langle s|\, [V_{_I}, \rho(0)]\, |s'\rangle - \int_0^t d\tau \langle s| [V_{_I}(t), [V_{_I}(t{-}\tau), \rho_{_I}(t{-}\tau)]] |s'\rangle, \tag{3.12}$$

where $|s\rangle$ can be $|+, E_p\rangle$, $|-, E_p\rangle$, or $|N{+}1, E_k\rangle$. The interaction Hamiltonian V has no diagonal elements in the representation for which H_0 and $\rho(0)$ are diagonal. Therefore, the first term on the right-hand side of Eq. (3.12) is equal to zero,

$$\langle s|\, \dot{\rho}_{_I}(t) |s'\rangle = -\int_0^t d\tau \langle s| [V_{_I}(t), [V_{_I}(t{-}\tau), \rho_{_I}(t{-}\tau)]] |s'\rangle. \tag{3.13}$$

Equation (3.13) implies that the evolution of the projected density matrix is proportional to V^2. Since interaction is assumed to be weak, the rate of change

of $\rho_{_I}(t-\tau)$ is slow compared to that of $V_{_I}(t)$. Therefore, one can approximate $\rho_{_I}(t-\tau)$ by $\rho_{_I}(t)$ in the right-hand side of Eq. (3.13) (for more details on the derivation see, for example, Refs. [48, 49]). Finally, going back to the original representation, we arrive at the following system of master equations

$$\begin{aligned}
\langle s|\,\dot{\rho}(t)\,|s'\rangle \;=\; & -i\,\langle s|\,(E_s-E_{s'})\rho(t)\,|s'\rangle \\
& -\;\pi\sum_{m,n}\langle s|\,V\,|m\rangle\,\langle m|\,V\,|n\rangle\,\langle n|\,\rho(t)\,|s'\rangle\,\delta(E_n-E_m) \\
& -\;\pi\sum_{m,n}\langle s|\,\rho(t)\,|m\rangle\,\langle m|\,V\,|n\rangle\,\langle n|\,V\,|s'\rangle\,\delta(E_m-E_n) \\
& +\;\pi\sum_{m,n}\langle s|\,V\,|m\rangle\,\langle m|\,\rho(t)\,|n\rangle\,\langle n|\,V\,|s'\rangle\,\delta(E_n-E_{s'}) \\
& +\;\pi\sum_{m,n}\langle s|\,V\,|m\rangle\,\langle m|\,\rho(t)\,|n\rangle\,\langle n|\,V\,|s'\rangle\,\delta(E_m-E_s),
\end{aligned} \tag{3.14}$$

where states $|m\rangle$, $|n\rangle$, $|s\rangle$, and $|s'\rangle$ denote $|+,E_p\rangle$, $|-,E_p\rangle$, or $|N+1,E_k\rangle$, and the sum runs over all possible configurations. The system of equations (3.14) describes the kinetics of the qubit in the presence of a quasiparticle in the Markovian approximation. We are interested in elements of the density matrix that are diagonal in quasiparticle subspace, *e.g.*, $P_{+-}(E_p,t)=\langle +,E_p|\,\rho(t)\,|E_p,-\rangle$, since at the end one should take the trace over quasiparticle degrees of freedom to obtain observable quantities. Note that Eq. (3.14) which describes evolution of a closed system (the qubit and the quasiparticle) does conserve its total energy. We will include the mechanisms of energy loss to the phonon bath and discuss the proper modifications of the master equation later in Sec. 3.5.

We now apply a secular approximation to Eq. (3.14). This is justified due to the separation of the characteristic time scales $E_{_J}^{-1}\ll\Gamma_{\rm out}^{-1}\ll\Gamma_{\rm in}^{-1}$ established in the previous section. When considering the evolution of the off-diagonal elements of the density matrix $P_{+-}(E_p,t)$, we need to keep only terms $\propto P_{+-}(E_p,t)$ in the right-hand-side of the corresponding master equation. The contribution of other elements of the density matrix to the evolution of the coherences $P_{+-}(E_p,t)$ is small as $\Gamma_{\rm out}/E_{_J}$ and $\Gamma_{\rm in}/E_{_J}$. Thus, we arrive at the equation governing the

evolution of the coherences

$$\dot{P}_{+-}(E_p,t) = -iE_J P_{+-}(E_p,t) - \frac{1}{2}\sum_k \left[W_+(E_p,E_k) + W_-(E_p,E_k)\right] P_{+-}(E_p,t). \quad (3.15)$$

The transition rates $W_+(E_p,E_k)$ and $W_-(E_p,E_k)$ are given by the Fermi golden rule

$$\begin{aligned} W_+(E_p,E_k) &= 2\pi |\langle E_p,+| H_T |N+1,E_k\rangle|^2 \delta(E_p+\omega_+-E_k), \\ W_-(E_p,E_k) &= 2\pi |\langle E_p,-| H_T |N+1,E_k\rangle|^2 \delta(E_p+\omega_--E_k) \end{aligned} \quad (3.16)$$

with $\omega_\pm$ of Eq. (2.4). The matrix elements $\langle E_p,\pm| H_T |N+1,E_k\rangle$ were calculated in the previous chapter, see Eq. (2.23),

$$\begin{aligned} W_+(E_p,E_k) &= \pi|t_{pk}|^2\left(1+\frac{\xi_p\xi_k+\Delta^2}{E_pE_k}\right)\delta(E_p+\omega_+-E_k), \\ W_-(E_p,E_k) &= \pi|t_{pk}|^2\left(1+\frac{\xi_p\xi_k-\Delta^2}{E_pE_k}\right)\delta(E_p+\omega_--E_k). \end{aligned} \quad (3.17)$$

Now we may relate tunneling matrix elements to the normal-state junction conductance

$$g_T = 8\pi^2 \sum_{p,k} |t_{pk}|^2 \delta(\xi_p)\delta(\xi_k).$$

Assuming that tunnel matrix elements t_{pk} are weakly dependent on the energies ξ_k, ξ_p, we can rewrite Eq. (3.17) in terms of the dimensionless conductance:

$$\begin{aligned} W_+(E_p,E_k) &= \frac{g_T\delta_r\delta_b}{8\pi}\left(1+\frac{\xi_p\xi_k+\Delta^2}{E_pE_k}\right)\delta(E_p+\omega_+-E_k), \\ W_-(E_p,E_k) &= \frac{g_T\delta_r\delta_b}{8\pi}\left(1+\frac{\xi_p\xi_k-\Delta^2}{E_pE_k}\right)\delta(E_p+\omega_--E_k), \end{aligned} \quad (3.18)$$

where $\delta_{r(b)}$ is the mean level spacing in the reservoir(box), $\delta_{r(b)} = (\nu_F V_{r(b)})^{-1}$ with ν_F being single-spin electron density of states at the Fermi level in the reservoir (box).

The system of equations for the diagonal part of the density matrix describes the evolution of the populations, and follows from Eq. (3.14). From now on we

adopt the short-hand notation for the diagonal elements of the density matrix $\langle s|\,\rho(t)\,|s\rangle = P_{ss}(E_s,t)$. In particular, we denote the probability of the qubit to be in the state $|+\rangle$ or in the state $|-\rangle$ and a quasiparticle to have energy E_p as $P_{++}(E_p,t)$ or $P_{--}(E_p,t)$, respectively; the probability $P_{\rm o}(E_k,t)$ corresponds to the state with a quasiparticle residing in the CPB and having energy E_k. In these notations the system of equations describing the dynamics of the populations for the states $|+,E_p\rangle$, $|-,E_p\rangle$ or $|N{+}1,E_k\rangle$ can be written as

$$\dot{P}_{++}(E_p,t)+\sum_k W_{+}(E_p,E_k)\left[P_{++}(E_p,t)-P_{\rm o}(E_k,t)\right]=0, \tag{3.19a}$$

$$\dot{P}_{--}(E_p,t)+\sum_k W_{-}(E_p,E_k)\left[P_{--}(E_p,t)-P_{\rm o}(E_k,t)\right]=0, \tag{3.19b}$$

$$\begin{aligned}\dot{P}_{\rm o}(E_k,t)\;+\;&\sum_p\left[W_{+}(E_p,E_k)+W_{-}(E_p,E_k)\right]P_{\rm o}(E_k,t)-\\ -\;&\sum_p\left[W_{+}(E_p,E_k)P_{++}(E_p,t)+W_{-}(E_p,E_k)P_{--}(E_p,t)\right]=0.\end{aligned} \tag{3.19c}$$

Here we neglected the contribution of the coherences. This is justified as long as $P_{+-}(E_p,0)=0$ in the initial moment of time, and the two parameters $\Gamma_{\rm out}/E_J$ and $\Gamma_{\rm in}/E_J$, are small. The transition rates in Eqs. (3.19) are given by the Fermi golden rule, see Eqs. (3.16).

At the end, experimentally observable quantities can be obtained from P_{ij} by taking the proper trace over the quasiparticle degrees of freedom

$$\sigma_{ij}(t)=\sum_p P_{ij}(E_p,t), \tag{3.20}$$

where $i,j=+,-$. This completes the derivation of the master equations without quasiparticle relaxation, and we proceed to the solution of these equations.

3.3 Evolution of the qubit coherences

We now discuss the solution for the off-diagonal elements of the density matrix. We assume that initially the qubit and quasiparticle are independent; the quasiparticle is in thermal equilibrium in the reservoir, and the qubit is prepared in a superposition state with $\sigma_{+-}(0) \neq 0$:

$$P_{+-}(E_p, 0) = \rho_{\rm odd}(E_p)\sigma_{+-}(0) \neq 0, \tag{3.21}$$

where $\rho_{\rm odd}(E_p)$ is the equilibrium distribution function with an odd number of electrons in reservoir at temperature $T \ll \Delta$,

$$\rho_{\rm odd}(E_p) = \frac{\exp\left(-E_p/T\right)}{Z_{\rm odd}}. \tag{3.22}$$

The normalization factor $Z_{\rm odd}$ here is

$$Z_{\rm odd} = \sum_p \exp\left(-\frac{E_p}{T}\right) = \frac{\sqrt{2\pi T\Delta}}{\delta_r}\exp\left(-\frac{\Delta}{T}\right).$$

The solution of Eq. (3.15) is straightforward. After tracing out quasiparticle degrees of freedom we obtain

$$\sigma_{+-}(t) = \sigma_{+-}(0)\sum_p \rho_{\rm odd}(E_p)\exp\left(-iE_{_J}t - \frac{1}{2}\Gamma_{\rm in}(E_p)t\right), \tag{3.23}$$

where $\Gamma_{\rm in}(E_p)$ is given by

$$\begin{aligned}\Gamma_{\rm in}(E_p) &= \sum_k \left[W_{+}(E_p, E_k) + W_{-}(E_p, E_k)\right] = \\ &= \frac{g_{_T}\delta_r}{4\pi}\left(\nu(E_p+\omega_+)\left(1+\frac{\Delta^2}{E_p(E_p+\omega_+)}\right)+\nu(E_p+\omega_-)\left(1-\frac{\Delta^2}{E_p(E_p+\omega_-)}\right)\right).\end{aligned} \tag{3.24}$$

In the low-temperature limit $T \ll \omega_-, \omega_+$, the expression for $\sigma_{+-}(t)$ can be simplified

$$\sigma_{+-}(t) = \sigma_{+-}(0)\exp\left(-iE_{_J}t - \frac{t}{T_2}\right). \tag{3.25}$$

Here the phase relaxation time T_2 is given by

$$\frac{1}{T_2} = \frac{g_T \delta_r}{8\pi} \left(\sqrt{\frac{2\Delta + \omega_+}{\omega_+}} + \sqrt{\frac{\omega_-}{2\Delta + \omega_-}} \right). \tag{3.26}$$

The decay of qubit coherences is determined by the rate of quasiparticle tunneling into the box as previously discussed in Sec. 3.1. This result remains valid also in the presence of quasiparticle relaxation. On the contrary, the evolution of the diagonal parts of the density matrix P_{++} and P_{--}, depends strongly on the relaxation of the quasiparticles. We will study this evolution with and without quasiparticle relaxation in the next sections.

3.4 Kinetics of the qubit populations without quasiparticle relaxation

The evolution of the diagonal elements of the density matrix is described by Eq. (3.19). We will assume that initially the qubit is prepared in the state $|+\rangle$, and the quasiparticle resides in the reservoir. As explained in Sec. 3.1 tunneling out of the box ($\sim\Gamma_{\rm out}$) is much faster than tunneling in ($\sim\Gamma_{\rm in}$) due to the differences in the volumes of the CPB and the reservoir. In fact, for a sufficiently small box, $1/\Gamma_{\rm out}$ is the shortest time scale in the system of Eqs. (3.19). Therefore, we may neglect term $\partial_t P_{\rm o}(E_k,t)$ in Eq. (3.19c); *i.e.*, the value of $P_{\rm o}(E_k,t)$ follows instantaneously the time variations of $P_{++}(E_p,t)$ and $P_{--}(E_p,t)$. This greatly simplifies the system of equations for the populations. The solution for $P_{\rm o}(E_k,t)$ in this approximation is

$$P_{\rm o}(E_k,t) = \frac{\sum_p W_+(E_p,E_k) P_{++}(E_p,t)}{\sum_{p''} \left[W_+(E_{p''},E_k) + W_-(E_{p''},E_k) \right]} + \frac{\sum_p W_-(E_p,E_k) P_{--}(E_p,t)}{\sum_{p''} \left[W_+(E_{p''},E_k) + W_-(E_{p''},E_k) \right]}. \tag{3.27}$$

After substituting this expression back into Eqs. (3.19a) and (3.19b), we obtain effective rate equations for the qubit in the presence of an unpaired electron in

the superconducting parts

$$\begin{aligned}\dot{P}_{++}(E_p,t) \;+\; \gamma_+(E_p)P_{++}(E_p,t)-\gamma_+(E_p)P_{--}(E_p+E_J,t)=0,\\ \dot{P}_{--}(E_p,t) \;+\; \gamma_-(E_p)P_{--}(E_p,t)-\gamma_-(E_p)P_{++}(E_p-E_J,t)=0\end{aligned} \tag{3.28}$$

with $\gamma_\pm(E_p)$ having the form

$$\begin{aligned}\gamma_+(E_p) \;&=\; \sum_{p',k}\frac{W_+(E_p,E_k)W_-(E_{p'},E_k)}{\sum_{p''}[W_+(E_{p''},E_k)+W_-(E_{p''},E_k)]},\\ \gamma_-(E_p) \;&=\; \sum_{p',k}\frac{W_-(E_p,E_k)W_+(E_{p'},E_k)}{\sum_{p''}[W_+(E_{p''},E_k)+W_-(E_{p''},E_k)]}.\end{aligned} \tag{3.29}$$

This structure of the transition rates reflects the nature of the transitions involving an intermediate state $|N+1,E_k\rangle$. The normalization condition

$$\sum_p[P_{++}(E_p,t)+P_{--}(E_p,t)]=1 \tag{3.30}$$

is preserved under evolution. This can be checked directly with the help of Eqs. (3.28) and the following relation for the rates:

$$\sum_p\gamma_+(E_p)X(E_p)=\sum_p\gamma_-(E_p)X(E_p-E_J) \tag{3.31}$$

(here $X(E_p)$ is an arbitrary smooth function of E_p).

Let us discuss the solution of the Eqs. (3.28). In the initial moment of time the qubit and quasiparticle are uncorrelated; the qubit is prepared in the excited state $|+\rangle$ and quasiparticle can be described by the equilibrium distribution function $\rho_{\rm odd}(E_p)$:

$$P_{++}(E_p,0)=\rho_{\rm odd}(E_p)\quad\text{and}\quad P_{--}(E_p+E_J,0)=0. \tag{3.32}$$

Upon solving Eqs. (3.28), we find expressions for the populations of the qubit

levels

$$\sigma_{++}(t) = \sum_p \frac{\rho_{\rm odd}(E_p)\gamma_-(E_p+E_J)}{\gamma_-(E_p+E_J)+\gamma_+(E_p)} + \sum_p \frac{\rho_{\rm odd}(E_p)\gamma_+(E_p)}{\gamma_-(E_p+E_J)+\gamma_+(E_p)} \exp\left(-\Gamma(E_p)t\right),$$

$$\begin{aligned}\sigma_{--}(t) &= \sum_p \frac{\rho_{\rm odd}(E_p-E_J)\gamma_-(E_p)}{\gamma_-(E_p)+\gamma_+(E_p-E_J)} \\ &- \sum_p \frac{\rho_{\rm odd}(E_p-E_J)\gamma_-(E_p)}{\gamma_-(E_p)+\gamma_+(E_p-E_J)} \exp\left(-\Gamma(E_p-E_J)t\right),\end{aligned} \tag{3.33}$$

where $\Gamma(E_p)$ is defined as

$$\Gamma(E_p) = \gamma_+(E_p) + \gamma_-(E_p+E_J). \tag{3.34}$$

In the low-temperature limit, we calculate the sums in Eq. (3.33) assuming $\Delta > \omega_+ > E_J \gg T$ to find

$$\sum_p \frac{\gamma_+(E_p)\rho_{\rm odd}(E_p)}{\Gamma(E_p)} \approx \sqrt{\frac{T}{\pi E_J}}, \tag{3.35}$$

and

$$\begin{aligned}\sigma_{++}(t) &= 1 - \sqrt{\frac{T}{\pi E_J}} + \sqrt{\frac{T}{\pi E_J}} \exp\left[-\frac{t}{T_1^*}\right], \\ \sigma_{--}(t) &= \sqrt{\frac{T}{\pi E_J}} \left(1 - \exp\left[-\frac{t}{T_1^*}\right]\right).\end{aligned} \tag{3.36}$$

The relaxation time T_1^* is defined as

$$\frac{1}{T_1^*} \approx \frac{g_T \delta_r}{4\pi} \sqrt{\frac{\omega_+}{2\Delta+\omega_+}} \left(1 + \frac{E_J}{\omega_+}\right). \tag{3.37}$$

In deriving this expression we assumed $E_J/\Delta \ll 1$ and kept only the leading terms.

The solution for the populations in this case (no quasiparticle relaxation, $\tau = \infty$) show that final qubit populations are determined by the tunneling rates, which, in turn, depend on the superconducting DOS at different energies $\nu(E_p)$

and $\nu(E_p+E_J)$. Since the states with higher DOS are more favorable, the quasiparticle can be found most of the time with energy close to Δ and rarely with energy $\Delta + E_J$. Therefore, at low temperatures $T \ll E_J$, the qubit will mostly remain in the excited state $|+\rangle$. The probability to find the qubit in the ground state is proportional to $\sim \sqrt{T/E_J}$ and thus is small, see Sec. 3.1. As soon as we include mechanisms of quasiparticle relaxation into consideration, the qubit populations will eventually reach equilibrium. In the next sections we investigate the equilibration of the qubit.

3.5 Kinetics of the Qubit populations with quasiparticle relaxation in the reservoir

3.5.1 Master equations with quasiparticle relaxation

In this section we consider a more realistic model by incorporating the mechanisms of quasiparticle relaxation into the rate equations. Such mechanisms were studied in the context of non-equilibrium superconductivity [46, 47]. In aluminum, a typical superconductor used in charge qubits, the dominant mechanism of quasiparticle relaxation is due to inelastic electron-phonon scattering. The relaxation time depends on the excess energy ε of a quasiparticle [46]

$$\frac{1}{\tau(\varepsilon)} = \frac{1}{\tau_0}\frac{64\sqrt{2}}{105}\left(\frac{\Delta}{T_c}\right)^3\left(\frac{\varepsilon}{\Delta}\right)^{7/2}, \tag{3.38}$$

where $\varepsilon = E_p - \Delta \ll \Delta$, and τ_0 is characteristic parameter defining electron-phonon scattering rate at $T = T_c$ (here T_c is superconducting transition temperature). For typical excess energies of the order of $E_J \sim 0.3$ K, the estimate for τ yields quite long relaxation time $\tau \sim 10^{-5} - 10^{-4}$ s.

The procedure developed in Sec. 3.2 allows us to include the mechanisms of quasiparticle relaxation into the master equations. One can start by writing an

equation of motion for the density matrix that includes the qubit, quasiparticle, and phonons, then expand the density matrix in the small coupling parameter - electron-phonon interaction as discussed in Sec. 3.2. Finally, one should trace out phonon degrees of freedom and obtain master equations for the qubit with quasiparticle relaxation. We will skip the cumbersome derivation and present only the results here. In the relaxation time approximation the collision integral has the form

$$\mathcal{I}_{\pm} = -\frac{1}{\tau}\left(P_{\pm\pm}(E_p,t) - \overline{P}_{\pm\pm}(E_p,t)\right), \tag{3.39}$$

where $\tau = \tau(\varepsilon \sim E_J)$. The probability $\overline{P}_{\pm\pm}(E_p,t)$ is proportional to the equilibrium distribution function of a quasiparticle $\rho_{\rm odd}(E_p)$ and the proper qubit population $\sigma_{\pm\pm}(t)$:

$$\overline{P}_{\pm\pm}(E_p,t) = \rho_{\rm odd}(E_p)\sum_p P_{\pm\pm}(E_p,t). \tag{3.40}$$

The form of $\overline{P}_{\pm\pm}(E_p,t)$ is dictated by the fact that phonons equilibrate the quasiparticle only, without affecting directly the qubit states. [8] The collision integral Eq. (3.39) replaces zero in the right-hand sides of Eqs. (3.19a) and (3.19b). However, Eq. (3.19c) for $P_{\rm o}(E_k,t)$ remains unchanged due to the short dwell time of a quasiparticle in the box (we assume that $\tau(\varepsilon\sim\omega_+) \gg \Gamma_{\rm out}^{-1}$, but set no constraints on $\tau\Gamma_{\rm in}$). Then, the system of Eqs. (3.28) for populations can be written as

$$\begin{aligned}
\dot{P}_{++}(E_p,t) \;+\; & \gamma_+(E_p)P_{++}(E_p,t) - \gamma_+(E_p)P_{--}(E_p+E_J,t) = \\
& -\frac{1}{\tau}\left(P_{++}(E_p,t) - \overline{P}_{++}(E_p,t)\right), \\
\dot{P}_{--}(E_p,t) \;+\; & \gamma_-(E_p)P_{--}(E_p,t) - \gamma_-(E_p)P_{++}(E_p-E_J,t) = \\
& -\frac{1}{\tau}\left(P_{--}(E_p,t) - \overline{P}_{--}(E_p,t)\right)
\end{aligned} \tag{3.41}$$

[8] We do not consider here qubit relaxation originating from the excitation of phonons by charge fluctuations across the Josephson junction [50]. The presence of a quasiparticle opens a relaxation channel that is faster than the mechanism considered in Ref. [50].

with the effective transition rates $\gamma_{\pm}(E_p)$ defined in Eq. (3.29). The obtained system of integro-differential equations (3.41) for $P_{\pm\pm}(E_p,t)$ describes the effect of quasiparticle relaxation on the dynamics of the qubit.

We solve Eqs. (3.41) first in the simple case of a short relaxation time ($\tau \ll \Gamma_{\rm in}^{-1}$). Under these assumptions, we can seek the solution in the form

$$P_{\pm\pm}(E_p,t) = \rho_{\rm odd}(E_p)\ \sigma_{\pm\pm}(t), \tag{3.42}$$

with $\sigma_{\pm\pm}(t)$ defined in Eq. (3.20), so that $P_{\pm\pm}(E_p,t) = \overline{P}_{\pm\pm}(E_p,t)$. Using this ansatz and performing the appropriate summation, Eqs. (3.41) reduce to the well-known Bloch-Redfield equations

$$\begin{aligned}
\dot\sigma_{++}(t) \quad &+ \quad \sum_p \gamma_+(E_p)\rho_{\rm odd}(E_p)\sigma_{++}(t) - \sum_p \gamma_+(E_p)\rho_{\rm odd}(E_p+E_J)\sigma_{--}(t) = 0, \\
\dot\sigma_{--}(t) \quad &+ \quad \sum_p \gamma_-(E_p)\rho_{\rm odd}(E_p)\sigma_{--}(t) - \sum_p \gamma_-(E_p)\rho_{\rm odd}(E_p-E_J)\sigma_{++}(t) = 0.
\end{aligned} \tag{3.43}$$

Utilizing the property of the rates Eq. (3.31), one can simplify the equations above,

$$\begin{aligned}
\dot\sigma_{++}(t) \quad &+ \quad \left\langle\gamma_+\right\rangle \sigma_{++}(t) = \left\langle\gamma_-\right\rangle \sigma_{--}(t), \\
\dot\sigma_{--}(t) \quad &+ \quad \left\langle\gamma_-\right\rangle \sigma_{--}(t) = \left\langle\gamma_+\right\rangle \sigma_{++}(t),
\end{aligned} \tag{3.44}$$

where thermal-averaged transition rates $\left\langle\gamma_+\right\rangle$ and $\left\langle\gamma_-\right\rangle$ are

$$\begin{aligned}
\left\langle\gamma_+\right\rangle &= \sum_p \gamma_+(E_p)\rho_{\rm odd}(E_p), \\
\left\langle\gamma_-\right\rangle &= \sum_p \gamma_-(E_p)\rho_{\rm odd}(E_p).
\end{aligned} \tag{3.45}$$

One can also check that due to the relation (3.31) rates $\left\langle\gamma_\pm\right\rangle$ comply with the detailed balance requirement

$$\frac{\left\langle\gamma_+\right\rangle}{\left\langle\gamma_-\right\rangle} = \exp\left(\frac{E_J}{T}\right).$$

For the initial conditions: $\sigma_{++}(0) = 1$, $\sigma_{--}(0) = 0$, the solution for populations is

$$\sigma_{++}(t) = \frac{e^{-E_J/T}}{1+e^{-E_J/T}} + \frac{e^{-(\langle\gamma_+\rangle+\langle\gamma_-\rangle)t}}{1+e^{-E_J/T}},$$

$$\sigma_{--}(t) = \frac{1}{1+e^{-E_J/T}}\left[1 - e^{-(\langle\gamma_+\rangle+\langle\gamma_-\rangle)t}\right]. \tag{3.46}$$

In the low-temperature limit ($T \ll E_J < \omega_+ < \Delta$) we find a simple form for the effective rates $\langle\gamma_\pm\rangle$ in the leading order in T/Δ and E_J/Δ:

$$\begin{aligned}\langle\gamma_-\rangle &= \frac{g\delta_r}{4\pi}\sqrt{\frac{\omega_+}{2\Delta+\omega_+}}\left(1+\frac{E_J}{\omega_+}\right)\sqrt{\frac{T}{\pi E_J}}\exp\left(-\frac{E_J}{T}\right),\\ \langle\gamma_+\rangle &= \frac{g\delta_r}{4\pi}\sqrt{\frac{\omega_+}{2\Delta+\omega_+}}\left(1+\frac{E_J}{\omega_+}\right)\sqrt{\frac{T}{\pi E_J}}.\end{aligned} \tag{3.47}$$

Factors of $\sqrt{T/\pi E_J}$ in the rates can be interpreted as the probability of flipping the qubit ($|+\rangle \to |-\rangle$), which is mainly determined by the ratio of the DOS of quasiparticles at energies $\nu(E_p)$ and $\nu(E_p+E_J)$, respectively (see the discussion in Sec. 3.1). We would like to point out here that energy relaxation rate $\langle\gamma_+\rangle + \langle\gamma_-\rangle$ is smaller than the phase relaxation rate by a factor of $\sqrt{T/\pi E_J}$.

3.5.2 General solution for the qubit populations in the relaxation time approximation

In this section we find the solution of Eqs. (3.41) at an arbitrary value of $\Gamma_{\rm in}\tau$. In order to find the solution for the qubit populations we will use Laplace transform

$$P(E_p, s) = \int_0^\infty dt P(E_p, t) e^{-st}, \tag{3.48}$$

and reduce the system of differential equations (3.41) supplied with the initial conditions Eq. (3.32) to the system of algebraic equations:

$$\begin{aligned} sP_{++}(E_p,s) \;-\; & \rho_{\rm odd}(E_p)+\gamma_+(E_p)P_{++}(E_p,s)-\gamma_+(E_p)\widetilde{P}_{--}(E_p,s) \\ = \; & -\frac{1}{\tau}\left(P_{++}(E_p,s)-\overline{P}_{++}(E_p,s)\right), \end{aligned} \tag{3.49}$$

$$\begin{aligned} s\widetilde{P}_{--}(E_p,s) \;+\; & \widetilde{\gamma}_-(E_p)\widetilde{P}_{--}(E_p,s)-\widetilde{\gamma}_-(E_p)P_{++}(E_p,s)= \\ = \; & -\frac{1}{\tau}\left(\widetilde{P}_{--}(E_p,s)-\overline{\widetilde{P}}_{--}(E_p,s)\right). \end{aligned}$$

Here tilde denotes the shift by E_J of the energy argument in a function, *e.g.* $\widetilde{P}_{--}(E_p,s) = P_{--}(E_p+E_J,s)$. The system of algebraic equations (3.49) can be solved for $P_{++}(E_p,s)$ and $P_{--}(E_p,s)$. Then, by summing these expressions over the momenta p and utilizing Eq. (3.40) we obtain a closed system of equations for qubit populations $\sigma_{\pm\pm}(s)$:

$$\begin{aligned} \sigma_{++}(s) \;&=\; A(s)+\frac{A(s)}{\tau}\sigma_{++}(s)+\frac{B(s)}{\tau}\sigma_{--}(s), \\ \\ \sigma_{--}(s) \;&=\; C(s)+\frac{C(s)}{\tau}\sigma_{++}(s)+\frac{D(s)}{\tau}\sigma_{--}(s), \end{aligned} \tag{3.50}$$

where the coefficients $A(s)$, $B(s)$, $C(s)$ and $D(s)$ are

$$\begin{aligned} A(s) \;&=\; \frac{1-Z(s)}{s+1/\tau}, \quad B(s)=\frac{Z(s)e^{-E_J/T}}{s+1/\tau}, \\ C(s) \;&=\; \frac{Z(s)}{s+1/\tau}, \quad D(s)=\frac{1-Z(s)e^{-E_J/T}}{s+1/\tau}. \end{aligned} \tag{3.51}$$

The function $Z(s)$ is given by

$$Z(s)=\sum_p \frac{\gamma_+(E_p)\rho_{\rm odd}(E_p)}{s+1/\tau+\Gamma(E_p)} \tag{3.52}$$

with $\gamma_+(E_p)$ and $\Gamma(E_p)$ being defined in Eqs. (3.16), (3.29) and (3.34), respectively. From now on we take thermodynamic limit and replace the sum by the integral in Eq. (3.52). (Thermodynamic limit is appropriate here, since $\delta_r \ll T$.)

$$Z(s)=\frac{2}{\delta_r}\int_\Delta^\infty dE_p\nu(E_p)\frac{\gamma_+(E_p)\rho_{\rm odd}(E_p)}{s+1/\tau+\Gamma(E_p)}. \tag{3.53}$$

The solution of Eqs. (3.50) yields the following results for $\sigma_{\pm\pm}(s)$:

$$\sigma_{++}(s) = \frac{1}{s}\left(1 - \frac{(\tau s+1)Z(s)}{\tau s + Z(s)(1+e^{-E_J/T})}\right),$$

$$\sigma_{--}(s) = \frac{1}{s}\frac{(\tau s+1)Z(s)}{\tau s + Z(s)(1+e^{-E_J/T})}. \tag{3.54}$$

Equations (3.54) allow us to analyze the dynamics of the qubit populations for arbitrary $\Gamma_{\rm in}\tau$. Let us point out that Eqs. (3.54) satisfy normalization condition $\sigma_{++}(s)+\sigma_{--}(s) = 1/s$. To find the evolution of the populations, it is sufficient to evaluate $\sigma_{++}(t)$.

The inverse Laplace transform is given by

$$\sigma_{++}(t) = \frac{1}{2\pi i}\int_{\eta-i\infty}^{\eta+i\infty} ds\, \sigma_{++}(s)e^{st}, \tag{3.55}$$

where η is chosen in such way that $\sigma_{++}(s)$ is analytic at $\mathrm{Re}[s] > \eta$. The integral (3.55) can be calculated using complex variable calculus by closing the contour of integration as shown in Fig. 3.3 and analyzing the enclosed points of nonanalytic behavior of $\sigma_{++}(s)$. In general, the singularities of $\sigma_{++}(s)$ consist of two poles and a cut. The latter is due to the singularities of the function $Z(s)$ causing $\sigma_{++}(s)$ to be nonanalytic along the cut $s \in (s_{\min}, s_{\max})$, where

$$s_{\min} = -\frac{1}{\tau} - \max\left[\,\Gamma(E_p)\,\right],$$
$$s_{\max} = -\frac{1}{\tau} - \min\left[\,\Gamma(E_p)\right].$$

The schematic plot of $\Gamma(E_p)$ is shown in Fig. C.1.

In addition to the cut, $\sigma_{++}(s)$ has 2 poles. The first one is at $s_1 = 0$; the second s_2 is the solutions of the following equation in the region of analyticity of the function $Z(s)$:

$$\tau s + Z(s)\left(1+e^{-E_J/T}\right) = 0. \tag{3.56}$$

The preceding discussion of the analytic properties of $\sigma_{++}(s)$ is general for any ratio of the relaxation time τ and quasiparticle escape rate $\Gamma_{\rm in}$. However, the

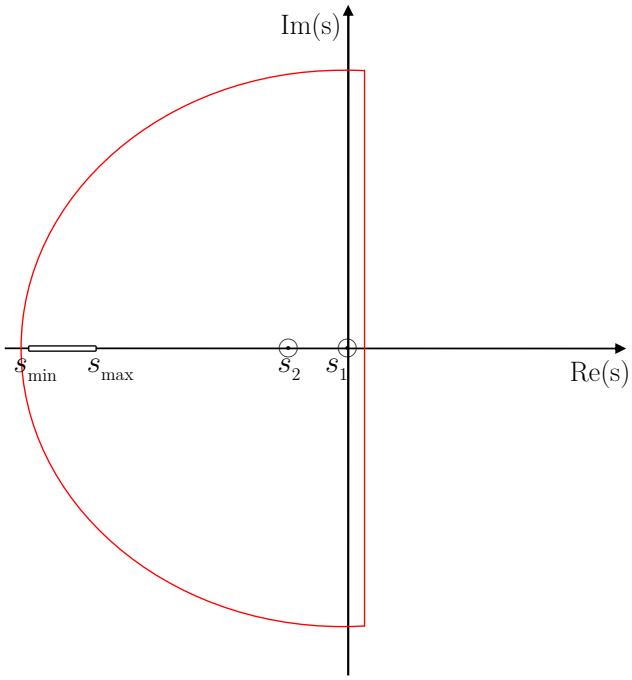

Figure 3.3: Contour of integration (red line) chosen to calculate inverse Laplace transform, see Eq. (3.55). Points of nonanalytic behavior of $\sigma_{++}(s)$ are shown. (Poles at s_1, s_2, and a cut $s \in (s_{\min}, s_{\max})$).

location of the singularities and their contribution to the integral (3.55) depends on $\Gamma_{\text{in}}\tau$. Below we briefly present results for two cases of interest: fast ($\Gamma_{\text{in}}\tau \ll 1$) and slow ($\Gamma_{\text{in}}\tau \gg 1$) quasiparticle relaxation. The detailed analysis of the singularities of $\sigma_{++}(s)$ is given in the Appendix C.

In the fast relaxation regime ($\Gamma_{\text{in}}\tau \ll 1$), the contributions from the cut is small (proportional to $\Gamma_{\text{in}}\tau$, see Appendix C) and thus can be neglected. Then, relevant poles of $\sigma_{++}(s)$ in this limit are

$$s_1 = 0,\ s_2 = -\left\langle \gamma_+ \right\rangle - \left\langle \gamma_- \right\rangle . \tag{3.57}$$

The integration of Eq. (3.55) yields, up to corrections vanishing in the limit $\Gamma_{\text{in}}\tau \ll 1$, Eqs. (3.46) for the populations.

In the slow relaxation case, $\Gamma_{\text{in}}\tau \gg 1$, the main contribution to the integral (3.55) comes from the cut, and poles $s_1 = 0$ and s_2. The latter may be found

by iterative solution of Eq. (3.56),

$$s_2 = -\frac{Z(0)}{\tau}\left(1+e^{-E_J/T}\right),$$

where function $Z(0)$ is defined in Eq. (3.53), and in the case of slow relaxation can be approximated as

$$Z(0) = \frac{2}{\delta_r}\int_\Delta^\infty dE_p \nu(E_p)\frac{\gamma_+(E_p)}{\Gamma(E_p)}\rho_{\rm odd}(E_p). \tag{3.58}$$

Taking integral in Eq. (3.55) along the contour enclosing the cut shown in Fig. 3.3, and accounting for poles s_1 and s_2, we find

$$\begin{aligned}\sigma_{++}(t) = &\frac{e^{-E_J/T}}{1+e^{-E_J/T}} + \left(\frac{1}{1+e^{-E_J/T}} - Z(0)\right)\exp\left(-Z(0)\left(1+e^{-E_J/T}\right)\frac{t}{\tau}\right) + \\ &+ \frac{2}{\delta_r}\int_\Delta^\infty dE_p \nu(E_p)\frac{\gamma_+(E_p)\rho_{\rm odd}(E_p)}{\Gamma(E_p)}\exp(-\Gamma(E_p)\,t)\,.\end{aligned} \tag{3.59}$$

Here we neglected the corrections to Eq. (3.59) of the order $1/\Gamma_{\rm in}\tau$. The obtained expression for $\sigma_{++}(t)$ describes the kinetics of the qubit populations in the slow relaxation regime. Note that the solution Eq. (3.59) satisfies initial conditions $\sigma_{++}(0) = 1$ and is consistent with previous results. Indeed, in the limit $\tau \to \infty$, the exponent in the second term goes to zero and we recover Eq. (3.33) (To show this one should use Eq. (3.31)).

Equation (3.59) becomes physically transparent in the low-temperature limit. Using the approximation (3.35) for $Z(0)$ and for the integral in the last term of Eq. (3.59) we find

$$\sigma_{++}(t) \;=\; \frac{e^{-E_J/T}}{1+e^{-E_J/T}} + \sqrt{\frac{T}{\pi E_J}}\exp\left(-\frac{t}{T_1^*}\right) + \left(\frac{1}{1+e^{-E_J/T}} - \sqrt{\frac{T}{\pi E_J}}\right)\exp\left(-\frac{t}{T_1}\right), \tag{3.60}$$

where relaxation times T_1 and T_1^* are

$$\frac{1}{T_1} = \frac{1}{\tau}\sqrt{\frac{T}{\pi E_J}} \text{ and } \frac{1}{T_1^*} = \frac{g_T\delta_r}{4\pi}\sqrt{\frac{\omega_+}{2\Delta+\omega_+}}\left(1+\frac{E_J}{\omega_+}\right). \tag{3.61}$$

Obtained results describe the relaxation of the qubit populations in the slow relaxation limit ($\Gamma_{\rm in}\tau \gg 1$) discussed qualitatively in Sec. 3.1. According to Eq. (3.60), the process of equilibration of qubit populations in this case occurs in two stages. The first stage ($t \sim T_1^*$) corresponds to a quasistationary state formation with qubit populations much larger than equilibrium ones. For the typical experimental temperatures $T \sim 20$ mK, the excited state population of the qubit is about 85%. The equilibrium populations are established in the second stage, on the time scale of T_1. The relaxation time T_1 sets an important experimental constraint on the frequency of repetition of qubit experiments.

We estimate now energy and phase relaxation times for the realistic experimental parameters [6, 12]: $\Delta \approx 2K$, $E_c \approx 0.5K$, $E_J \approx 0.3K$, $g_T \sim 1$, and $T \approx 20mK$. For the volume of the reservoir $10^{-19} - 10^{-17}m^3$, Eq. (3.26) yields the phase relaxation time $T_2 \sim 10^{-5} - 10^{-3}s$. Energy relaxation depends on the relation between Γ_{in} and $1/\tau$. Taking $\tau \sim 10^{-4}s$ and $\Gamma_{in}^{-1} \sim 10^{-5}s$, which corresponds to the lower end of the volume range, energy relaxation is described by Eq. (3.60) with $T_1^* \sim 10^{-5}s$ and $T_1 \sim 10^{-3}s$.

We considered so far the effect of a single quasiparticle on the qubit kinetics. It is possible to generalize our results onto the case of many quasiparticles $N_{\rm qp}$ residing in the system. In this case T_2 becomes shorter since the quasiparticle tunneling rate $\Gamma_{\rm in}$, see Eq. (3.1), should be multiplied by the number of quasiparticles in the superconducting reservoir

$$\frac{1}{T_2} \simeq \Gamma_{\rm in} \cdot N_{\rm qp} \simeq \frac{g_{\rm T} n_{\rm qp}}{4\pi\nu_F}. \tag{3.62}$$

Note that the volume of the reservoir does not enter in Eq. (3.62). A finite density of quasiparticles in the reservoir affects also the process of energy relaxation of the qubit. The most clear example corresponds to the limit $\Gamma_{\rm in}\tau \ll 1$ in which quasiparticle relaxation in the reservoir occurs fast compared to the time needed for the quasiparticle to reenter the CPB. In this limit $T_1/T_2 \sim \sqrt{E_J/T}$.

The comparison of the theoretical prediction for T_2 and T_1 with experimental

data is complicated by the unknown value of $N_{\rm qp}$ in a qubit. The quasiparticle density in a system with a massive lead is known to deviate from the equilibrium value in a number of experiments [31, 51]. The estimate of $n_{\rm qp}$ can be obtained from the kinetics of "quasiparticle poisoning" studied in the recent experiments [36, 37]. The observed rate of quasiparticle entering the CPB was $10^5 - 10^4$ Hz. Assuming that the bottleneck for the quasiparticles was tunneling through the junction (rather than the diffusion in the lead), we estimate the density of quasiparticles in the lead to be $n_{\rm qp} \sim 10^{19} - 10^{18}\,{\rm m}^{-3}$. The same quasiparticle density in a qubit with the reservoir volume $10^{-19} - 10^{-17} m^3$ would result in $N_{\rm qp} \sim 1 - 100$.

3.6 Conclusion

We studied the kinetics of a superconducting charge qubit in the presence of an unpaired electron. The presence of a quasiparticle in the system leads to the decay of quantum oscillations. We obtained master equations for the coherences and populations of the qubit, which take into account energy exchange between the quasiparticle and the qubit, and include the mechanisms of quasiparticle relaxation due to electron-phonon interaction. Finally, we found decay exponents governing the dynamics of the qubit for different cases: fast and slow quasiparticle relaxation in the reservoir.

We have shown that phase relaxation is determined by the quasiparticle tunneling rate to the box $\Gamma_{\rm in} \sim g_{_T}\delta_r/4\pi$. Kinetics of the qubit populations depends on the ratio of the quasiparticle relaxation time τ and escape time $\Gamma_{\rm in}^{-1}$. In this Chapter, we considered two limits - fast ($\tau\Gamma_{\rm in} \ll 1$) and slow ($\tau\Gamma_{\rm in} \gg 1$) quasiparticle relaxation. In the latter case, the decay of qubit populations occurs in two stages. In the first stage at $t \sim \Gamma_{\rm in}^{-1}$ a quasistationary regime is established with large nonequilibrium excited state population. The second stage describes

the attainment of the equilibrium populations and occurs on the time scale of $\tau\sqrt{\pi E_J/T}$. In the fast relaxation case, equilibrium qubit populations are established at $t \sim \Gamma_{\rm in}^{-1}\sqrt{\pi E_J/T}$.

Chapter 4

Statistics of charge fluctuations

4.1 Introduction

In this Chapter we study the statistics of charge fluctuations induced by quasiparticles in time domain.

Properties of mesoscopic superconducting circuits may depend crucially on the presence of quasiparticles in its elements. The operation of the most superconducting single-charge devices, such as Cooper-pair box qubit and single Cooper-pair transistor, require two-electron periodicity of its charge states [31–33, 35–38]. This periodicity may be interrupted by the entrance of an unpaired electron into the Cooper-pair box resulting in the shift of its charge state from even to odd. Such quasiparticle tunneling, often referred to as "quasiparticle poisoning", can degrade the performance of these superconducting circuits causing their operating point to shift stochastically on the scale comparable to the measurement time. For a typical CPB size and tunnel conductances of the order of unit quantum, the quasiparticle dwell times are of the order of a few μs. This time scale is at the edge of accessibility for the modern experiments [52]. Individual quasiparticle tunneling events were resolved and the statistics of quasiparticle entrances and exists from CPB box was investigated in Refs. [37, 38].

The observed statistics of entrances was well described by a standard Poissonian process [37, 38]. For the quasiparticle exits, the results are less clear. In many cases, it may be well described by the Poissonian statistics [37, 38]. However, there are indications of deviation from that simple law in some samples [53, 54].

In this Chapter, we develop a kinetic theory of "quasiparticle poisoning". We find the distribution of times $N_{\rm o}(t)$ and $N_{\rm ev}(t)$ the CPB dwells, respectively, in odd- and even-electron states. We also find the spectrum of charge noise produced by the poisoning processes.

The conventional Poissonian statistics of the quasiparticle exits would yield an exponential distribution for odd-electron lifetime in the box. We see two reasons for the distribution function $N_{\rm o}(t)$ to deviate from that simple form. The first one is related to the thermalization of a quasiparticle within the CPB. If the rates of energy relaxation and of tunneling out for a quasiparticle from CPB are of the same order, then two different time scales control the short-time and long-time parts of the distribution function $N_{\rm o}(t)$. The shorter time scale is defined by the escape rate $\Gamma_{\rm out}$ of unequilibrated quasiparticle from the CPB. The longer time scale is defined by the rate of activation of equilibrated quasiparticle to the energy level allowing an escape from CPB. The second reason for the deviations from the exponential distribution controlled by a single rate, comes from the singular energy dependence of the quasiparticle density of states in a superconductor. Because of it, the tunneling-out rate depends strongly on the quasiparticle energy. Thus, even in the absence of thermalization the quasiparticle escapes from CPB cannot be described by an exponential distribution.

The conventional Poissonian statistics for both entrances and exits of the quasiparticle would lead to a Lorentzian spectral density $S_Q(\omega)$ of CPB charge fluctuations [55]. The interplay of tunneling and relaxation rates may result in deviations from the Lorentzian function. In the case of slow quasiparticle thermalization rate compared to the quasiparticle tunneling-out rate $\Gamma_{\rm out}$, the

function $S_Q(\omega)$ roughly can be viewed as a superposition of two Lorentzians. The width of the narrower one is controlled by the processes involving quasiparticle thermalization and activation by phonons, while the width of the broader one is of the order of the escape rate $\Gamma_{\rm out}$.

4.2 Qualitative considerations and main results

4.2.1 Relevant time scales

Dynamics of the Cooper-pair box coupled to the superconducting lead through the Josephson junction, see Fig. 2.1a, is described by Eq. (2.7). The energy of the system as a function of the gate voltage is shown in Fig. 4.1. At $N_g = 1$ the electrostatic energy of the Cooper-pair box is minimized when unpaired electron resides in it. Thus, at $N_g = 1$ the CPB is a trap for a quasiparticle. The trap depth δE is equal to the ground state energy difference between the even-charge state (no quasiparticles in the CPB) and odd-charge state (an unpaired electron in the CPB). For equal gap energies in the box and the lead, $\Delta_l = \Delta_b = \Delta$, the trap is formed due to Coulomb blockade effect. In the case $E_c \gg E_J$ [9] one has

$$\delta E \approx E_c - \frac{E_J}{2} \gg T, \tag{4.1}$$

and only two lowest charge states are important, see Fig. 4.1. Also, we assume here that there is at most one quasiparticle in the box in the odd state [10].

At $N_g = 1$ the transition probability per unit time between odd and even-charge states $W_{\text{-}}(E_p, E_k)$ can be obtained using the Fermi golden rule ($\hbar = 1$),

$$W_{\text{-}}(E_p, E_k) = 2\pi |\langle p, - | V | N+1, k\rangle|^2 \delta(E_p + \delta E - E_k). \tag{4.2}$$

The transition rate $W_{\text{-}}(E_p, E_k)$ can be calculated using the Bogoliubov transformation, and is given by Eq. (3.17). Using Eq. (4.2), one can calculate the level

[9] In Chapter 5 we calculate δE for general ratio of E_c and E_J.

[10] We assume the system is at low temperature $T \ll T_b^*$, where T_b^* is a characteristic temperature at which thermal quasiparticles appear in the CPB, *i.e.* $T_b^* = \frac{\Delta}{\ln(\Delta/\delta_b)}$

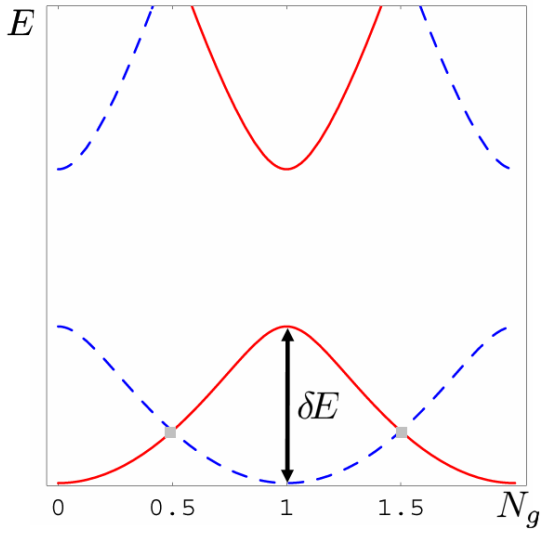

Figure 4.1: Energy of the Cooper-pair box as a function of dimensionless gate voltage N_g in units of e. Solid line corresponds to even-charge state of the box, dashed line corresponds to the odd-charge state of the box. The trap depth δE is the ground state energy difference between the even-charge state (no quasiparticles in the CPB), and odd-charge state (an unpaired electron in the CPB) at $N_g = 1$. (We assume here equal gap energies in the box and the lead, $\Delta_l = \Delta_b = \Delta$.)

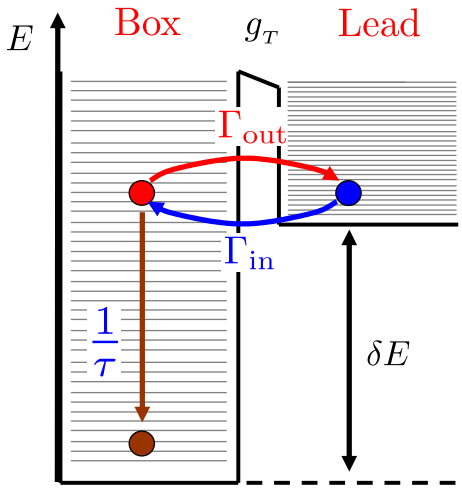

Figure 4.2: Schematic picture of the CPB-lead system showing allowed transitions for the quasiparticle injected into the excited state of the box. At $N_g = 1$ the Cooper-pair box is a trap for quasiparticle.

width of the state $|N+1,k\rangle$ with respect to quasiparticle tunneling through the junction to the lead,

$$\Gamma_{\rm out}(E_k) \equiv \sum_p W_{\text{-}}(E_p,E_k) = \frac{g_{\rm T}\delta_b}{4\pi}\frac{(E_k-\delta E)E_k-\Delta^2}{(E_k-\delta E)E_k}\nu(E_k-\delta E)\Theta(E_k-E_{\rm thd}). \tag{4.3}$$

The Heaviside function $\Theta(x)$ appears in Eq. (4.3) because there are no states to tunnel into for a quasiparticle with energy lower than the threshold energy $E_{\rm thd}$, see Fig. 4.2,

$$E_{\rm thd} = \Delta + \delta E. \tag{4.4}$$

The quasiparticle density of states $\nu(E_k)$ (in units of the normal density of states at the Fermi level) is given by

$$\nu(E_k) = \frac{E_k}{\sqrt{E_k^2-\Delta^2}}. \tag{4.5}$$

Due to the square-root singularity here, the rate $\Gamma_{\rm out}(E_k)$ has square-root divergence at $E_k = E_{\rm thd}$, see Fig. (4.3).

The quasiparticle may enter and subsequently leave the Cooper-pair box without changing its energy. For such elastic process, the excess energy of the exiting quasiparticle equals to its initial energy, and is of the order of the temperature, *i.e.* $E_k - E_{\rm thd} \sim T$. Therefore, the corresponding escape rate is

$$\Gamma_{\rm out} = \frac{g_{\rm T}\delta_b}{4\pi}\nu(T)\frac{\delta E}{\delta E+\Delta}. \tag{4.6}$$

Here for brevity we denote $\nu(T) \equiv \nu(E_k = \Delta + T)$. For the system with $g_{\rm T} \lesssim 1$, volume of the CPB $V_b \lesssim 1\mu m^3$, temperature $T \sim 50$mK and $\delta E \sim 0.5$K, the typical escape time $\Gamma_{\rm out}^{-1}$ is of the order of a μs.

To find the average rate $\Gamma_{\rm in}$ of quasiparticle tunneling from the lead to the CPB, we integrate the transition probability per unit time (4.2) with the distribution function $f(E_p)$ of quasiparticles in the lead,

$$\Gamma_{\rm in} = \sum_{p,k} W_{\text{-}}(k,p) f(E_p). \tag{4.7}$$

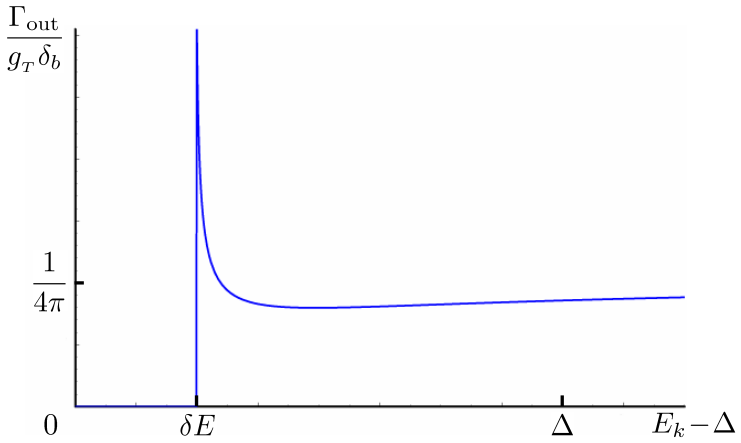

Figure 4.3: The dependence of the escape rate $\Gamma_{\rm out}(E_k)$ on energy E_k.

Upon elastically tunneling into the excited state in the CPB the quasiparticle can relax to the bottom of the trap, see Fig. (4.2). For that, the quasiparticle needs to give away energy $\sim \delta E$. At low temperatures the dominant mechanism of quasiparticle energy relaxation is due to electron-phonon inelastic scattering rate $1/\tau(E_k)$. At low temperature quasiparticles are tunneling into the box through the energy levels just above the threshold energy $E_k \sim E_{\rm thd}$, see Eq. (4.4). Assuming $\delta E \ll \Delta$, the typical quasiparticle relaxation time τ is given by [46]

$$\tau \equiv \tau(E_k \sim E_{\rm thd}) \approx \tau_0 \left(\frac{\Delta}{T_c}\right)^{-3} \left(\frac{\delta E}{\Delta}\right)^{-\frac{7}{2}}. \tag{4.8}$$

Here τ_0 is characteristic parameter defining the average electron-phonon scattering rate at $T = T_c$ with T_c being superconducting transition temperature. In aluminum, a typical material used for CPB, $\tau_0 \approx 0.1 - 0.5\,\mu s$ [46, 47, 56]. As one can see from Eq. (4.8), the quasiparticle relaxation rate is a strong function of the trap depth δE. Therefore, depending on δE there are two kinds of traps - "shallow" traps corresponding to $\tau\Gamma_{\rm out} \gg 1$, and "deep" traps with $\tau\Gamma_{\rm out} \ll 1$. (Note, for shallow traps we still assume $\delta E \gg T$.) The important quantity characterizing the traps is the probability $P_{\rm tr}$ for a quasiparticle to relax to the bottom of

the trap before an escape,

$$P_{\rm tr} = \frac{1/\tau}{1/\tau + \Gamma_{\rm out}}. \tag{4.9}$$

4.2.2 Lifetime distribution function

Experimentally observable quantity [37, 38], which reveals the kinetics of quasiparticle trapping, is the lifetime distribution function $N_{\rm o}(t)$ of odd-charge states of the CPB. The distribution of lifetimes $N_{\rm o}(t)$ depends on the internal dynamics of the quasiparticle in the CPB, *i.e* the ratio of $\tau\Gamma_{\rm out}$.

We start with the discussion of the long time asymptote of the lifetime distribution function. At $t > \tau$ the dwell-time distribution $N_{\rm o}(t)$ is governed by phonon-assisted activation of the thermalized quasiparticle in the trap. The phonon adsorption processes are statistically independent from each other. Hence, the lifetime distribution exponentially decays with time

$$N_{\rm o}(t) \propto \exp(-\gamma t) \tag{4.10}$$

with the rate

$$\gamma \approx \frac{1}{\tau}\frac{\nu(\delta E)}{\nu(T)} \exp\left(-\frac{\delta E}{T}\right)(1 - P_{\rm tr})\,. \tag{4.11}$$

This expression can be understood as follows. The rate of thermal activation of the quasiparticle from the bottom of the trap to the threshold energy is $\frac{1}{\tau}\frac{\nu(\delta E)}{\nu(T)} \exp\left(-\frac{\delta E}{T}\right)$, for brevity we define $\nu(\delta E) \equiv \nu(E_k = E_{\rm thd})$. The additional factor $\nu(\delta E)/\nu(T)$ here comes from the difference of the quasiparticle density of states at the bottom of the trap $\nu(T)$ and at the threshold energy $\nu(\delta E)$. The last term $(1 - P_{\rm tr})$ in Eq. (4.11) corresponds to the probability of the quasiparticle escape to the lead upon activation. Equation (4.11) allows us to consider limiting cases of $\tau\Gamma_{\rm out} \ll 1$ and $\tau\Gamma_{\rm out} \gg 1$.

In the case of "deep" traps ($\tau\Gamma_{\rm out} \ll 1$) most quasiparticles upon entering the excited state in the box quickly thermalize . Therefore, the main contribution to

lifetime distribution function comes from phonon-assisted escapes described by Eq. (4.10), see also Fig. (4.4). The activation escape rate of Eq. (4.11) in this limit equals

$$\gamma_{\rm f} \approx \Gamma_{\rm out} \frac{\nu(\delta E)}{\nu(T)} \exp\left(-\frac{\delta E}{T}\right), \tag{4.12}$$

since $1 - P_{\rm tr} \simeq \Gamma_{\rm out}\tau$, see Eq. (4.9).

In the opposite limit $\tau\Gamma_{\rm out} \gg 1$, *i.e.* "shallow" traps, the probability for a quasiparticle to relax to the bottom of the trap is small $P_{\rm tr} \ll 1$. Therefore, upon elastically tunneling into the excited state in the CPB the quasiparticles will predominantly return to the reservoir unequilibrated. Nevertheless, there is a small fraction of quasiparticles ($\sim 1/\tau\Gamma_{\rm out}$) that do relax to the bottom of the trap, and stay in the box much longer than unequilibrated ones. Thus, at $t > \tau$ the dwell-time distribution function $N_{\rm o}(t)$ has an exponentially decaying tail (4.10), see Fig. (4.4), with phonon-activated escape rate

$$\gamma_{\rm s} \approx \frac{1}{\tau}\frac{\nu(\delta E)}{\nu(T)} \exp\left(-\frac{\delta E}{T}\right). \tag{4.13}$$

At $t \sim \tau$ the typical value of the lifetime distribution function is $N_{\rm o}(t \sim \tau) \sim \gamma_{\rm s}/\tau\Gamma_{\rm out}$.

At short times, $t \ll \tau$, the lifetime distribution function $N_{\rm o}(t)$ describes the kinetics of unequilibrated quasiparticles. Quasiparticles tunnel into the box through the energy levels $E_k = E_{\rm thd} + \varepsilon$ (here $\varepsilon \geq 0$), and predominantly reside there till the escape with the rates $\Gamma_{\rm out}(\varepsilon)$. For a given energy level ε the lifetime distribution is exponential

$$N_{\rm o}(\varepsilon, t) \propto \exp(-\Gamma_{\rm out}(\varepsilon)t). \tag{4.14}$$

Note that upon entering into the CPB from the reservoir the quasiparticles can populate different levels within the energy strip $\sim T$, see Eq. (4.32). Therefore, experimentally observable quantity $N_{\rm o}(t)$, obtained by the statistical averaging

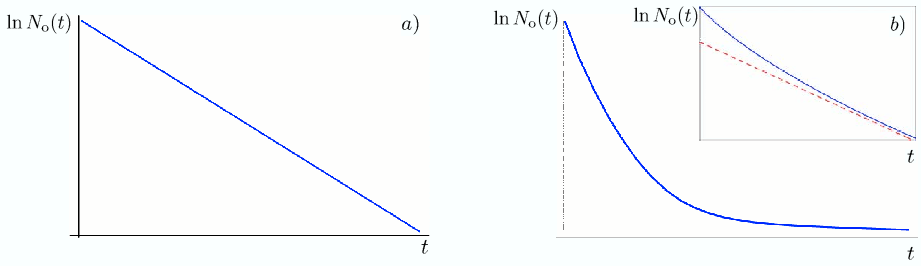

Figure 4.4: a) Schematic picture of the lifetime distribution function for "deep" traps ($\tau\Gamma_{\rm out} \ll 1$). b) Schematic picture of the lifetime distribution function for "shallow" traps ($\tau\Gamma_{\rm out} \gg 1$). Inset: Deviations of $N_{\rm o}(t)$ from exponential distribution at short times.

over large number of the tunneling events, is given by

$$N_{\rm o}(t) \propto \int_0^\infty d\varepsilon \exp\left(-\frac{\varepsilon}{T} - \Gamma_{\rm out}(\varepsilon)t\right). \tag{4.15}$$

Taking into account the singularity of $\Gamma_{\rm out}(\varepsilon)$ at small energies $\Gamma_{\rm out}(\varepsilon) \propto \varepsilon^{-1/2}$, we find that $N_{\rm o}(t)$ deviates from the simple exponential distribution [see also Fig. (4.4)],

$$N_{\rm o}(t) \propto \exp\left(-3\left(\frac{\Gamma_{\rm out}t}{2}\right)^{2/3}\right) \tag{4.16}$$

at times $t \gtrsim 1/\Gamma_{\rm out}$. See Sec. (4.4) for more details.

4.2.3 Charge Noise Power Spectrum

Anomalies in the lifetime distribution should also lead to a specific spectrum of charge fluctuations. We define the spectral density of charge fluctuations $S_Q(\omega)$ in the Cooper-pair box as

$$S_Q(\omega) = \int_{-\infty}^{\infty} dt e^{i\omega t} \left(\langle \delta Q(t)\delta Q(0)\rangle + \langle \delta Q(0)\delta Q(t)\rangle\right) \tag{4.17}$$

with $\delta Q(t) = Q(t) - \langle Q\rangle$. The variance of the fluctuations of charge Q in the CPB

$$\langle \delta Q^2\rangle = \int_0^\infty \frac{d\omega}{2\pi} S_Q(\omega) \tag{4.18}$$

is a thermodynamic, not a kinetic, quantity, and is known from statistical mechanics. The kinetics of the system is reflected in the dependence of the noise spectrum (4.17) on the frequency ω.

In the limit of fast relaxation $\tau\Gamma_{\rm out} \ll 1$ the escapes from the CPB are given by one timescale (4.12). The quasiparticle entrances into and exits from the CPB are random, and can be described by Poisson processes. Thus, $S_Q(\omega)$ is given by the Lorentzian function corresponding to random telegraph noise [55],

$$S_Q(\omega) \approx 4e^2\bar{\sigma}_{\rm o}(1-\bar{\sigma}_{\rm o})\frac{\tau_{\rm eff}}{(\omega\tau_{\rm eff})^2+1}. \tag{4.19}$$

Here $\bar{\sigma}_{\rm o}$ is an equilibrium average occupation of the odd-charge state in the CPB ($0 \le \bar{\sigma}_{\rm o} \le 1$), see Eq. (4.71) for details. At low temperature ($T \ll \delta E$) the box is predominantly in the odd-charge state, *i.e* $(1-\bar{\sigma}_{\rm o}) \propto \exp(-\delta E/T)$. The rate of activated quasiparticle escape processes has the same small exponent, therefore the width of the Lorentzian (4.19) is mainly given by the transitions from even to odd-electron state,

$$\frac{1}{\tau_{\rm eff}} \approx \Gamma_{\rm in}. \tag{4.20}$$

For the full result see Eq. (4.79).

In the limit of slow relaxation ($\tau\Gamma_{\rm out} \gg 1$) the charge noise power spectrum $S_Q(\omega)$ deviates significantly from the Lorentzian. These deviations stem from the fact that a quasiparticle may escape from the box before or after the equilibration, which results in two characteristic timescales for the escapes [57], see Fig. 4.4. Consequently, the function $S_Q(\omega)$ can be roughly viewed as a superposition of two Lorentzians, and is similar to carrier concentration fluctuations in semiconductors due to trapping [58]. The "narrow" Lorentzian describes the dynamics of slow fluctuations due to phonon-assisted trapping of quasiparticles

$$S_Q^{(1)}(\omega) \sim e^2\frac{\bar{\sigma}_{\rm o}(1-\bar{\sigma}_{\rm o})\tau_{\rm eff}}{(\omega\tau_{\rm eff})^2+1}, \quad \frac{1}{\tau_{\rm eff}} \approx \frac{1}{\tau}\frac{\Gamma_{\rm in}}{\Gamma_{\rm in}+\Gamma_{\rm out}}. \tag{4.21}$$

The width $\tau_{\rm eff}^{-1}$ here is determined by the probability of quasiparticle trapping per unit time. (Like above, we assume here $T \ll \delta E$ and neglect activated

escape rate.) The second (quasi) Lorentzian function $S_Q^{(2)}(\omega)$ is associated with fast charge fluctuations reflecting the kinetics of unequilibrated quasiparticles. Assuming $\omega \gg \Gamma_{\rm out} \gg \Gamma_{\rm in}$ the asymptote of $S_Q^{(2)}(\omega)$ is

$$S_Q^{(2)}(\omega) \sim e^2 \frac{\bar{\sigma}_{\rm o}}{\Gamma_{\rm out}} \exp(-\delta E/T) \left(\frac{\Gamma_{\rm out}}{\omega}\right)^2. \tag{4.22}$$

The width of $S_Q^{(2)}(\omega)$ is determined by the typical escape rate of unequilibrated quasiparticles from the box $\Gamma_{\rm out}$ defined in Eq. (4.6). Similar to the lifetime distribution, see Fig. 4.4, we predict deviations of $S_Q^{(2)}(\omega)$ from the Lorentzian function at $\omega \sim \Gamma_{\rm out}$ due to the peculiarity of the quasiparticle density of states.

The high-frequency tail of $S_Q(\omega)$ is provided by Eq. (4.22). However, the contribution of $S_Q^{(2)}(\omega)$ to the sum rule (4.18) is much smaller than that from $S_Q^{(1)}(\omega)$. In other words, the main contribution to the noise power comes from slow fluctuations. It resembles the case of the current noise in superconducting detectors [51].

In the rest of the Chapter, we provide detailed derivation of the results discussed qualitatively in this section.

4.3 Lifetime distribution of an even-charge state

Let us assume that the system switched to the even state at $t = 0$, and introduce the probability density $N_{\rm ev}(E_k, t)$ for a quasiparticle to enter the CPB for the first time through the state E_k. Then, the probability density for the CPB to reside in the even state until time t is

$$N_{\rm ev}(t) = \sum_k N_{\rm ev}(E_k, t). \tag{4.23}$$

$N_{\rm ev}(E_k, t)$ is given by the conditional probability of quasiparticle entering the CPB into an empty state E_k during the interval $(t, t + dt)$ times the probability that any quasiparticle has not entered into any state in the CPB during the

preceding interval $(0, t)$,

$$N_{\rm ev}(E_k, t)dt = \sum_p W_{\text{-}}(k,p) f(E_p) \left(1 - \sum_{k'} \int_0^t dt' N_{\rm ev}(E_{k'}, t')\right) dt. \qquad (4.24)$$

Summing Eq. (4.24) over states k and solving for $N_{\rm ev}(t)$ one finds

$$N_{\rm ev}(t) = \Gamma_{\rm in} \exp\left(-\Gamma_{\rm in} t\right), \qquad (4.25)$$

which corresponds to a homogenous Poisson process. The quasiparticle tunneling rate from the lead to the CPB $\Gamma_{\rm in}$ is given by Eq. (4.7).

Recent experiments by Aumentado *et. al.* [31, 37] indicate that the density of quasiparticles $n^l_{\rm qp}$ in the lead exceeds the equilibrium one at the temperature of the cryostat. The origin of non-equilibrium quasiparticles is not clear, but it is plausible to assume that quasiparticle distribution function in the lead $f(E_p)$ is given by the Boltzman function

$$f(E_p) = \exp\left(-\frac{E_p - \mu_l}{T}\right) \qquad (4.26)$$

with some effective chemical potential and temperature, μ_l and T, respectively. The chemical potential μ_l is related to the quasiparticle density by the equation

$$n^l_{\rm qp} = \frac{1}{V_l} \sum_p f(E_p). \qquad (4.27)$$

Here V_l is the volume of the lead. We consider the density of quasiparticles $n^l_{\rm qp}$ and their effective temperature as input parameters here, which can be estimated from the experimental data [31, 37, 38]. Taking into account Eq. (4.26) we can evaluate the r.h.s of Eq. (4.7) to obtain

$$\Gamma_{\rm in} = \frac{g_{\rm T} n^l_{\rm qp}}{4\pi\nu_{_F}} \nu(\delta E) \frac{\delta E}{\Delta + \delta E}. \qquad (4.28)$$

Here ν_F is the normal density of states at the Fermi level.

The average waiting time in the even-charge state is

$$\langle T_{\rm e} \rangle = \int_0^\infty N_{\rm ev}(t) t dt = \Gamma_{\rm in}^{-1}. \qquad (4.29)$$

This result is expected for conventional Poisson process.

4.4 Lifetime distribution of an odd-charge state

4.4.1 Master equation for survival probability

The distribution of dwell times for odd-charge state is more complicated than for even state due to the internal dynamics of the quasiparticle in the CPB. Upon tunneling elastically into the box the quasiparticle enters into the excited state with typical excess energy δE above the gap in the island. The dwell time of the quasiparticle in the box depends on whether upon tunneling into the excited state it relaxes to the bottom of the trap or tunnels out un-equilibrated, see Fig. 4.2. In order to describe the physics of quasiparticle tunneling we develop a formalism similar to the rate equations theory. We will include electron-phonon collision integral into our equations to account for the internal dynamics of the quasiparticle inside the CPB. The experimentally accessible quantity is the probability density $N_{\rm o}(t)$ of leaving an odd state in the time interval $(t, t+dt)$ assuming that quasiparticle resided continuously in the box during the time interval $(0, t)$. The object convenient for evaluation is the conditional probability $S_{\rm o}(t)$ (or survival probability) for a quasiparticle to occupy given level, under the condition that the unpaired electron continuously resided in the box over the time interval $(0, t)$. The lifetime distribution $N_{\rm o}(t)$ can be easily obtained from $S_{\rm o}(t)$,

$$N_{\rm o}(t) = \frac{d}{dt}(1 - S_{\rm o}(t)) = -\frac{dS_{\rm o}(t)}{dt}. \tag{4.30}$$

Probability $S_{\rm o}(t)$ is simply related to the conditional probability $S(E_k, t)$ for a quasiparticle to occupy level E_k at the moment t in the box assuming that a quasiparticle entered CPB at $t = 0$ and resided continuously in the box during the time interval $(0, t)$:

$$S_{\rm o}(t) = \sum_k S_{\rm o}(E_k, t). \tag{4.31}$$

We assume that in the initial moment of time the quasiparticle has just entered the state E_k in the box. Therefore, the initial probability $S_{\rm o}(E_k, 0)$ of the

occupation of the level E_k in the box is determined by the tunneling rate into the state E_k

$$S_{\rm o}(E_k,0)=\frac{1}{\Gamma_{\rm in}}\sum_p W_{\text{-}}(E_p,E_k)f(E_p). \tag{4.32}$$

The normalization of $S_{\rm o}(E_k,0)$ is chosen to satisfy $S_{\rm o}(0)=\sum_k S_{\rm o}(E_k,0)=1$. According to Eq. (4.32) the initial conditional probability $S_{\rm o}(E_k,0)$ is zero below the threshold energy $E_k<E_{\rm thd}$, and is proportional to Gibbs factor above the threshold $E_k>E_{\rm thd}$. This reflects out-of-equilibrium quasiparticle distribution at $t=0$.

The conditional probability $S_{\rm o}(E_k,t)$ consistent with initial conditions (4.32) satisfies the following master equation

$$\dot{S}_{\rm o}(E_k,t)+\Gamma_{\rm out}(E_k)S_{\rm o}(E_k,t)=-\frac{S_{\rm o}(E_k,t)-S_{\rm o}^{\rm eq}(E_k,t)}{\tau}. \tag{4.33}$$

The second term in the l.h.s corresponds to the loss from the state E_k due to the tunneling through the junction to the lead with the rate $\Gamma_{\rm out}(E_k)$ of Eq. (4.3). Note that unlike in the theory of the rate equations there is no "gain" term in Eq. (4.33). This is due to the condition that the box is occupied at $t=0$ and remains occupied continuously until some time t. The r.h.s of Eq. (4.33) corresponds to the electron-phonon collision integral in the relaxation time approximation with τ of Eq. (4.8) and

$$S_{\rm o}^{\rm eq}(E_k,t)=S_{\rm o}(t)\cdot\rho_{\rm odd}^{b}(E_k).$$

Note that Eq. (4.33) is nonlocal in E_k due the dependence of the collision integral on $S_{\rm o}(t)$ (see Eq. (4.31)). The collision integral in Eq. (4.33) describes the phonon-induced relaxation of the trapped quasiparticle to the equilibrium distribution,

$$\rho_{\rm odd}^{b}(E_k)=\frac{\exp\left(-E_k/T\right)}{Z_{\rm odd}}. \tag{4.34}$$

Here T is the quasiparticle temperature in the box. (For simplicity, we assume that the effective quasiparticle temperature in the lead is the same as in the box,

$T_l = T_b = T$.) The normalization factor $Z_{\rm odd}$ at $T \ll T^*$ is given by

$$Z_{\rm odd} = \frac{\sqrt{2\pi T\Delta}}{\delta_b} \exp\left(-\frac{\Delta}{T}\right). \tag{4.35}$$

4.4.2 General solution for $S_{\rm o}(t)$

Using Laplace transform,

$$S_{\rm o}(E_k, s) = \int_0^\infty dt S_{\rm o}(E_k, t) e^{-st}, \tag{4.36}$$

we reduce differential equation (4.33) supplied with the initial conditions Eq. (4.32) to an algebraic one

$$\left(s+\Gamma_{\rm out}(E_k)+\frac{1}{\tau}\right) S_{\rm o}(E_k, s) = \frac{S_{\rm o}^{\rm eq}(E_k, s)}{\tau} + S_{\rm o}(E_k, 0). \tag{4.37}$$

Equation (4.37) can be solved for $S_{\rm o}(E_k, s)$. Then, by summing that solution over momenta k and utilizing Eqs. (4.31) and (4.32) we find the survival probability

$$S_{\rm o}(s) = \frac{B(s)}{1 - A(s)}. \tag{4.38}$$

Here functions $B(s)$ and $A(s)$ are defined as

$$\begin{aligned} B(s) &= \frac{1}{\Gamma_{\rm in}} \sum_k \frac{f(E_k - \delta E)\Gamma_{\rm out}(E_k)}{s + 1/\tau + \Gamma_{\rm out}(E_k)}, \\ A(s) &= \frac{1}{\tau} \sum_k \frac{\rho_{\rm odd}^b(E_k)}{s + 1/\tau + \Gamma_{\rm out}(E_k)}. \end{aligned} \tag{4.39}$$

At $T \gg \delta_b$ one can take thermodynamic limit and replace the sums with the integrals in Eq. (4.39). Further simplification of the denominator in Eq. (4.38) is possible if one splits the integral in $A(s)$ into the intervals $(\Delta, E_{\rm thd})$, where $\Gamma_{\rm out}(E_k) = 0$, and $(E_{\rm thd}, \infty)$. Then, Equation (4.38) becomes

$$S_{\rm o}(s) = \left(s + \frac{1}{\tau}\right) \frac{B(s)}{s + X(s)} \tag{4.40}$$

with the functions $B(s)$ and $X(s)$ defined as

$$B(s) \;=\; \frac{2}{\Gamma_{\rm in}}\int_{E_{\rm thd}}^{\infty}\frac{dE_k}{\delta_b}\nu(E_k)\frac{f(E_k-\delta E)\Gamma_{\rm out}(E_k)}{s+1/\tau+\Gamma_{\rm out}(E_k)},$$

$$X(s) \;=\; \frac{2}{\tau}\int_{E_{\rm thd}}^{\infty}\frac{dE_k}{\delta_b}\nu(E_k)\frac{\rho^b_{\rm odd}(E_k)\Gamma_{\rm out}(E_k)}{s+1/\tau+\Gamma_{\rm out}(E_k)}. \tag{4.41}$$

The inverse Laplace transform is given by

$$S_{\rm o}(t)=\frac{1}{2\pi i}\int_{\eta-i\infty}^{\eta+i\infty}ds\,S_{\rm o}(s)e^{st}, \tag{4.42}$$

where η is chosen in such way that $S_{\rm o}(s)$ is analytic at ${\rm Re}[s] > \eta$. The integral (4.42) can be calculated using complex variable calculus by closing the contour of integration as shown in Fig. 4.5 and analyzing the enclosed points of non-analytic behavior of $S_{\rm o}(s)$. In general, the singularities of $S_{\rm o}(s)$ consist of 2 poles and a cut. The latter is due to the singularities of the function $B(s)$ causing $S_{\rm o}(s)$ to be non-analytic along the cut $s \in (-\infty, -s_{\rm min})$, where

$$s_{\rm min} \;=\; \frac{1}{\tau}+\min\left[\,\Gamma_{\rm out}(E_k)\,\right]. \tag{4.43}$$

The plot of $\Gamma_{\rm out}(E_k)$ is shown in Fig. (4.3). The function $\Gamma_{\rm out}(E_k)$ has a minimum at $E_k^{\rm min} = E_{\rm thd}+\delta E/2$. (For the estimate of the minimum we assumed $\delta E \ll \Delta$.) In addition to the cut, $S_{\rm o}(s)$ has 2 poles. The poles s_1 and s_2 are the solutions of the following equation in the region of analyticity of $B(s)$

$$s + X(s) = 0. \tag{4.44}$$

We now analyze the singularities $S_{\rm o}(s)$ and find their contribution to the integral (4.42).

The contribution from the cut to Eq. (4.42) corresponds to the kinetics of unequilibrated quasiparticles. Formally it comes from the non-analyticity of $S_{\rm o}(s)$ due to the singularities of the function $B(s)$ itself. The proper contribution to Eq. (4.42) can be calculated by integrating along the contour enclosing the cut,

$$I_{\rm cut} \;=\; \frac{-1}{2\pi i}\int_{s_{\rm min}}^{\infty}ds e^{st}\left(S_{\rm o}(s+i\epsilon)-S_{\rm o}(s-i\epsilon)\right). \tag{4.45}$$

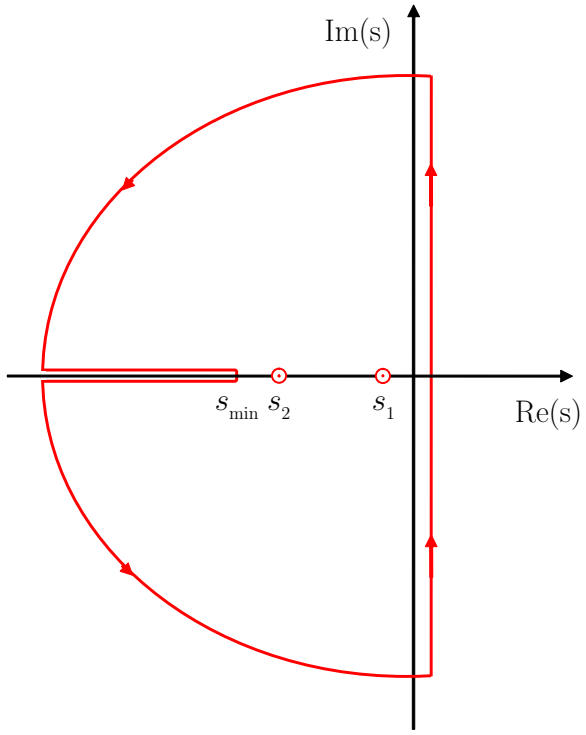

Figure 4.5: Contour of integration chosen to calculate inverse Laplace transform Eq. (4.42). Points of non-analytic behavior of $\sigma_{++}(s)$ are shown. Poles at s_1, s_2, and a cut $s \in (-\infty, -s_{\min})$.

At low temperature $T \ll \delta E$, the discontinuity of the imaginary part of $S_{\rm o}(s)$ at the cut is

$$S_{\rm o}(s+i\epsilon)-S_{\rm o}(s-i\epsilon) = 2i\left(s+\frac{1}{\tau}\right)\frac{{\rm Im}B(s+i\epsilon)}{s}. \tag{4.46}$$

Substitution of this expression into Eq. (4.45) yields

$$\begin{aligned} I_{\rm cut} \;&=\; \frac{2}{\Gamma_{\rm in}}\int_{E_{\rm thd}}^{\infty}\frac{dE_k}{\delta_b}\,\nu(E_k)f(E_k-\delta E)\Gamma_{\rm out}(E_k) \\ &\times\; \frac{\tau\Gamma_{\rm out}(E_k)}{1+\tau\Gamma_{\rm out}(E_k)}\exp\!\left(-\frac{t}{\tau}-\Gamma_{\rm out}(E_k)t\right). \end{aligned} \tag{4.47}$$

To simplify above expression we introduce the dimensionless variable z

$$z = \frac{E_k - E_{\rm thd}}{T}, \tag{4.48}$$

and write the integral in $I_{\rm cut}$ in terms of z

$$I_{\rm cut} = \int_0^{\infty} dz \frac{\nu(z)\Gamma_{\rm out}(z)}{\sqrt{\pi}\Gamma_{\rm out}\nu(\delta E)}\frac{\tau\Gamma_{\rm out}(z)}{1+\tau\Gamma_{\rm out}(z)}\exp\left(-z-\Gamma_{\rm out}(z)t-t/\tau\right). \tag{4.49}$$

Here and thereafter $\Gamma_{\rm out}(z)$ and $\nu(z)$ are given by Eqs. (4.3) and (4.5), respectively, with $E_k = E_{\rm thd} + Tz$.

We now analyze the contribution to Eq. (4.42) from the poles. The pole at s_1 may be found from the iterative solution of Eq. (4.44) at small s ($s \ll s_{\rm min}$)

$$s_1 \approx -X(s=0) \tag{4.50}$$

with $X(s)$ given by Eq. (4.41). The contribution from the pole at s_1 is calculated using residue calculus yielding

$$I_1 \;=\; Y(0)\exp\left(-X(0)t\right). \tag{4.51}$$

Equation (4.51) describes the kinetics of thermalized quasiparticles. At low temperature $X(0) \propto \exp(-\delta E/T)$, which justifies the approximation used in

Eq. (4.50), see also next section. The function $Y(0)$ depends on $\tau\Gamma_{\rm out}$, and is approximately given by

$$Y(0) \approx \frac{1}{\sqrt{\pi}} \int_0^\infty dz \frac{\exp(-z)}{\sqrt{z} + \tau\Gamma_{\rm out}}. \tag{4.52}$$

Here we used small-z asymptote ($z \ll \frac{\delta E}{2T}$) for the escape rate,

$$\Gamma_{\rm out}(z) \approx \frac{\Gamma_{\rm out}}{\sqrt{z}}. \tag{4.53}$$

The second pole s_2 is given by the solution of Eq. (4.44) at large s. At small temperature $T \ll \delta E$ one can show that the contribution of the second pole s_2 to Eq. (4.42) is small, and thus can be neglected. (For details, see Appendix in Ref. [59])

4.4.3 Results and Discussions

Combining all relevant contributions to the inverse Laplace transform, Eqs. (4.49) and (4.51), we obtain the solution for the survival probability

$$S_{\rm o}(t) \;\; = \;\; Y(0) \exp(-\gamma t) + F(t). \tag{4.54}$$

The first term here corresponds to the kinetics of the quasiparticle that relaxed to the bottom of the trap. The thermally activated decay rate γ, found with the help of Eqs. (4.50) and (4.48), is

$$\gamma = \frac{1}{\tau} \frac{\nu(\delta E)}{\nu(T)} \exp\left(-\frac{\delta E}{T}\right) \left(1 - \int_0^\infty dz \frac{e^{-z}/\tau}{1/\tau + \Gamma_{\rm out}/\sqrt{z}}\right). \tag{4.55}$$

The integral in Eq. (4.55) reflects the probability for a quasiparticle to relax to the bottom of the trap [cf. Eq. (4.9)]. The second term in Eq. (4.54) describes the kinetics of unequilibrated quasiparticles with $F(t)$ given by

$$F(t) = \int_0^\infty dz \frac{\nu(z)\Gamma_{\rm out}(z)}{\sqrt{\pi}\Gamma_{\rm out}\nu(\delta E)} \frac{\tau\Gamma_{\rm out}(z)}{1 + \tau\Gamma_{\rm out}(z)} \exp\left(-z - t\Gamma_{\rm out}(z) - \frac{t}{\tau}\right). \tag{4.56}$$

In the next paragraphs we will analyze $S_{\rm o}(t)$ for fast and slow relaxation limits.

In the case $\tau\Gamma_{\rm out} \ll 1$ ("deep" trap), the leading contribution to the survival probability $S_{\rm o}(t)$ comes from the first term in Eq. (4.54), the second term in Eq. (4.54) is proportional to $\tau\Gamma_{\rm out}$, and can be neglected. Consequently, the survival probability is given by

$$S_{\rm o}(t) \approx \exp\left(-\gamma_{\rm f} t\right). \tag{4.57}$$

Using Eq. (4.30) we find the lifetime distribution function

$$N_{\rm o}(t) = \gamma_{\rm f} \exp\left(-\gamma_{\rm f} t\right), \tag{4.58}$$

cf. Eqs. (4.10) and (4.12). As discussed qualitatively in Sec. 4.2 in the fast relaxation limit the majority of quasiparticles entering the CPB into excited state $E_k \sim E_{\rm thd}$ relax to the bottom of the trap and stay in the box until they are thermally excited out of the trap by phonons with the rate $\gamma_{\rm f}$ of Eq. (4.12). Finally, using Eq. (4.57) we find the average lifetime of the odd-charge state

$$\langle T_{\rm o} \rangle = \int_0^\infty S_{\rm o}(t) dt = 1/\gamma_{\rm f}. \tag{4.59}$$

In the opposite limit of "shallow" trap, $\tau\Gamma_{\rm out} \gg 1$, the majority of quasiparticles tunnel out unequilibrated to the lead ($P_{\rm tr} \approx 1/\tau\Gamma_{\rm out}$). The expression for the survival probability (4.54) in this limit becomes

$$S_{\rm o}(t) = F(t) + \frac{1}{\sqrt{\pi}\tau\Gamma_{\rm out}} \exp(-\gamma_{\rm s} t). \tag{4.60}$$

Note that in addition to first term describing the kinetics of unequilibrated quasiparticles the survival probability has a tail corresponding to the small fraction of quasiparticles that do relax to the bottom of the trap. These quasiparticles reside in the box until they are thermally excited by phonons. In the slow relaxation limit the activation exponent (4.55) can be reduced to

$$\gamma_{\rm s} \approx \frac{1}{\sqrt{\pi}\tau} \frac{\nu(\delta E)}{\nu(T)} \exp\left(-\frac{\delta E}{T}\right). \tag{4.61}$$

[Rigorous evaluation produces a difference in the numerical factor here compared to Eq. (4.13).] The tail of the distribution function (4.60) describes the processes that are much slower than $1/\Gamma_{\rm out}$, thus it has to be retained despite its small amplitude, see also Eq. (4.67).

The function $F(t)$ defined in Eq. (4.56) can be evaluated using small-z asymptote of $\Gamma_{\rm out}(z)$, see Eq. (4.53). This approximation substantially simplifies $F(t)$,

$$F(t) \approx \frac{1}{\sqrt{\pi}} \int_0^\infty \frac{dz}{\sqrt{z}} \frac{\tau\Gamma_{\rm out}}{\sqrt{z}+\tau\Gamma_{\rm out}} \exp\left(-z - \frac{t\Gamma_{\rm out}}{\sqrt{z}} - \frac{t}{\tau}\right). \tag{4.62}$$

Here we assumed that the main contribution to the $F(t)$ comes from small-z region, $z \ll \delta E/2T$, which limits the applicability of Eq. (4.62) to $t \ll \Gamma_{\rm out}^{-1} \left(\frac{\delta E}{2T}\right)^{3/2}$. The asymptotic expression for $F(t)$ in Eq. (4.60) can be obtained using the saddle-point approximation

$$F(t) \approx \frac{2}{\sqrt{3}} \frac{\tau\Gamma_{\rm out}}{\tau\Gamma_{\rm out} + \left(\frac{1}{2}\Gamma_{\rm out} t\right)^{1/3}} \exp\left(-3\left(\frac{\Gamma_{\rm out} t}{2}\right)^{2/3} - \frac{t}{\tau}\right). \tag{4.63}$$

The integral (4.62) can be also expressed in the analytic form in terms of the Meijer's G-function [60]. As one can see from Fig. 4.6 at low temperature $T \ll \delta E$ there is time window

$$\frac{1}{\Gamma_{\rm out}} \lesssim t \ll \frac{1}{\Gamma_{\rm out}} \left(\frac{\delta E}{2T}\right)^{3/2}, \tag{4.64}$$

when the survival probability deviates from the exponentially decaying function. We assumed in Eq. (4.64) that the upper limit is more restrictive than $t \ll \frac{1}{\Gamma_{\rm out}} \left(\Gamma_{\rm out}\tau\right)^3$ so that τ-dependent term in the exponent of Eq. (4.63) can be neglected.

The fractional power 2/3 in Eq. (4.63) stems from the peculiarity of superconducting density of states at low energies. Assuming the quasiparticle distribution in the lead is given by Eq. (4.26), every time a quasiparticle tunnels into the box

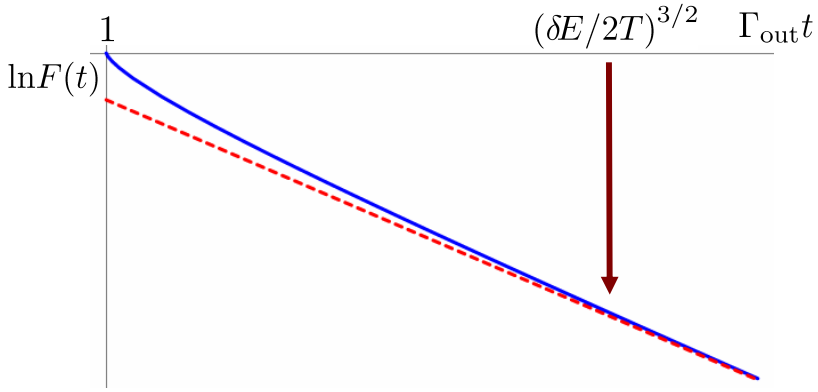

Figure 4.6: Deviation of $F(t)$ (solid line) defined in Eq. (4.56) from the exponentially decaying function at $\Gamma_{\rm out}t \gtrsim 1$. (We assumed $\tau = \infty$ here.)

it may occupy a different energy level, which is reflected in the initial conditions, see Eq. (4.32). However, due to the singularity of the escape rate $\Gamma_{\rm out}(E_k)$ at $E_k \sim E_{\rm thd}$, this results in a strong energy dependence of the dwell time of a quasiparticle. Therefore, averaging over many such events leads to the deviation of $F(t)$ from the simple exponential function, as shown in Fig. 4.6.

At $t \gtrsim \frac{1}{\Gamma_{\rm out}} \left(\frac{\delta E}{2T}\right)^{3/2}$ the minimum of the exponent in (4.62) is beyond the limit of applicability of small-z approximation for the rate $\Gamma_{\rm out}(z)$ given by Eq. (4.53), and instead of Eq. (4.62) one should use Eq. (4.56). Since at $z \sim \delta E/2T$ the escape rate $\Gamma_{\rm out}(z)$ is a smooth function, $F(t)$ decays exponentially

$$F(t) \propto \exp\left(-\frac{\delta E}{2T} - \Gamma_{\rm out}(z_{\rm min})t - \frac{t}{\tau}\right). \tag{4.65}$$

Here $\Gamma_{\rm out}(z_{\rm min}) \approx \frac{g_{\rm T}\delta_b}{2\pi}\sqrt{\frac{\delta E}{\Delta}}$.

The lifetime distribution function $N_{\rm o}(t)$ for the odd-charge state can be obtained from $S_{\rm o}(t)$ by substituting Eq. (4.60) into Eq. (4.30). Under conditions of Eq. (4.64) the lifetime distribution function $N_{\rm o}(t)$ will deviate from the exponential distribution

$$N_{\rm o}(t) \approx \frac{2^{4/3}}{\sqrt{3}} \frac{\Gamma_{\rm out}}{(\Gamma_{\rm out}t)^{1/3}} \exp\left(-3\left(\frac{\Gamma_{\rm out}t}{2}\right)^{2/3}\right). \tag{4.66}$$

This result is consistent with experimental observations [53, 54].

The average lifetime of the odd-charge state $\langle T_{\rm o}\rangle$ in the slow relaxation case is

$$\langle T_{\rm o}\rangle = \int_0^\infty S_{\rm o}(t)dt \;\approx\; \frac{1}{\sqrt{\pi}\tau\Gamma_{\rm out}\gamma_s} = \frac{1}{\gamma_f}. \tag{4.67}$$

Despite the quasiparticle having small probability of relaxing to the bottom of the trap, the main contribution to the average dwell time $\langle T_{\rm o}\rangle$ is given by the tail of $S_{\rm o}(t)$. This is because once the quasiparticle is trapped in the CPB it spends there exponentially long time, see Eq. (4.61). As expected $\langle T_{\rm o}\rangle$ is the same for fast and slow relaxation cases because the average lifetime determines the thermodynamic probability to occupy given charge state, and should not depend on the kinetics of the equilibration process.

4.5 Charge Noise

The complex statistics of capture and emission processes discussed in the previous section also manifest itself in the spectral density of charge fluctuations of the Cooper-pair box. In this section we study the charge noise power spectrum for "deep" ($\tau\Gamma_{\rm out} \ll 1$) and "shallow" ($\tau\Gamma_{\rm out} \gg 1$) traps.

The kinetic equations for occupational probabilities of odd- and even-charge state have the form [59]

$$\dot{P}_{\rm e}(E_p,t) + \sum_k W_{\text{-}}(E_p,E_k)\left(P_{\rm e}(E_p,t) - P_{\rm o}(E_k,t)\right) = 0, \tag{4.68}$$

$$\dot{P}_{\rm o}(E_k,t) + \sum_p W_{\text{-}}(E_p,E_k)\left(P_{\rm o}(E_k,t) - P_{\rm e}(E_p,t)\right) = -\frac{1}{\tau}\left(P_{\rm o}(E_k,t) - P_{\rm o}^{\rm eq}(E_k,t)\right).$$

Here $P_{\rm o}^{\rm eq}(E_k,t) = \rho_{\rm odd}^b(E_k)\sigma_{\rm o}(t)$ with $\sigma_{\rm o}(t) = \sum_k P_{\rm o}(E_k,t)$, and the quasiparticle transition rate $W_{\text{-}}(E_p,E_k)$ is defined in Eq. (4.2). Assuming that the lead is a heat bath of quasiparticles we can write even-charge occupational probability as $P_{\rm e}(E_p,t) = f(E_p)\sigma_{\rm e}(t)$ with $f(E_p)$ being the distribution function of the quasiparticles in the lead, and $\sigma_{\rm e}(t) = \sum_p P_{\rm e}(E_p,t)$ being occupational probability of

the even state. This allows us to reduce Eqs. (4.68) to

$$\dot{\sigma}_{\rm e}(t) \; + \; \sum_{k,p} W_{\text{-}}(E_p,E_k)\left(f(E_p)\sigma_{\rm e}(t) - P_{\rm o}(E_k,t)\right) = 0 \tag{4.69}$$

$$\dot{P}_{\rm o}(E_k,t) \; + \; \sum_{p} W_{\text{-}}(E_p,E_k)\left(P_{\rm o}(E_k,t) - f(E_p)\sigma_{\rm e}(t)\right) = -\frac{1}{\tau}\left(P_{\rm o}(E_k,t) - P_{\rm o}^{\rm eq}(E_k,t)\right).$$

One can see that Eqs. (4.69) satisfy the normalization condition:

$$\sigma_{\rm e}(t) + \sigma_{\rm o}(t) = 1. \tag{4.70}$$

The stationary occupational probabilities $\bar{\sigma}_{\rm e}$ and $\bar{\sigma}_{\rm o}$ are given by the Gibbs equilibrium state. Assuming that $f(E_p)$ is given by Eq. (4.26), we obtain

$$\bar{\sigma}_{\rm e} = \frac{1}{1 + n_{\rm qp}^{l} V_b \exp\left(\frac{\delta E}{T}\right)},\; \bar{\sigma}_{\rm o} = 1 - \bar{\sigma}_{\rm e}. \tag{4.71}$$

Here $n_{\rm qp}^{l}$ is the quasiparticle density in the lead, see Eq. (4.27), and V_b is the volume of the CPB.

The fluctuations around this equilibrium state can be taken into account within the Boltzmann-Langevin approach, which assumes that the occupational probabilities fluctuate around the stationary solution (4.71) due to the randomness of the tunneling and scattering events as well as partial occupations of the quasiparticle states [11].

The kinetic equations for the charge fluctuations can be derived by properly varying Eqs. (4.69) and adding Langevin sources corresponding to the relevant random events [61, 62]

$$\begin{aligned}
&\left(\frac{d}{dt} + \Gamma_{\rm in}\right)\delta\sigma_{\rm e}(t) = \sum_{k,p} W_{\text{-}}(E_p,E_k)\delta P_{\rm o}(E_k,t) + \sum_{p}\xi_p^{\rm T}(t),\\
&\left(\partial_t + \sum_{p} W_{\text{-}}(E_p,E_k) + \frac{1}{\tau}\right)\delta P_{\rm o}(E_k,t) = -\frac{\delta\sigma_{\rm e}(t)}{\tau}\rho_{\rm odd}^{b}(E_k)\\
&+\sum_{p} W_{\text{-}}(E_p,E_k) f(E_p)\delta\sigma_{\rm e}(t) + \xi_k^{\rm T}(t) + \xi_k^{ph}(t).
\end{aligned} \tag{4.72}$$

[11] Boltzmann-Langevin approach is adequate for calculating noise at low frequencies $\omega \ll T$ (classical limit). This frequency domain is broad enough to include the rates of the relevant processes affecting the noise spectrum, see Eqs. (4.6)-(4.8)

Here the relation $\delta\sigma_{\rm e}(t) = -\delta\sigma_{\rm o}(t)$ was taken into account. The Langevin sources $\xi^{\rm T}_{p(k)}(t)$ and $\xi^{ph}_k(t)$ correspond to quasiparticle tunneling from/to the state $|p\rangle\,/\,|k\rangle$ through the junction, and inelastic electron-phonon scattering, respectively. [Note that $\sum_p \xi^{\rm T}_p(t) = -\sum_k \xi^{\rm T}_k(t)$ and $\sum_k \xi^{ph}_k(t) = 0$.] These random processes are considered to be Poissonian with the following correlation functions

$$\begin{aligned}\langle \xi^{\rm T}_k(t)\xi^{\rm T}_{k'}(t')\rangle &= 2\delta(t-t')\delta_{k,k'}\sum_p W_{\text{-}}(E_p,E_k)f(E_p)\bar\sigma_{\rm e}\\ &= 2\delta(t-t')\delta_{k,k'}\Gamma_{\rm out}(E_k)f(E_k-\delta E)\bar\sigma_{\rm e},\end{aligned}$$

$$\begin{aligned}\langle \xi^{ph}_k(t)\xi^{ph}_{k'}(t')\rangle &= \delta(t-t')\frac{2P^{\rm eq}_{\rm o}(E_k)}{\tau}\left(\delta_{k,k'}-\frac{P^{\rm eq}_{\rm o}(E_{k'})}{\sigma_{\rm o}}\right)\\ &= \delta(t-t')\frac{2\bar\sigma_{\rm o}\rho^b_{\rm odd}(E_k)}{\tau}\left(\delta_{k,k'}-\rho^b_{\rm odd}(E_{k'})\right).\end{aligned} \tag{4.73}$$

The latter expression is consistent with the collision integral in the relaxation time approximation and conservation of the probability $\sigma_{\rm o}(t)$ by the electron-phonon scattering [63, 64].

The spectral density of charge fluctuations in the CPB defined in Eq. (4.17) can be written in the Fourier domain as

$$S_Q(\omega) = 2e^2\langle\delta\sigma_{\rm e}(\omega)\delta\sigma_{\rm e}(-\omega)\rangle, \tag{4.74}$$

and can be obtained from Eqs. (4.72) and (4.73). The solution of the second equation of the system (4.72) in frequency domain is

$$\delta P_{\rm o}(E_k,\omega)=\frac{\Gamma_{\rm out}(E_k)f(E_k-\delta E)-\frac{1}{\tau}\rho^b_{\rm odd}(E_k)}{-i\omega+\Gamma_{\rm out}(E_k)+\frac{1}{\tau}}\delta\sigma_{\rm e}(\omega)+\frac{\xi^{\rm T}_k(\omega)+\xi^{ph}_k(\omega)}{-i\omega+\Gamma_{\rm out}(E_k)+\frac{1}{\tau}}. \tag{4.75}$$

Substituting this expression into equation for $\delta\sigma_{\rm e}(\omega)$ we find

$$\mathcal{L}(\omega)\delta\sigma_{\rm e}(\omega)=\sum_k\frac{(i\omega-\frac{1}{\tau})\xi^{\rm T}_k(\omega)+\Gamma_{\rm out}(E_k)\xi^{ph}_k(\omega)}{-i\omega+\Gamma_{\rm out}(E_k)+\frac{1}{\tau}}, \tag{4.76}$$

where the function $\mathcal{L}(\omega)$ is given by

$$\mathcal{L}(\omega)=\frac{1}{\tau}\sum_k \frac{\rho^b_{\rm odd}(E_k)\Gamma_{\rm out}(E_k)}{-i\omega+\Gamma_{\rm out}(E_k)+\frac{1}{\tau}}+\sum_k f(E_k-\delta E)\frac{\Gamma_{\rm out}(E_k)(-i\omega+\frac{1}{\tau})}{-i\omega+\Gamma_{\rm out}(E_k)+\frac{1}{\tau}}-i\omega. \tag{4.77}$$

Finally, using Eqs. (4.74) and (4.76) we can find the correlation function $\langle\delta\sigma_{\rm e}(\omega)\delta\sigma_{\rm e}(-\omega)\rangle$, and obtain charge noise power spectrum $S_Q(\omega)$,

$$\begin{aligned} S_Q(\omega) &= \frac{2e^2}{\mathcal{L}(\omega)\mathcal{L}(-\omega)} \\ &\times \sum_{k,k'}\frac{(\omega^2+\frac{1}{\tau^2})\langle\xi^{\rm T}_k(\omega)\xi^{\rm T}_{k'}(-\omega)\rangle+\Gamma_{\rm out}(E_k)\Gamma_{\rm out}(E_{k'})\langle\xi^{ph}_k(\omega)\xi^{ph}_{k'}(-\omega)\rangle}{\left(-i\omega+\Gamma_{\rm out}(E_k)+\frac{1}{\tau}\right)\left(i\omega+\Gamma_{\rm out}(E_{k'})+\frac{1}{\tau}\right)}. \end{aligned} \tag{4.78}$$

Upon substituting correlation functions (4.73) into Eq. (4.78), the general solution for $S_Q(\omega)$ can be obtained (after cumbersome but straightforward calculations, see Appendix D). Rather than going through the full derivation, we study here $S_Q(\omega)$ in the limiting cases $\tau\Gamma_{\rm out}\ll 1$ and $\tau\Gamma_{\rm out}\gg 1$, which can be derived from Eqs. (4.73), (4.77) and (4.78).

First, we consider fast relaxation limit $\tau\Gamma_{\rm out}\ll 1$. In this case one can neglect the second term in the numerator of Eq. (4.78). For $\omega\tau\ll 1$ one can simplify Eqs. (4.77) and (4.78) further. After straightforward manipulations one finds that the leading contribution to the noise is given by Eq. (4.19) with the rate

$$\frac{1}{\tau_{\rm eff}}=\gamma_{\rm f}+\Gamma_{\rm in}, \tag{4.79}$$

which includes all processes changing the population $\bar{\sigma}_{\rm e}$. The first term in Eq. (4.79) corresponds to the rate of thermal activation of the quasiparticles by phonons from the bottom of the trap to the lead, see Eq. (4.12); the second term is the rate of quasiparticle tunneling from the lead to the box given by Eq. (4.7), also cf. Eq. (4.20).

In the opposite limit $\tau\Gamma_{\rm out}\gg 1$, the charge noise power spectrum $S_Q(\omega)$ can be roughly viewed as the superposition of two Lorentzians, see Fig. 4.7. The

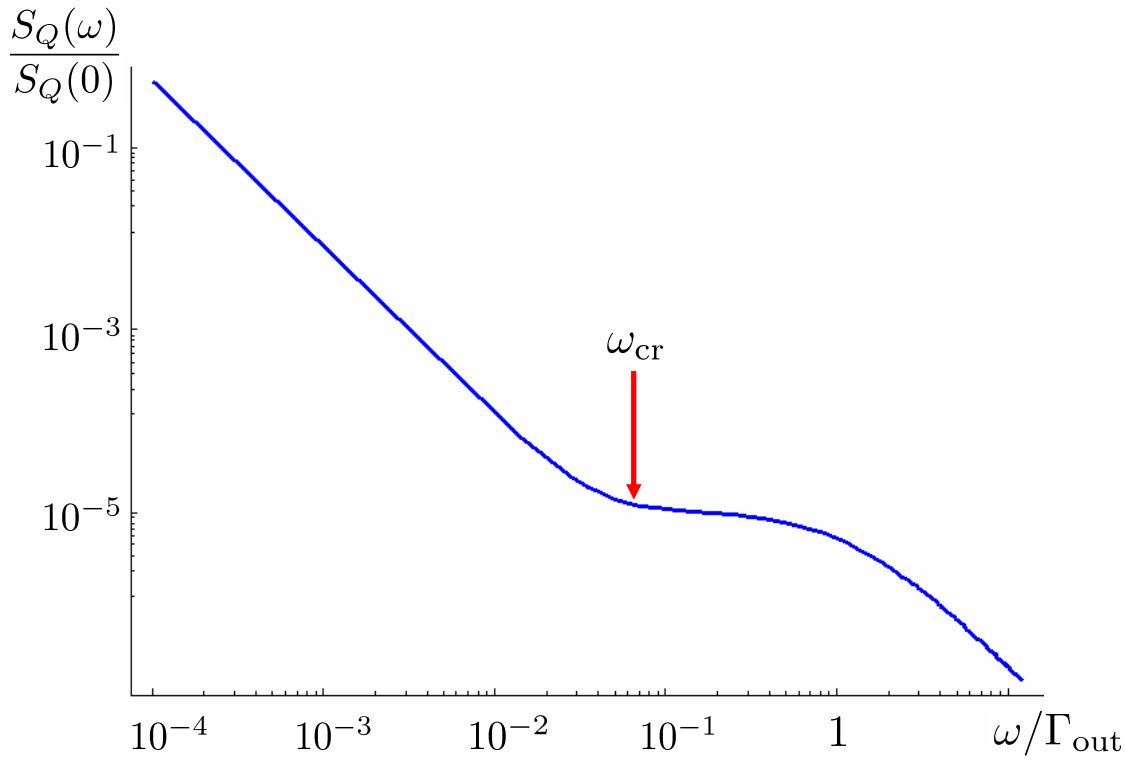

Figure 4.7: Spectral density of charge fluctuations generated by quasiparticle capture and emission processes in the Cooper-pair box for the slow relaxation case ($\tau\Gamma_{\rm out} = 10^3$). Here $\omega_{\rm cr} \approx \sqrt{\Gamma_{\rm out}/\tau}$ is a crossover frequency between two different regimes governed by Eqs. (4.80) and (4.83).

first one corresponds to the processes involving quasiparticle thermalization and activation by phonons, and is dominant at low frequencies. The second (quasi) Lorentzian describes the fast processes ($\omega \sim \Gamma_{\rm out}$) associated with the escape of unequilibrated quasiparticles from the box.

At low frequencies $\omega \ll \omega_{\rm cr}$, see Fig. 4.7, the noise power spectrum is well approximated by the Lorentzian function. This can be obtained by neglecting the first term in the numerator of Eq. (4.78), and keeping the leading terms in $1/\tau\Gamma_{\rm out}$ and $\omega/\Gamma_{\rm out}$ in Eqs. (4.77) and (4.78), see Appendix D for more details. After straightforward manipulations one finds

$$S_Q(\omega) \approx 4e^2\bar{\sigma}_{\rm o}\,(1-\bar{\sigma}_{\rm o})\,\frac{1-D}{1+C}\cdot\frac{\tau_{\rm eff}}{(\omega\tau_{\rm eff})^2+1}. \tag{4.80}$$

The constants C and D here are defined as

$$C = \frac{1}{\sqrt{\pi}}\frac{\Gamma_{\rm in}}{\Gamma_{\rm out}}, \text{ and } D = \frac{1}{\sqrt{\pi}}\frac{\nu(\delta E)}{\nu(T)}\exp\left(-\frac{\delta E}{T}\right). \tag{4.81}$$

The width of the Lorentzian (4.80) is given by

$$\frac{1}{\tau_{\rm eff}} = \frac{1}{\tau}\frac{\Gamma_{\rm in}}{\Gamma_{\rm in}+\sqrt{\pi}\Gamma_{\rm out}} + \gamma_{\rm s}\frac{\sqrt{\pi}\Gamma_{\rm out}}{\Gamma_{\rm in}+\sqrt{\pi}\Gamma_{\rm out}}. \tag{4.82}$$

The first term here corresponds to the transitions from even- to odd-charge state involving the relaxation of a quasiparticle to the bottom of the trap. [cf. Eq. (4.21); difference in the numerical coefficients comes from rigorous solution of Eqs. (4.73), (4.77) and (4.78).] It is determined by the quasiparticle relaxation rate $1/\tau$ times the fraction of the time the unequilibrated quasiparticle spends in the box. The second term in Eq. (4.82) describes the transitions from odd to even state involving the escapes of a thermalized quasiparticle from the CPB by phonon activation. It is proportional to the phonon-assisted quasiparticle escape rate from the box to the lead γ_s times the probability to find an empty trap upon the escape of the thermalized quasiparticle. This probability is determined by the fraction of the time the trap spends in the even state upon the escape of the thermalized quasiparticle, and is determined by the fast processes involving $\Gamma_{\rm out}$ and $\Gamma_{\rm in}$.

At high frequencies, $\omega \gg \omega_{\rm cr}$, the dominant is the first term in the numerator of Eq. (4.78). Then, in the leading order in $1/\tau\Gamma_{\rm out}$ the power spectrum becomes

$$S_Q(\omega) \approx \frac{4e^2}{\Gamma_{\rm out}} \cdot \frac{CZ_1(\omega)\bar{\sigma}_{\rm e}}{\left(1+CZ_2(\omega)\right)^2 + \left(\frac{\omega}{\Gamma_{\rm out}}\right)^2 \left(CZ_1(\omega)\right)^2}. \tag{4.83}$$

Here the sums over momentum k in Eq. (4.78) are replaced with the integrals ($T \gg \delta_b$). In terms of the dimensionless variable z (4.48) these integrals are denoted as $Z_1(\omega)$ and $Z_2(\omega)$ [see Appendix D],

$$Z_1(\omega) \approx \int_0^\infty dz \frac{e^{-z}\sqrt{z}}{\left(\omega/\Gamma_{\rm out}\right)^2 z + 1},$$

$$Z_2(\omega) \approx \int_0^\infty dz \frac{e^{-z}}{\left(\omega/\Gamma_{\rm out}\right)^2 z + 1}. \tag{4.84}$$

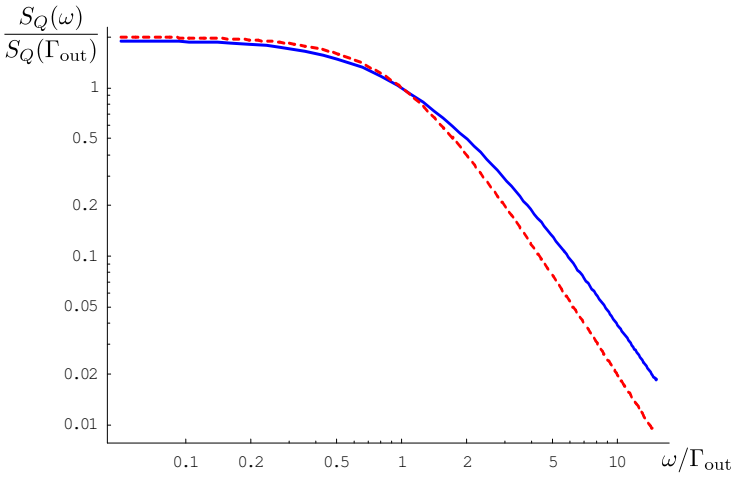

Figure 4.8: The deviations of the charge noise power spectrum $S_Q(\omega)$ from the Lorentzian function at high frequencies $\omega \sim \Gamma_{\rm out}$. Solid line corresponds to $S_Q(\omega)$ given by Eq. (4.86), dashed line is the normalized Lorentzian function with the width $\Gamma_{\rm out}$.

As shown in Fig. 4.7, in the frequency window $\omega_{\rm cr} \ll \omega \ll \Gamma_{\rm out}$ the noise power $S_Q(\omega)$ becomes flat with the amplitude

$$S_Q(\omega) \approx \frac{2\sqrt{\pi}e^2}{\Gamma_{\rm out}} \frac{C\bar{\sigma}_{\rm e}}{(1+C)^2}. \tag{4.85}$$

At higher frequencies $\omega \gtrsim \Gamma_{\rm out}$ and $C \ll 1$ the noise power spectrum (4.83) can be approximated by

$$S_Q(\omega) \approx \frac{4e^2}{\Gamma_{\rm out}} C Z_1(\omega) \bar{\sigma}_{\rm e} \tag{4.86}$$

with $Z_1(\omega)$ of Eq. (4.84). At these frequencies the charge noise power spectrum $S_Q(\omega)$ describes charge fluctuations due the tunneling of the unequilibrated quasiparticles from the box to the lead. By taking a Fourier transform of Eq. (4.86), one can notice that the noise power spectrum in time domain has the same functional form as $F(t)$ of Eq. (4.63). Therefore, charge noise power spectrum also reveals the deviations from the conventional Poisson statistics due to the singularity of the quasiparticle density of states at low energies. The deviations of the charge noise power spectrum (4.86) from the Lorentzian function at $\omega \sim \Gamma_{\rm out}$

are illustrated in Fig. (4.8). At higher frequencies $\omega \gg \Gamma_{\rm out}$ charge noise power spectrum $S_Q(\omega)$ decays as $1/\omega^2$, see Eq. (4.22).

4.6 Conclusion

In this Chapter we studied the kinetics of quasiparticle trapping and releasing in the mesoscopic superconducting island (Cooper-pair box). We found the lifetime distribution of even- and odd-charge states of the Cooper-pair box. We also calculated charge noise power spectrum generated by quasiparticle capture and emission processes.

The lifetime of the even-charge state is exponentially distributed random variable corresponding to homogenous Poisson process. However, the lifetime distribution of the odd-charge state may deviate from the exponential one. The deviations come from two sources - the peculiarity of the quasiparticle density of states in a superconductor, and the possibility of quasiparticle energy relaxation via phonon emission. Odd-charge-state lifetime distribution function depends on the ratio of the escape rate of unequilibrated quasiparticle from the box $\Gamma_{\rm out}$ and quasiparticle energy relaxation rate $1/\tau$.

The conventional Poissonian statistics for both quasiparticle entrances to and exits from the Cooper-pair box would lead to a Lorentzian spectral density $S_Q(\omega)$ of CPB charge fluctuations [55]. The interplay of tunneling and relaxation rates in the exit events may result in deviations from the Lorentzian function. In the case of slow quasiparticle thermalization rate compared to the quasiparticle tunneling out rate $\Gamma_{\rm out}$, the function $S_Q(\omega)$ roughly can be viewed as a superposition of two Lorentzians. The width of the first one is controlled by the processes involving quasiparticle thermalization and activation by phonons, while the width of the broader one is of the order of the escape rate $\Gamma_{\rm out}$.

Chapter 5

Renormalization of the even-odd energy difference by quantum charge fluctuations

From the viewpoint of quantum many-body phenomena, superconducting quantum circuits are good systems to study the effect of quantum fluctuations of an environment on the discrete spectrum of charge states [34, 65–68] (similar to the Lamb shift in a hydrogen atom). While most of the studies of superconducting nanostructures focus on smearing of the charge steps in the Coulomb staircase measurements [69–71], here we consider another observable quantity - even-odd-electron energy difference δE in the Cooper-pair box (CPB). This quantity is important for understanding of the quasiparticle "poisoning" effect, see Ch. 4, and it has been recently studied experimentally [37, 38]. It was conjectured that δE may be reduced in the strong tunneling regime $g_{_T} = R_q/R_{_T} > 1$ by quantum fluctuations of the charge [37]. Here R_q and $R_{_T}$ are the resistance quantum, $R_q = h/e^2$, and normal-state resistance of the tunnel junction, respectively.

In this Chapter, we study the renormalization of the discrete spectrum of

charge states of the Cooper-pair box by quantum charge fluctuations. We show that virtual tunneling of electrons across the tunnel junction may lead to a substantial reduction of the even-odd energy difference δE. We consider here the case of the tunnel junction with a large number of low transparency channels [12].

The dynamics of the system is described by the Hamiltonian

$$H = H_{_C} + H^b_{\rm BCS} + H^r_{\rm BCS} + H_{_T}. \tag{5.1}$$

Here $H^b_{\rm BCS}$ and $H^r_{\rm BCS}$ are BCS Hamiltonians for the CPB and superconducting reservoir; $H_{_C} = E_c(\hat{Q}/e - N_g)^2$ with E_c, N_g, and $\hat{Q}$ being the charging energy, dimensionless gate voltage and charge of the CPB, respectively. The tunneling Hamiltonian $H_{_T}$ is defined in the conventional way, see Eq. (2.8). We assume that the island and reservoir are isolated from the rest of the circuit; *i.e.*, total number of electrons in the system is fixed. At low temperature $T < T^*$, thermal quasiparticles are frozen out. [Here $T^* = \frac{\Delta}{\ln(\Delta/\delta)}$ with Δ and δ being the superconducting gap and mean level spacing in the reservoir, respectively]. If the total number of electrons in the system is even, then the only relevant degree of freedom at low energies is the phase difference across the junction φ. In the case of an odd number of electrons, a quasiparticle resides in the system even at zero temperature. The presence of $1e$-charged carriers changes the periodicity of the CPB energy spectrum (see Fig. 5.1) since an unpaired electron can reside in the island or in the reservoir. Note that at $N_g = 1$, a working point for the charge qubit, the odd-electron state of the CPB may be more favorable, resulting in trapping of a quasiparticle in the island [37, 38, 72]. In order to understand the energetics of this trapping phenomenon, one has to look at the ground state energy difference δE between the even-charge state (no quasiparticles in the CPB),

[12] The effective action method used here is applicable for tunnel junctions of a wide area with large number of transverse channels $N_{ch} \sim Sk_F^2 \gg 1$. This approach does not take into account the possibility of higher-order tunneling processes, *e.g.*, Andreev tunneling. However, such processes can be neglected as long as the effective number of transverse channels is large, see Ch. 6 and references therein for more details.

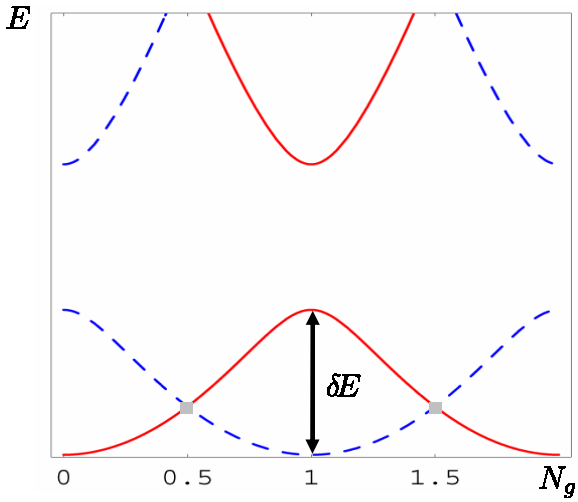

Figure 5.1: Energy of the Cooper-pair box as a function of dimensionless gate voltage N_g in units of e. The solid line corresponds to even-charge state of the box; dashed line corresponds to the odd-charge state of the box. Here, δE is the ground state energy difference between the even-charge state (no quasiparticles in the CPB) and odd-charge state (an unpaired electron in the CPB) at $N_g = 1$. (We assume here equal gap energies in the box and reservoir, $\Delta_r = \Delta_b = \Delta$.)

and odd-charge state (with a quasiparticle in the CPB):

$$\delta E = E_{\rm even}(N_g{=}1) - E_{\rm odd}(N_g{=}1), \tag{5.2}$$

see also Fig. 5.1. For equal gap energies in the box and the reservoir ($\Delta_r = \Delta_b = \Delta$), the activation energy δE is determined by the effective charging energy of the CPB. Note that tunneling of an unpaired electron into the island shifts the net charge of the island by $1e$. Thus, one can find δE of Eq. (5.2) as the energy difference at two values of the induced charge, $N_g = 1$ and $N_g = 0$, on the even-electron branch of the spectrum (see Fig. 5.1):

$$\delta E \;=\; E_{\rm even}(N_g{=}1) - E_{\rm even}(N_g{=}0). \tag{5.3}$$

Here we assumed that subgap conductance due to the presence of an unpaired electron is negligible [59].

In order to find the activation energy δE given by Eq. (5.3), we calculate the partition function $Z(N_g)$ for the system, island and reservoir, with an even

number of electrons. For the present discussion, it is convenient to calculate the partition function using the path-integral description developed by Ambegaokar *et. al* [73–75]. In this formalism, the quadratic in $\hat{Q}$ interaction in Eq. (5.1) is decoupled with the help of Hubbard-Stratonovich transformation by introducing an auxiliary field φ (conjugate to the excess number of Cooper pairs on the island). Then, the fermion degrees of freedom are traced out, and around the BCS saddle-point, the partition function becomes

$$Z(N_g) = \sum_{m=-\infty}^{\infty} e^{i\pi N_g m} \int d\varphi_0 \int_{\varphi(0)=\varphi_0}^{\varphi(\beta)=\varphi_0+2\pi m} D\varphi(\tau) e^{-S}. \tag{5.4}$$

Here, the summation over winding numbers accounts for the discreteness of the charge [76, 77] and the action S reads ($\hbar = 1$)

$$\begin{aligned} S &= \int_0^\beta d\tau \left[\frac{C_{\rm geom}}{2} \left(\frac{\dot{\varphi}(\tau)}{2e} \right)^2 - E_{_J} \cos\varphi(\tau) \right] \\ &+ \int_0^\beta d\tau \int_0^\beta d\tau' \alpha(\tau-\tau') \left\{ 1 - \cos\left[\frac{\varphi(\tau)-\varphi(\tau')}{2} \right] \right\}, \end{aligned} \tag{5.5}$$

with β being the inverse temperature, $\beta = 1/T$. Here $C_{\rm geom}$ is the geometric capacitance of the CPB, which determines the bare charging energy $E_c = e^2/2C_{\rm geom}$, and $E_{_J}$ is Josephson coupling given by the Ambegaokar-Baratoff relation. The last term in Eq. (5.5) accounts for single electron tunneling with kernel $\alpha(\tau)$ decaying exponentially at $\tau \gg \Delta^{-1}$ [73–75]. For sufficiently large capacitance, the evolution of the phase is slow in comparison with Δ^{-1}, and we can simplify the last term in Eq. (5.5) as

$$\int_0^\beta d\tau \int_0^\beta d\tau' \alpha(\tau-\tau') \left\{ 1 - \cos\left(\frac{\varphi(\tau)-\varphi(\tau')}{2} \right) \right\} \approx \frac{3\pi^2}{128} \frac{1}{2\pi e^2 R_{_T} \Delta} \int_0^\beta d\tau \left(\frac{d\varphi(\tau)}{d\tau} \right)^2.$$

It follows from here that virtual tunneling of electrons between the island and reservoir leads to the renormalization of the capacitance [73–75]

$$C_{\rm geom} \to \tilde{C} = C_{\rm geom} + \frac{3\pi}{32} \frac{1}{R_{_T}\Delta}. \tag{5.6}$$

Within the approximation (5.6), the effective action acquires a simple form

$$S_{\text{eff}} = \int_0^\beta d\tau \left[\frac{\tilde{C}}{2} \left(\frac{\dot{\varphi}(\tau)}{2e} \right)^2 - E_J \cos\varphi(\tau) \right]. \tag{5.7}$$

To calculate $Z(N_g)$, one can use the analogy between the present problem and that of a quantum-particle moving in a periodic potential, and write the functional integral as a quantum mechanical propagator from $\varphi_i = \varphi_0$ to $\varphi_f = \varphi_0 + 2\pi m$ during the (imaginary) "time" β

$$\int_{\varphi(0)=\varphi_0}^{\varphi(\beta)=\varphi_0+2\pi m} D\varphi(\tau) \exp(-S_{\text{eff}}) = \langle \varphi_0 | e^{-\beta \hat{H}_{\text{eff}}} | \varphi_0 + 2\pi m \rangle \,. \tag{5.8}$$

The time-independent "Shrödinger equation" corresponding to this problem has the form [78]

$$\hat{H}_{\text{eff}} \Psi(\varphi) = E\Psi(\varphi), \; \hat{H}_{\text{eff}} = \left(-4\tilde{E}_c \frac{\partial^2}{\partial \varphi^2} - E_J \cos\varphi \right). \tag{5.9}$$

Here, $\tilde{E}_c$ denotes renormalized charging energy

$$\tilde{E}_c = \frac{E_c}{1 + \frac{3}{32} g_T \frac{E_c}{\Delta}}. \tag{5.10}$$

One can notice that Eq. (5.9) corresponds to the well-known Mathieu equation, for which eigenfunctions $\Psi_{k,s}(\varphi)$ are known [79, 80], see also Appendix A. Here, quantum number s labels Bloch band ($s = 0, 1, 2, ...$), and k corresponds to the "quasimomentum". By rewriting the propagator (5.8) in terms of the eigenfunctions of the Shrödinger equation (5.9), we obtain

$$\begin{aligned} \langle \varphi_0 | \, e^{-\beta \hat{H}_{\text{eff}}} \, | \varphi_0 + 2\pi m \rangle &= \sum_{k,k'} \langle \varphi_0 \| \, k \rangle \langle k | \, e^{-\beta \hat{H}_{\text{eff}}} \, | k' \rangle \langle k' \| \varphi_0 + 2\pi m \rangle \\ &= \sum_{k,s} \Psi^*_{k,s}(\varphi_0) \Psi_{k,s}(\varphi_0 + 2\pi m) \exp(-\beta E_s(k)) \,, \end{aligned} \tag{5.11}$$

where $E_s(k)$ are eigenvalues of Eq. (5.9).

According to the Bloch theorem, the eigenfunctions should have the form $\Psi_{k,s}(\varphi) = e^{ik\varphi/2} u_{k,s}(\varphi)$, with $u_{k,s}(\varphi)$ being 2π-periodic functions, $u_{k,s}(\varphi) =$

$u_{k,s}(\varphi + 2\pi)$. We can now rewrite Eq. (5.4) as

$$\begin{aligned} Z(N_g) &= \sum_{m=-\infty}^{\infty} e^{i\pi N_g m} \int d\varphi_0 \sum_{k,s} \Psi^*_{k,s}(\varphi_0)\Psi_{k,s}(\varphi_0+2\pi m) \exp\left(-\beta E_s(k)\right) \\ &= \sum_{s=0,1}^{\infty} \exp\left(-\beta E_s\left(N_g\right)\right). \end{aligned} \tag{5.12}$$

The eigenvalues $E_s(N_g)$ are given by the Mathieu characteristic functions $M_A(r,q)$ and $M_B(r,q)$ [60, 81]. At $N_g = 0$ and $N_g = 1$, the exact solution for the lowest band reads

$$\begin{aligned} E_0(N_g = 0) &= \tilde{E}_c M_A\left(0, -\frac{E_{_J}}{2\tilde{E}_c}\right), \\ E_0(N_g = 1) &= \tilde{E}_c M_A\left(1, -\frac{E_{_J}}{2\tilde{E}_c}\right). \end{aligned} \tag{5.13}$$

The activation energy δE can be calculated from Eq. (5.12) by evaluating the free energy at $T = 0$:

$$\delta E = \tilde{E}_c \left[M_A\left(1, -\frac{E_{_J}}{2\tilde{E}_c}\right) - M_A\left(0, -\frac{E_{_J}}{2\tilde{E}_c}\right)\right]. \tag{5.14}$$

The plot of δE as a function of $E_{_J}/2\tilde{E}_c$ is shown in Fig. (5.2). Even-odd energy difference δE has the following asymptotes:

$$\delta E \approx \begin{cases} \tilde{E}_c - \frac{1}{2}E_{_J}, & E_{_J}/2\tilde{E}_c \ll 1, \\ 2^5\sqrt{\frac{2}{\pi}}\tilde{E}_c \left(\frac{E_{_J}}{2\tilde{E}_c}\right)^{3/4} \exp\left(-4\sqrt{\frac{E_{_J}}{2\tilde{E}_c}}\right), & E_{_J}/2\tilde{E}_c \gg 1. \end{cases}$$

These asymptotes can also be obtained using perturbation theory and Wentzel-Kramers-Brillouin approximation, respectively.

As one can see from Eq. (5.14), δE can be reduced by quantum charge fluctuations. For realistic experimental parameters [37], $\Delta \approx 2.5$K, $E_c \approx 2$K and $g_{_T} \approx 2$, we find that even-odd energy difference δE is 15% smaller with respect to its bare value, *i.e.*, $\delta E \approx 1.45$K and $\delta E^{\rm bare} \approx 1.7$K. Since the reduction of the

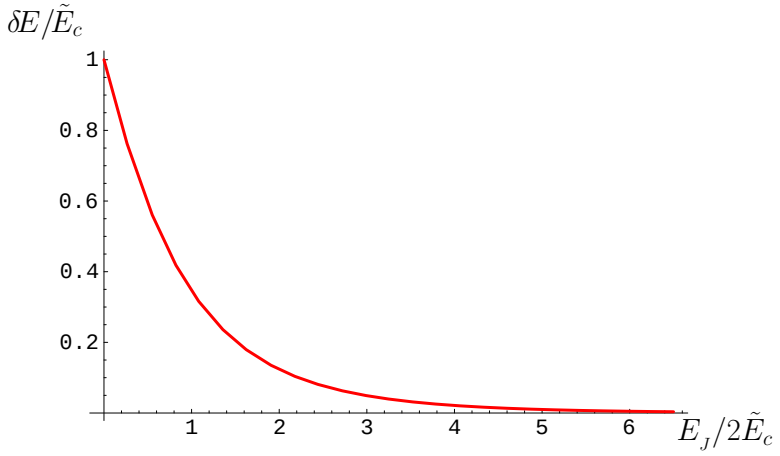

Figure 5.2: Dependence of the even-odd energy difference δE on the dimensionless parameter $E_J/2\tilde{E}_c$.

activation energy by quantum fluctuations is much larger than the temperature, this effect can be observed experimentally. The renormalization of δE can be studied systematically by decreasing the gap energy Δ, which can be achieved by applying magnetic field B [34]. The dependence of the activation energy δE on $\Delta(B)$ in Eq. (5.14) enters through the Josephson energy E_J, which is given by the Ambegaokar-Baratoff relation, and renormalized charging energy $\tilde{E}_c$ of Eq. (5.10).

The renormalization of the discrete spectrum of charge states in the CPB becomes more pronounced in the strong tunneling regime. However, the adiabatic approximation leading to the effective action $S_{\rm eff}$ (5.7) is valid when the evolution of the phase is slow, *i.e.*, the adiabatic parameter ω_J/Δ is small. (Here, ω_J is the plasma frequency of the Josephson junction, $\omega_J \sim \sqrt{E_c E_J}$.) Thus, at large conductances g_T, the adiabatic approximation holds only when the geometric capacitance is large $C_{\rm geom} \gg e^2 g_T/\Delta$. Under such conditions, the renormalization effects lead to a small correction of the capacitance, see Eq. (5.6). If $\omega_J/\Delta > 1$, the dynamics of the phase is described by the integral equation (5.5), and retardation effects have to be included.

In a similar circuit corresponding to the Cooper-pair box qubit [20, 21], it is

possible to achieve the strong tunneling regime, $g_T \gg \Delta C_{\rm geom}/e^2$, and satisfy the requirements for adiabatic approximation ($\omega_J/\Delta \ll 1$). In this circuit, a single Josephson junction is replaced by two junctions in a loop configuration [20, 21]. This allows one to control the effective Josephson energy using the external flux Φ_x. (For the CPB qubit, the Josephson energy E_J in Eq. (5.7) should be replaced with $E_J(\Phi_x) = E_{J,\max}\cos(\pi\Phi_x/\Phi_0)$; here, Φ_0 is the magnetic flux quantum, $\Phi_0 = h/2e$.) In this setup, even at large conductance $g_T \gg \Delta C_{\rm geom}/e^2$ one can decrease $\omega_J \sim \sqrt{E_c E_J(\Phi_x)}$ by adjusting the external magnetic flux to satisfy $\omega_J/\Delta \ll 1$. Under such conditions, the quantum contribution to the capacitance $\tilde{C}$ (see Eq. (5.6)) becomes larger than the geometric one, while the dynamics of the phase is described by the simple action of Eq. (5.7). It would be interesting to study experimentally the renormalization of the discrete energy spectrum of the qubit in this regime. We propose to measure, for example, the even-odd energy difference δE. In this case, δE is determined by the conductance of the junctions g_T, superconducting gap Δ, and magnetic flux Φ_x, and is given by Eq. (5.14) with $\tilde{E}_c \approx 32\Delta/3g_T$ [see Eq. (5.10)] and $E_J = E_{J,\max}\cos(\pi\Phi_x/\Phi_0)$.

In conclusion, we studied the renormalization of the discrete spectrum of charge states of the Cooper-pair box by virtual tunneling of electrons across the junction. In particular, we calculated the reduction of even-odd energy difference δE by quantum charge fluctuations. We showed that under certain conditions, the contribution of quantum charge fluctuations to the capacitance of the Cooper-pair box may become larger than the geometric one. We propose to study this effect experimentally using the Cooper-pair box qubit.

Chapter 6

Energy relaxation of a charge qubit via Andreev processes

6.1 Introduction

In this Chapter we study fundamental limitations on the energy relaxation time in a charge qubit with a large-gap Cooper-pair box. For equal gap energies in the box and reservoir, $\Delta_b = \Delta_r$, the mechanisms of energy relaxation rate due to quasiparticles were discussed in Chapter 3. The energy relaxation rate was found to be

$$\frac{1}{T_1} \propto \frac{g_T n_{\rm qp}}{\hbar \nu_F} \sqrt{\frac{T}{E_J}} \tag{6.1}$$

with $n_{\rm qp}$, g_T and ν_F being the density of quasiparticles in the reservoir, dimensionless conductance of the junction and density of states at the Fermi level, respectively. The relaxation rate $1/T_1$ in Eq. (6.1) was derived under the assumption that an unpaired electron tunnels from the reservoir to the box to minimize the energy of the system. Indeed, for $\Delta_b = \Delta_r$, the odd-charge state of the CPB has lower energy at $N_g = 1$ due to the Coulomb blockade effect. By

properly engineering superconducting gap energies (*i.e.* by inducing large gap mismatch, $\Delta_b > \Delta_r$), one can substantially reduce quasiparticle tunneling rate to the Cooper-pair box. Gap energies in superconductors can be modified by oxygen doping [31], applying magnetic field [32, 82], and adjusting layer thickness [38, 39]. Suppose initially the qubit is in the excited state with energy $E_{|+\rangle}$, and the quasiparticle is in the reservoir with energy E_p. Upon quasiparticle tunneling to the box, the minimum energy of the final state is $E_f^{\min} = \Delta_b + E_{N+1}$ with E_{N+1} being the energy of the CPB in the odd-charge state. Therefore, the threshold energy for a quasiparticle to tunnel to the box is $E_p^{\min} = \Delta_b + E_{N+1} - E_{|+\rangle}$, see also Fig. 6.1. If $E_p^{\min} - \Delta_r \gtrsim E_J \gg T$, only exponentially small fraction of quasiparticles in the reservoir are able to tunnel into the island. (Note that the energy difference between excited and ground state of a charge qubit is E_J, while the energy of the qubit in the excited state is $E_{|+\rangle} = E_c + E_J/2$. Here E_c, E_J and T are the charging energy of the CPB, the Josephson energy associated with the tunnel junction, and the temperature, respectively.) Thus, the contribution to the qubit relaxation rate T_1^{-1} from the processes involving real quasiparticle tunneling to the island becomes

$$\frac{1}{T_1} \propto \frac{g_T n_{\rm qp}}{\hbar \nu_F} \exp\left(-\frac{\Delta_b - \Delta_r - E_c - E_J/2}{T}\right), \tag{6.2}$$

and is much smaller than the one of Eq. (6.1). However, there is also a mechanism of qubit energy relaxation originating from the higher order tunneling processes (Andreev reflection). The contribution of these processes to the qubit relaxation is activationless, and can be much larger than the one of Eq. (6.2). In this Chapter we discuss qubit energy relaxation due to Andreev processes in detail.

Figure 6.1: The spectrum of the Cooper-pair box as a function of the dimensionless gate voltage in the case of a large gap mismatch, $\Delta_b > \Delta_r$. The solid and dashed lines correspond to an even- and odd-charge state of the box, respectively.

6.2 Theoretical model

Dynamics of the Cooper-pair box coupled to the superconducting reservoir through the tunnel junction is described by the Hamiltonian

$$H = H_C + H^b_{\rm BCS} + H^r_{\rm BCS} + H_T. \tag{6.3}$$

Here $H^b_{\rm BCS}$ and $H^r_{\rm BCS}$ are BCS Hamiltonians for the box and reservoir; $H_C = E_c(Q/e - N_g)^2$ with N_g and Q being the dimensionless gate voltage and the charge of the CPB, respectively. We consider the following energy scale hierarchy: $\Delta_b > \Delta_r, E_c > E_J \gg T$. In order to distinguish between Cooper pair and quasiparticle tunneling, we present the Hamiltonian (6.3) in the form [44]

$$H = H_0 + V, \text{ and } V = H_T - H_J. \tag{6.4}$$

Here $H_0 = H_C + H^b_{\rm BCS} + H^r_{\rm BCS} + H_J$, and H_J is the Hamiltonian describing Josephson tunneling

$$H_J = |N\rangle \langle N| H_T \frac{1}{E - H_0} H_T |N+2\rangle \langle N+2| + \text{H.c.}$$

The matrix element $\langle N|\, H_{_T} \frac{1}{E-H_0} H_{_T}\, |N+2\rangle$ is proportional to the Josephson energy $E_{_J}$. The perturbation Hamiltonian V defined in Eq. (6.4) is suitable for calculation of the quasiparticle tunneling rate. The tunneling Hamiltonian for homogeneous insulating barrier is

$$H_T = \sum_\sigma \int d\mathbf{x} d\mathbf{x}' \left(T(\mathbf{x},\mathbf{x}') \Psi_\sigma^\dagger(\mathbf{x}) \Psi_\sigma(\mathbf{x}') + \text{H.c.} \right), \tag{6.5}$$

where $\mathbf{x}$ and $\mathbf{x}'$ denote the coordinates in the CPB and reservoir, respectively, and $T(\mathbf{x},\mathbf{x}')$, in the limit of a barrier with low transparency, is defined as

$$T(\mathbf{x},\mathbf{x}') = \frac{1}{4\pi^2} \sqrt{\frac{\mathcal{T}}{\nu_F^2}} \delta^2(\mathbf{r}-\mathbf{r}') \delta(z) \delta(z') \frac{\partial}{\partial z} \frac{\partial}{\partial z'}. \tag{6.6}$$

Here $\mathcal{T}$ is the transmission coefficient of the barrier, $\mathbf{r}$ and z are the coordinates in the plane of the tunnel junction and perpendicular to it, respectively. The Hamiltonian (6.5) along with the above definition of $T(\mathbf{x},\mathbf{x}')$ properly takes into account the fact in the tunnel-Hamiltonian approximation the wavefunctions turn to zero at the surface of the junction [70, 83]. In terms of the transmission coefficient $\mathcal{T}$, the dimensionless conductance of the tunnel junction $g_{_T}$ can be defined as $g_{_T} = \mathcal{T} S_J k_F^2 / 4\pi = \frac{1}{3} \mathcal{T} N_{\text{ch}}$, where S_J is the area of the junction, and N_{ch} is the number of transverse channels in the junction.

The energy relaxation rate of the qubit due to higher-order processes is given by

$$\Gamma_A = \frac{2\pi}{\hbar} \sum_{p,p'} \; 2 \; |A_{p'p}|^2 \delta(E_{p'} - E_p - E_{_J}) f_{_F}(E_p)(1 - f_{_F}(E_{p'})). \tag{6.7}$$

Here $f_{_F}(E_p)$ is the Fermi distribution function with $E_p = \sqrt{\varepsilon_p^2 + \Delta_r^2}$ being the energy of a quasiparticle in the reservoir. The amplitude $A_{p'p}$ is given by the second order perturbation theory in V,

$$A_{p'p} = \langle -, E_{p'\uparrow}|\, V \frac{1}{E_i - H_0} V\, |+, E_{p\uparrow}\rangle\,. \tag{6.8}$$

At $E_c \gg E_J$ and $N_g = 1$, the eigenstates of the qubit are given by the symmetric and antisymmetric superposition of two charge states, *i.e.* $|-\rangle = \frac{|N\rangle+|N+2\rangle}{\sqrt{2}}$ and $|+\rangle = \frac{|N\rangle-|N+2\rangle}{\sqrt{2}}$ with the corresponding eigenvalues $E_{|\pm\rangle} = E_c \pm E_J/2$. In the initial moment of time, the qubit is prepared in the excited state and the quasiparticle is in the reservoir, *i.e* $|+, E_{p\uparrow}\rangle \equiv |+\rangle \otimes |E_{p\uparrow}\rangle$. The energy of the initial state of the system is $E_i = E_p + E_{|+\rangle}$. The denominator in the amplitude (6.8) corresponds to the formation of the virtual intermediate state when the quasiparticle has tunnelled to the island from the reservoir. Since a quasiparticle is a superposition of a quasi-electron and quasi-hole, the contributions to $A_{p'p}$ come from two interfering paths:

$$A_{p'p} = \frac{1}{2}\left[\left\langle N+2, p'_\uparrow\right| V \frac{1}{E_i - H_0} V \left|N, p_\uparrow\right\rangle - \left\langle N, p'_\uparrow\right| V \frac{1}{E_i - H_0} V \left|N+2, p_\uparrow\right\rangle\right]. \tag{6.9}$$

To calculate the amplitude $A_{p'p}$ we use particle-conserving Bogoliubov transformation [41, 42]

$$\begin{aligned} \gamma^\dagger_{n\sigma} &= \int d\mathbf{x}\left[U_n(\mathbf{x})\Psi^\dagger_\sigma(\mathbf{x}) - \sigma V_n(\mathbf{x})\Psi_{-\sigma}(\mathbf{x})R^\dagger\right], \\ \gamma_{n\sigma} &= \int d\mathbf{x}\left[U_n(\mathbf{x})\Psi_\sigma(\mathbf{x}) - \sigma V_n(\mathbf{x})\Psi^\dagger_{-\sigma}(\mathbf{x})R\right]. \end{aligned} \tag{6.10}$$

The operators $R^\dagger$ and R transform a given state in an N-particle system into the corresponding state in the $N+2$ and $N-2$ particle system, respectively, leaving the quasiparticle distribution unchanged, *i.e.* $R^\dagger |N\rangle = |N+2\rangle$. Thus, quasiparticle operators $\gamma^\dagger_{n\sigma}$ and $\gamma_{n\sigma}$ defined in Eq. (6.10) do conserve particle number [13]. The transformation coefficients $U_n(\mathbf{x})$ and $V_n(\mathbf{x})$ are given by the solution of Bogoliubov-de Gennes equation. For spatially homogenous superconducting gap Δ, the functions $U_n(\mathbf{x})$ and $V_n(\mathbf{x})$ can be written as $U_n(\mathbf{x}) = u_n\phi_n(\mathbf{x})$ and $V_n(\mathbf{x}) = v_n\phi_n(\mathbf{x})$. The coherence factors u_n and v_n are given by

$$u_n^2 = \frac{1}{2}\left(1 + \frac{\varepsilon_n}{E_n}\right), \text{ and } v_n^2 = \frac{1}{2}\left(1 - \frac{\varepsilon_n}{E_n}\right).$$

[13] We apply this transformation to a Cooper-pair box assuming that it is not very small, *i.e* $\Delta_b \gg T \gg \delta_b$. Here δ_b is the mean level spacing in the box

Here $E_n = \sqrt{\varepsilon_n^2 + \Delta^2}$; ε_n and $\phi_n(\mathbf{x})$ are exact eigenvalues and eigenfunctions of the single-particle Hamiltonian, which may include random potential $\mathcal{V}(\mathbf{x})$, *e.g.*, due to impurities. The single-particle energies ε_n and wavefunctions $\phi_n(\mathbf{x})$ are defined by the following Shrödinger equation:

$$\left[-\frac{\hbar^2}{2m}\vec{\nabla}^2 + \mathcal{V}(\mathbf{x})\right]\phi_n(\mathbf{x}) = \varepsilon_n\phi_n(\mathbf{x}).$$

In the presence of time-reversal symmetry u_n, v_n and $\phi_n(\mathbf{x})$ can be taken to be real. Then with the help of Eq. (6.10), we obtain the amplitude of the process $A_{p'p}$:

$$\begin{aligned} A_{p'p} \;=\; & \frac{1}{2}\int d\mathbf{x_1}d\mathbf{x_1'}d\mathbf{x_2}d\mathbf{x_2'}T(\mathbf{x_1},\mathbf{x_1'})T(\mathbf{x_2},\mathbf{x_2'})\left[U_{p'}(\mathbf{x_1'})V_p(\mathbf{x_2'}) - U_p(\mathbf{x_1'})V_{p'}(\mathbf{x_2'})\right] \\ & \times \sum_k \frac{U_k(\mathbf{x_1})V_k(\mathbf{x_2})}{E_p + \omega_+ - E_k}, \end{aligned} \tag{6.11}$$

where $\omega_+ \equiv E_{|+\rangle} - E_{N+1} = E_c + E_J/2$. The minus sign in parenthesis here reflects the destructive interference between quasi-electron and quasi-hole contributions, see also Eq. (6.9).

6.3 Disorder averaging

It is well-known that Andreev conductance is sensitive to disorder, see, for example, Refs. [84, 85]. Similarly, the rate Γ_A is affected by coherent electron backscattering to the tunnel junction, see Fig. 6.2. If a quasiparticle bounces off the walls of the box or impurities many times, it is reasonable to expect the chaotization of its motion. Thus, one is prompted to consider ensemble-averaged quantities rather than their particular realization. Using Eqs. (6.7) and (6.11), we obtain

$$\begin{aligned} \langle\Gamma_A\rangle = \; & \frac{\pi}{\hbar}\langle\sum_{p,p'}\int\prod_{i=1..4} d\mathbf{x_i}d\mathbf{x_i'}T(\mathbf{x_1},\mathbf{x_1'})T(\mathbf{x_2},\mathbf{x_2'})T(\mathbf{x_3},\mathbf{x_3'})T(\mathbf{x_4},\mathbf{x_4'}) \\ & \times \left(u_{p'}v_p\phi_{p'}(\mathbf{x_1'})\phi_p(\mathbf{x_2'}) - u_pv_{p'}\phi_p(\mathbf{x_1'})\phi_{p'}(\mathbf{x_2'})\right)\left(u_{p'}v_p\phi_{p'}(\mathbf{x_3'})\phi_p(\mathbf{x_4'}) - u_pv_{p'}\phi_p(\mathbf{x_3'})\phi_{p'}(\mathbf{x_4'})\right) \\ & \times \sum_k \frac{u_kv_k\phi_k(\mathbf{x_1})\phi_k(\mathbf{x_2})}{E_p+\omega_+-E_k}\sum_{k'}\frac{u_{k'}v_{k'}\phi_{k'}(\mathbf{x_3})\phi_{k'}(\mathbf{x_4})}{E_p+\omega_+-E_{k'}}\delta(E_{p'}-E_p-E_J)f_F(E_p)(1-f_F(E_{p'}))\rangle. \end{aligned} \tag{6.12}$$

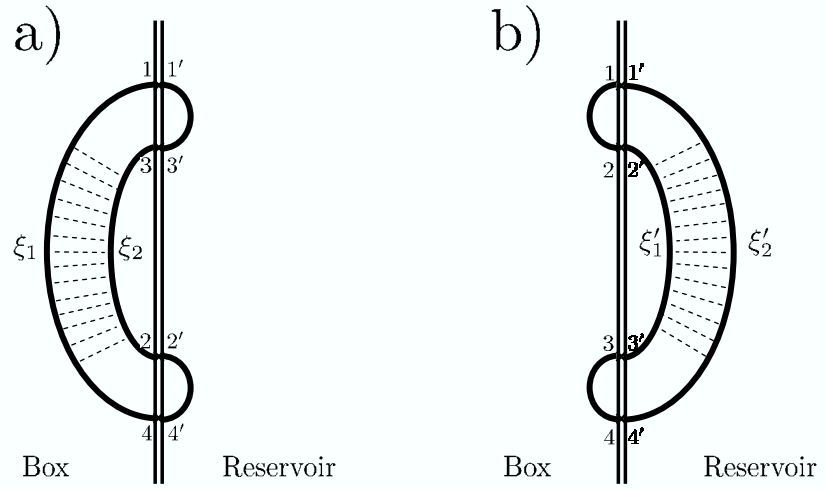

Figure 6.2: The diagrams corresponding to the interference of electron trajectories in the box (a) and reservoir (b). The contribution of the diagrams with interference in both electrodes (not shown) is much smaller than the one of the above diagrams [84].

Here the brackets $\langle ... \rangle$ denote averaging independently over different realizations of the random potential in the box and reservoir. In order to average over the disorder in the CPB, one has to calculate the following correlation function:

$$I \equiv \left\langle \sum_{k,k'} \frac{u_k v_k \phi_k(\mathbf{x_1})\phi_k(\mathbf{x_2})}{E_p+\omega_+-E_k} \frac{u_{k'} v_{k'} \phi_{k'}(\mathbf{x_3})\phi_{k'}(\mathbf{x_4})}{E_p+\omega_+-E_{k'}} \right\rangle$$

$$= \int \frac{\Delta_b^2 d\xi_1 d\xi_2}{4E(\xi_1)E(\xi_2)} \frac{\langle K_{\xi_1}(\mathbf{x_1},\mathbf{x_2}) K_{\xi_2}(\mathbf{x_3},\mathbf{x_4})\rangle}{[E_p+\omega_+-E(\xi_1)][E_p+\omega_+-E(\xi_2)]}, \tag{6.13}$$

where $K_\xi(\mathbf{x_1},\mathbf{x_2}) = \sum_k \phi_k(\mathbf{x_1})\phi_k(\mathbf{x_2})\delta(\epsilon_k - \xi)$, and $E(\xi) = \sqrt{\xi^2+\Delta_b^2}$. The correlation function $\langle K_{\xi_1}(\mathbf{x_1},\mathbf{x_2}) K_{\xi_2}(\mathbf{x_3},\mathbf{x_4})\rangle$ consists of reducible and irreducible parts,

$$\begin{aligned} \langle K_{\xi_1}(\mathbf{x_1},\mathbf{x_2}) K_{\xi_2}(\mathbf{x_3},\mathbf{x_4})\rangle &= \langle K_{\xi_1}(\mathbf{x_1},\mathbf{x_2})\rangle \langle K_{\xi_2}(\mathbf{x_3},\mathbf{x_4})\rangle \\ &+ \langle K_{\xi_1}(\mathbf{x_1},\mathbf{x_2}) K_{\xi_2}(\mathbf{x_3},\mathbf{x_4})\rangle_{\rm ir} \end{aligned} \tag{6.14}$$

The reducible part can be easily calculated by relating $\langle K_\xi(\mathbf{x_1},\mathbf{x_2})\rangle$ to the ensemble-averaged Green function: $\langle K_\xi(\mathbf{x_1},\mathbf{x_2})\rangle \equiv -\frac{1}{\pi}\mathrm{Im}\langle G^R_\xi(\mathbf{x_1},\mathbf{x_2})\rangle = \nu_F f_{12}$. [Upon averaging over disorder, one can neglect energy dependence of the density of states here, *i.e.* $\langle\nu_F(\xi)\rangle = \nu_F$. The function f_{12} is given by $f_{12} = \langle e^{i\mathbf{k}(\mathbf{x_1}-\mathbf{x_2})}\rangle_{\mathrm{FS}}$ with $\langle ...\rangle_{\mathrm{FS}}$ being the average over electron momentum on the Fermi surface. For 3D system the function f_{12} is equal to $f_{12} = \frac{\sin(k_F|\mathbf{x_1}-\mathbf{x_2}|)}{k_F|\mathbf{x_1}-\mathbf{x_2}|}$.] The irreducible part $\langle K_{\xi_1}(\mathbf{x_1},\mathbf{x_2})K_{\xi_2}(\mathbf{x_3},\mathbf{x_4})\rangle_{\mathrm{ir}}$ can be expressed in terms of the classical diffusion propagators - diffusons and Cooperons, see, for example, Aleiner *et. al.* [86]. In the absence of magnetic field, diffusons and Cooperons coincide, $\mathcal{P}_\omega(\mathbf{x}_1,\mathbf{x}_2) = \mathcal{P}^D_\omega(\mathbf{x}_1,\mathbf{x}_2) = \mathcal{P}^C_\omega(\mathbf{x}_1,\mathbf{x}_2)$, and the irreducible part of the correlation function (6.14) reads

$$\begin{aligned}\langle K_{\xi_1}(\mathbf{x_1},\mathbf{x_2})K_{\xi_2}(\mathbf{x_3},\mathbf{x_4})\rangle_{\mathrm{ir}} &= \\ &= \frac{\nu_F}{\pi}\mathrm{Re}\left[f_{14}f_{23}\mathcal{P}_{|\xi_2-\xi_1|}(\mathbf{x}_1,\mathbf{x}_3)+f_{13}f_{24}\mathcal{P}_{|\xi_2-\xi_1|}(\mathbf{x}_1,\mathbf{x}_4)\right].\end{aligned} \tag{6.15}$$

The spectral expansion of $\mathcal{P}_\omega(\mathbf{x}_1,\mathbf{x}_2)$ for the diffusive system is

$$\mathcal{P}_\omega(\mathbf{x}_1,\mathbf{x}_2) = \sum_n \frac{f^*_n(\mathbf{x}_1)f_n(\mathbf{x}_2)}{-i\omega+\gamma_n}. \tag{6.16}$$

Here γ_n and $f_n(\mathbf{x})$ are the corresponding eigenvalues and eigenfunctions of the diffusion equation, $-D\vec{\nabla}^2 f_n(\mathbf{x}) = \gamma_n f_n(\mathbf{x})$, satisfying von Neumann boundary conditions in the box.

Equation (6.15) can be simplified in the case of large Thouless energy, *i.e.* $E_{_T} \gg \Delta_b, \Delta_r, E_c, E_{_J}$. (Here $E_{_T} = \hbar/\tau_D$ with $\tau_D \sim S_b/D$ being the time to diffuse through the box, and $S_b = \pi R_b^2$ being the area of the island, see Fig 6.3.) This condition is fulfilled for a small aluminum island [14] with $S_b \ll 1\mu m^2$ and mean free path $l \gtrsim 25nm$ [56], when the time spent by the virtual quasiparticle in the box, $t \sim \hbar/(\Delta_b - \Delta_r - \omega_+)$, is much longer than the classical diffusion time

[14] For an island shown in Fig. 6.3, $E_{_T} = 14.7\pi\hbar D/S_b$. The superconducting gap Δ_b can be expressed in terms of the diffusion constant D and the coherence length in a system with disorder, ξ_{dirty} - $\Delta_b = \frac{1.74}{2\pi}\hbar D/\xi^2_{dirty}$. Thus, the ratio $\Delta_b/E_{_T} \approx 6\cdot 10^{-3} S_b/\xi^2_{dirty} \ll 1$ sets the constraints on the size of the box.

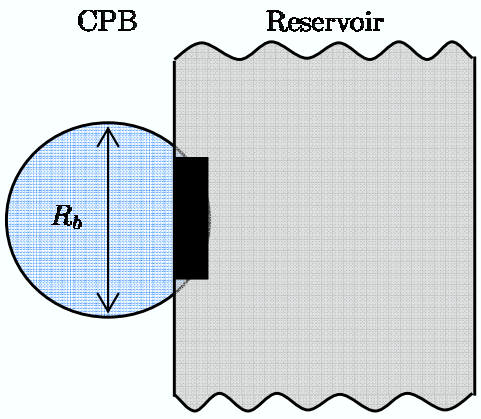

Figure 6.3: The layout of the Cooper-pair box qubit considered in the text.

τ_D [87]. In this case the irreducible part in Eq. (6.14) is given by the universal limit,

$$\langle K_{\xi_1}(\mathbf{x_1},\mathbf{x_2})K_{\xi_2}(\mathbf{x_3},\mathbf{x_4})\rangle_{\rm ir} = \frac{\nu_F}{V_b}\delta(\xi_1-\xi_2)(f_{14}f_{23}+f_{13}f_{24}). \tag{6.17}$$

Here V_b is the volume of the box. Upon substituting Eqs. (6.14) and (6.17) into Eq. (6.13) and evaluating the integrals over energies ξ_1 and ξ_2, we obtain

$$I = 4\nu_F^2 f_{12}f_{34}L_1\left[\frac{E_p+\omega_+}{\Delta_b}\right]+\nu_F^2\frac{\delta_b}{2\Delta_b}\left(f_{14}f_{23}+f_{13}f_{24}\right)L_2\left[\frac{E_p+\omega_+}{\Delta_b}\right], \tag{6.18}$$

where $\delta_b = 1/\nu_F V_b$ is the mean level spacing in the box. The functions $L_1(y)$ and $L_2(y)$ are defined as

$$\begin{aligned} L_1(y) &= \frac{1}{1-y^2}\arctan^2\left(\sqrt{\frac{1+y}{1-y}}\right), \\ L_2(y) &= \int_1^\infty dx \frac{1}{\sqrt{x^2-1}}\frac{1}{x(x-y)^2}. \end{aligned} \tag{6.19}$$

The expressions above are valid for $y<1$. The function $L_2(y)$ has the following asymptotes

$$L_2(y)\approx\begin{cases} \frac{\pi}{4}+\frac{4}{3}y, & y\ll 1, \\ \\ \frac{\pi}{2\sqrt{2}(1-y)^{3/2}}, & 1-y\ll 1. \end{cases} \tag{6.20}$$

After substituting Eq. (6.18) into Eq. (6.12) and averaging over disorder in the reservoir, we obtain the following expression for $\langle\Gamma_A\rangle$:

$$\begin{aligned}\langle\Gamma_A\rangle &= \frac{\pi\nu_F^2}{2\hbar}\int d\xi_1' d\xi_2' \delta(E(\xi_2')-E(\xi_1')-E_J) f_F[E(\xi_1')](1-f_F[E(\xi_2')]) \\ &\times \int\prod_{i=1..4} d\mathbf{x}_i d\mathbf{x}_i' T(\mathbf{x_1},\mathbf{x_1'})T(\mathbf{x_2},\mathbf{x_2'})T(\mathbf{x_3},\mathbf{x_3'})T(\mathbf{x_4},\mathbf{x_4'}) \\ &\times \left(4f_{12}f_{34}L_1\left[\frac{E(\xi_1')+\omega_+}{\Delta_b}\right]+\frac{\delta_b}{2\Delta_b}\left(f_{14}f_{23}+f_{13}f_{24}\right)L_2\left[\frac{E(\xi_1')+\omega_+}{\Delta_b}\right]\right) \\ &\times \left(1-\frac{\Delta_r^2}{E(\xi_1')E(\xi_2')}\right)\langle K_{\xi_1'}(\mathbf{x'}_1,\mathbf{x'}_3)K_{\xi_2'}(\mathbf{x'}_2,\mathbf{x'}_4)\rangle. \end{aligned} \tag{6.21}$$

Here the energy $E(\xi')$ is given by $E(\xi')=\sqrt{\xi'^2+\Delta_r^2}$. The correlation function in the reservoir $\langle K_{\xi_1'}(\mathbf{x'}_1,\mathbf{x'}_3)K_{\xi_2'}(\mathbf{x'}_2,\mathbf{x'}_4)\rangle$ follows from Eqs. (6.14) and (6.15). Using Eq. (6.6) and evaluating the spatial integrals over the area of the junction as well as the integrals over energies ξ_1', and ξ_2', we finally obtain the answer for $\langle\Gamma_A\rangle$:

$$\langle\Gamma_A\rangle = \Gamma_1+\Gamma_2 \tag{6.22}$$

with Γ_1 and Γ_2 being defined as

$$\Gamma_1 \approx \frac{2\pi}{\hbar}\frac{3C_1}{(4\pi^2)^2}\frac{g_T^2}{N_{\rm ch}}\sqrt{\frac{E_J}{2\Delta_r+E_J}}\frac{n_{\rm qp}}{\nu_F}L_1\left[\frac{\Delta_r+\delta E_+}{\Delta_b}\right], \tag{6.23}$$

and

$$\Gamma_2 \approx \frac{2\pi}{\hbar}\frac{g_T^2}{8(4\pi^2)^2}\frac{\delta_b}{\Delta_b}\sqrt{\frac{E_J}{2\Delta_r+E_J}}\frac{n_{\rm qp}}{\nu_F}L_2\left[\frac{\Delta_r+\delta E_+}{\Delta_b}\right]. \tag{6.24}$$

Here C_1 is a numerical constant of the order of one:

$$C_1 = \frac{1}{\pi^3 k_F^2 S_J}\int_{k_F^2 S_J} d\mathbf{y}_1 d\mathbf{y}_2 d\mathbf{y}_3 d\mathbf{y}_4 P_{12}P_{13}P_{24}P_{34}$$

with $\mathbf{y}$ being a dimensionless coordinate in the plane of a tunnel junction, and $P_{12}=\frac{\sin(|\mathbf{y}_1-\mathbf{y}_2|)-|\mathbf{y}_1-\mathbf{y}_2|\cos(|\mathbf{y}_1-\mathbf{y}_2|)}{|\mathbf{y}_1-\mathbf{y}_2|^3}$. The functions L_1 and L_2 are defined in Eq. (6.19), and their dependence on the ratio $(\Delta_r+\delta E_+)/\Delta_b$ is shown in Fig. 6.4. The rate

Γ_1 describes the contribution from the reducible terms, see Eq. (6.14), and is similar to the ballistic case when electron backscattering from the impurities or boundaries is negligible. The other term, Γ_2, reflects the enhancement of $\langle\Gamma_A\rangle$ in the diffusive limit due to the quantum interference of quasiparticle return trajectories [15], and originates from the irreducible contributions, see Fig. 6.2. In the case of $N_{\rm ch}\delta_b/\Delta_b \gg 1$, the contribution of this interference term becomes dominant, $\Gamma_2 \gg \Gamma_1$. The contribution of the interference in the reservoir to the rate Γ_2, see Fig. 6.2b, is geometry dependent. For a typical Cooper-pair box qubit with a small junction connected to a large electrode, backscattering of electrons to the junction from the reservoir side gives much smaller contribution to Γ_2 than the similar one for the box side of the junction. In particular, for the layout of the qubit shown in Fig. 6.3, the contribution of the interference in the reservoir to Γ_2 is smaller than the one in the box by a factor $\frac{d_b}{d_r}\frac{\Delta_b}{E_T}\ln\left[\frac{\hbar D}{\Delta_r S_J}\right]\frac{L_1(a_0)}{L_2(a_0)} \ll 1$. [Here $a_0 = (\Delta_r + \delta E_+)/\Delta_b$, and $d_{b(r)}$ is the thickness of the superconducting film in the box(reservoir).] Therefore, we neglected the terms corresponding to the interference in the reservoir in Eq. (6.24).

6.4 Conclusion

In this Chapter we have studied the fundamental limitations on the energy relaxation time in a charge qubit with a large-gap Cooper-pair box, $\Delta_b > \Delta_r$. For sufficiently large Δ_b, real quasiparticle transitions can be exponentially suppressed, and the dominant contribution to T_1 comes from the higher-order (Andreev) processes, see Eq. (6.22). For realistic geometry of the charge qubits and the density of nonequilibrium quasiparticles in the reservoir $n_{\rm qp} \sim 10^{19} - 10^{18}{\rm m}^{-3}$ [59],

[15] In the presence of a strong magnetic field, $B \gg B_c$, the quantum interference pattern is altered leading to a suppression of the rate Γ_2. Here B_c is the correlation field $B_c \sim \Phi_0/S_b\sqrt{g}$ with Φ_0, S_b and g being the flux quantum, the area and dimensionless conductance of the island, respectively. (See for details Aleiner *et. al.* [86] and references therein.) At the same time, rate Γ_1 remains unchanged. However, for a weak magnetic field $B \ll B_c$, Eq. (6.24) still holds.

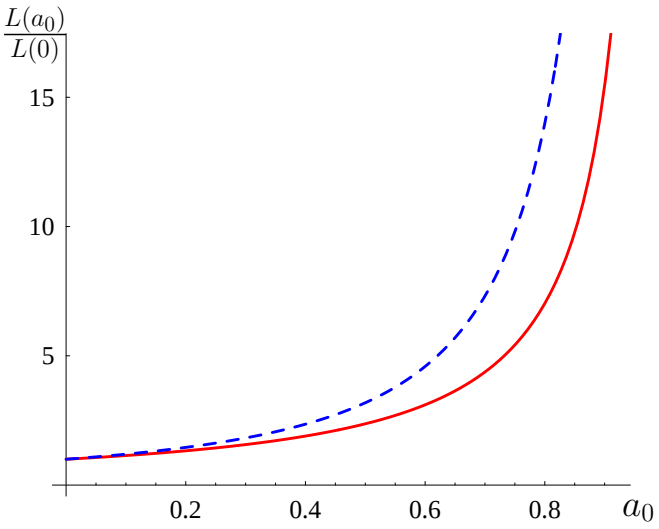

Figure 6.4: The dependence of the functions $L_1(a_0)$ and $L_2(a_0)$ (normalized by $L_1(0)$ and $L_2(0)$, respectively) on the dimensionless parameter $a_0 = (\Delta_r + \delta E_+)/\Delta_b$. The solid and dashed lines correspond to L_1 and L_2, respectively, and reflect the increase of the rates Γ_1 and Γ_2 with a_0. The expressions for $L_1(a_0)$ and $L_2(a_0)$ given by Eq. (6.19) are valid for $a_0 \ll 1 - T/\Delta_b$.

we estimate Andreev relaxation rate to be $\langle \Gamma_A \rangle \sim 10^{-1} - 10^{-2}$Hz. Thus, in the absence of other relaxation channels, the design of the qubit with a mismatch of gap energies leads to extremely long T_1-times. (For comparison, the quasiparticle-induced T_1 found in Ch. 3 for the charge qubit with equal gap energies was $T_1^{-1} \sim 10^5 - 10^3$Hz.)

The charge qubit with a large gap in the box also permits to reduce quasiparticle-induced decoherence. Since real quasiparticle transitions into the island are suppressed, see Eq. (6.2), the dephasing time of the qubit is limited by the energy relaxation processes, *i.e.* $T_2 \approx 2/\langle \Gamma_A \rangle$. Therefore, the design of a qubit with large gap mismatch is optimal from the point of view of quasiparticle-induced decoherence. It provides the desired stability of the charge states with respect to quasiparticle tunneling, and should restore $2e$-periodicity in these single-charge devices on time scales comparable to the measurement times.

Appendix A

The spectrum of the Cooper-pair box qubit: exact solution

In this Appendix we discuss the general solution for the energy spectrum of Cooper-pair box qubit. From the commutation relation of the operators $\hat{N}$ and $\hat{\varphi}$ given by Eq. (1.2), we can write the qubit Hamiltonian in the phase representation

$$H_{\rm qb} = E_c \left(\frac{2}{i} \frac{\partial}{\partial \varphi} - N_g \right)^2 - E_{_J} \cos(\varphi). \tag{A.1}$$

This Hamiltonian is similar to that of a quantum particle moving in a periodic potential with N_g being a "quasimomentum". The solution of the corresponding Shrödinger equation,

$$\left[E_c \left(\frac{2}{i} \frac{\partial}{\partial \varphi} - N_g \right)^2 - E_{_J} \cos(\varphi) \right] \Psi_{N_g,s}(\varphi) = E_s(N_g) \Psi_{N_g,s}(\varphi), \tag{A.2}$$

can be found exactly. It is easy to see that Eq. (A.2) at $N_g = 0$ can be mapped on the Mathieu equation

$$y''(x) + [a - 2q\cos(2x)]y(x) = 0 \tag{A.3}$$

with $a = E_s/E_c$, $q = -E_{_J}/2E_c$ and $\varphi = 2x$. The solution of Eq. (A.3) can be written in terms of the symmetric and antisymmetric Mathieu functions, $M_C(a, q, x)$

and $M_S(a,q,x)$, respectively [60]. The dependance of the wavefunctions $\Psi_{N_g,s}(\varphi)$ on the gate voltage N_g can be easily restored by a unitary transformation:

$$\Psi_{N_g,s}(\varphi) = \exp\left(iN_g\frac{\varphi}{2}\right)\left[C_1 M_C\left(\frac{E_s}{E_c}, -\frac{E_J}{2E_c}, \frac{\varphi}{2}\right) + C_2 M_S\left(\frac{E_s}{E_c}, -\frac{E_J}{2E_c}, \frac{\varphi}{2}\right)\right]. \tag{A.4}$$

Here C_1 and C_2 are the normalization constants. For any value of N_g the wave-

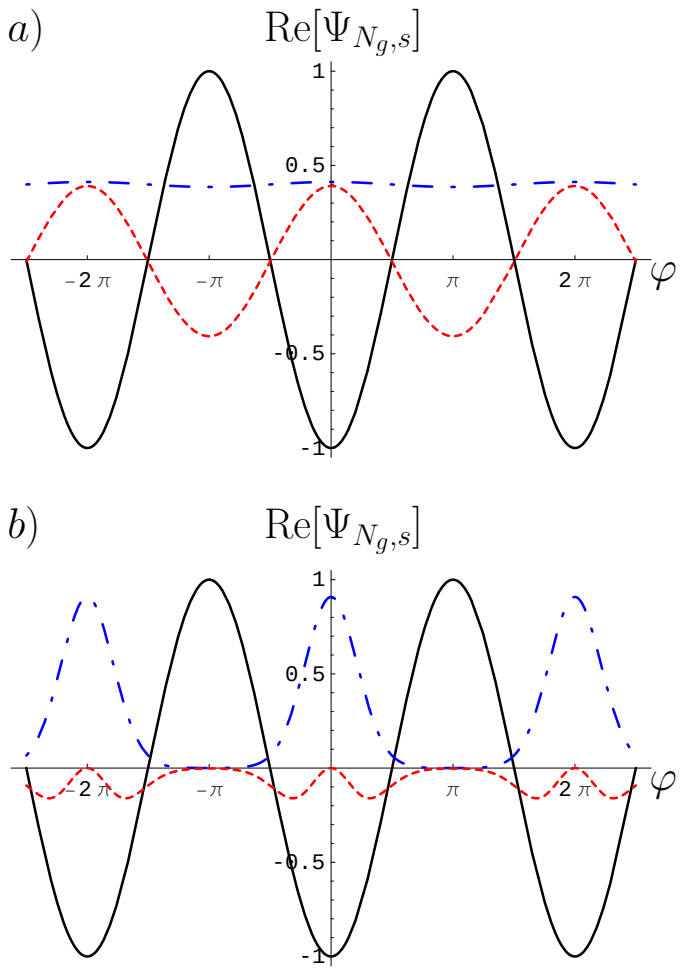

Figure A.1: The plot of the wavefunction $\Psi_{N_g,s}(\varphi)$ at $N_g = 0.5$ for different ratios of E_J and E_c: insets a) and b) correspond to $E_J/E_c = 0.1$ and $E_J/E_c = 10$, respectively. Here the dash-dot and dashed lines correspond to the ground and excited states of the qubit. The solid line reflects the periodic cosine potential of the Josephson junction, $i.e\ -\cos(\varphi)$, and is provided for reference.

function $\Psi_{N_g,s}(\varphi)$ should satisfy the following periodic boundary conditions:

$$\Psi_{N_g,s}(\varphi) = \Psi_{N_g,s}(\varphi + 2\pi). \tag{A.5}$$

These boundary conditions lead to a discrete spectrum of charge states. To see this we write $M_C(a,q,x)$ and $M_S(a,q,x)$ in the Floquet form

$$M_C(a,q,x) = \exp(irx)mc(x),$$
$$M_S(a,q,x) = \exp(irx)ms(x).$$

Here r is a real parameter and depends on a and q, $mc(x)$ and $ms(x)$ are π-periodic functions in x. One can notice that boundary conditions (A.5) are fulfilled if $\frac{1}{2}[N_g + r] \in Z$. This leads to the discrete spectrum of charge states, where the eigenvalues E_s associated with a given wavefunction can be expressed as a function of the parameters q and r_s via Mathieu characteristic functions $M_A(r,q)$ and $M_B(r,q)$[7]:

$$E_s(N_g) \;=\; E_c M_{A/B}\left(r_s, -\frac{E_J}{2E_c}\right) \tag{A.6}$$

Here $s = 0, 1, ...,$ and labels the energy band. Following the treatment in Ref. [81, 88], one finds that for $N_g \in]0,1[$ the function $r_s(N_g)$ is given by

$$r_s(N_g) = -N_g + (-1)^{s+1}\{(s+1) - (s+1) \bmod 2\}. \tag{A.7}$$

Here, $a \bmod b$ denotes the usual modulo operation. Thus, the wavefunction $\Psi_{N_g,s}(\varphi)$ is

$$\Psi_{N_g,s}(\varphi) = \frac{\exp\left(iN_g\frac{\varphi}{2}\right)}{\sqrt{2\pi}}\left[M_C\left(\frac{E_s}{E_c}, -\frac{E_J}{2E_c}, \frac{\varphi}{2}\right) + i(-1)^{s+1}M_S\left(\frac{E_s}{E_c}, -\frac{E_J}{2E_c}, \frac{\varphi}{2}\right)\right]. \tag{A.8}$$

The plot of the wavefunction $\Psi_{N_g,s}(\varphi)$ is shown in Fig. A.1.

[7] If r is not an integer $M_A(r,q) = M_B(r,q)$.

Appendix B

Quasiparticle tunneling rates

In this Appendix we calculate quasiparticle tunneling rates for general ratio E_J/E_c. For simplicity we assume here equal gap energies in the CPB and reservoir, $\Delta_r = \Delta_b = \Delta$. The quasiparticle transition rates are given by Fermi's golden rule

$$\Gamma = \frac{2\pi}{\hbar} \sum_{i,f} |\langle f| V |i\rangle|^2 \delta(E_i - E_f) \rho_{\rm odd}(E_p). \tag{B.1}$$

Here $\rho_{\rm odd}(E_p)$ is the distribution function for an odd number of electrons in the superconductor. The Hamiltonian $V = H_T - H_J$ takes into account quasiparticle tunneling only. Initially the Cooper-pair box can be either in the excited $|+\rangle$ or ground $|-\rangle$ state, and quasiparticles are in the reservoir

$$\Gamma_\pm = \frac{2\pi}{\hbar} \sum_{p,k} |\langle N+1, E_k| H_T |\pm, E_p\rangle|^2 \delta(E_k - E_p - \omega_\pm) \rho_{\rm odd}(E_p). \tag{B.2}$$

The matrix elements of the tunneling Hamiltonian H_T are easy to find in the charge basis, while the solution of $H_{\rm qb}$ is obtained in the phase representation, see Appendix A. Therefore, we calculate matrix elements in the following way:

$$\begin{aligned} &\langle N+1, E_k| H_T |\pm, E_p\rangle \\ &\quad = \int_0^{2\pi} d\varphi \int_0^{2\pi} d\varphi' \sum_{N,N'} \langle N+1\|\varphi\rangle\langle\varphi|N\rangle\langle N, E_k| H_T |E_p, N'\rangle\langle N'\|\varphi'\rangle\langle\varphi'|\pm\rangle . \end{aligned} \tag{B.3}$$

Here N is the the charge of the CPB in units of e. The matrix elements $\langle N+1; E_k| H_{_T} |N'; E_p\rangle$ can be calculated using particle conserving Bogoliubov transformation

$$\langle N+1; E_k| H_{_T} |N'; E_p\rangle = t_{kp}u_k u_p \delta_{N,N'} - t_{pk}v_k v_p \delta_{N,N'-2}. \tag{B.4}$$

Upon substituting this result into Eq. (B.3) one finds

$$\langle N+1, E_k|H_{_T}|\pm, E_p\rangle = A_{\pm}^{(1)} t_{kp}u_k u_p - A_{\pm}^{(2)} t_{pk}v_k v_p \tag{B.5}$$

with $A_{\pm}^{(1)}$ and $A_{\pm}^{(2)}$ being the following overlap integrals:

$$\begin{aligned} A_{\pm}^{(1)} &= \int_0^{2\pi} d\varphi \Psi^*_{N_g=0,0}(\varphi)\Psi_{N_g=1,\pm}(\varphi), \\ A_{\pm}^{(2)} &= \int_0^{2\pi} d\varphi \Psi^*_{N_g=0,0}(\varphi)\Psi_{N_g=1,\pm}(\varphi)e^{-i\varphi}. \end{aligned} \tag{B.6}$$

The overlap integrals $A_{\pm}^{(1)}$ and $A_{\pm}^{(2)}$ take into account the shake-up of the collective mode due to tunneling of a quasiparticle into the Cooper-pair box. Following similar derivation steps as for Eq. (2.29) we obtain

$$\Gamma_{\pm}(N_g) = \frac{g_{_T} n^r_{\rm qp}}{4\pi\nu_F} \frac{\left[|A_{\pm}^{(1)}|^2 + |A_{\pm}^{(2)}|^2\right](\Delta+\omega_{\pm}) - 2{\rm Re}\left[A_{\pm}^{(2)}A_{\pm}^{(1)*}\right]\Delta}{\sqrt{(\Delta+\omega_{\pm})^2-\Delta^2}}. \tag{B.7}$$

Here $n^r_{\rm qp}$ is the density of quasiparticles in the reservoir, and in the equilibrium $n^r_{\rm qp} = \sqrt{2\pi\Delta T}\nu_F \exp(-\Delta/T)$. Equation (B.7) is a general expression for the quasiparticle tunneling rate valid for $\omega_{\pm} \gg T$. In the limit corresponding to the charge qubit, $E_{_J} \ll E_c$, we recover results of Eq. (2.29).

Recently, the proposal for the Cooper-pair box qubit with large Josephson energy, $E_{_J} \gg E_c$, attracted great interest due to the insensitivity of such qubit to the charge fluctuations [88]. In this limit, the transition from the even-charge state $|E_p, s=1\rangle$ to the odd-charge state $|E_k, s=0\rangle$ is given by

$$\Gamma_{0\leftarrow 1} = \frac{g_{_T} n^r_{\rm qp}}{2\pi\nu_F}\left(\frac{2E_c}{E_{_J}}\right)^{1/2}\sqrt{\frac{2\Delta+\delta E_{10}}{\delta E_{10}}}. \tag{B.8}$$

Here s refers to the band index of the Cooper-pair-box energy spectrum, and $\delta E_{10} = E_{s=1}(N_g = 1) - E_{s=0}(N_g = 0)$ is approximately given by the Josephson plasma frequency, $\delta E_{10} \approx \sqrt{8E_c E_J}$.

Appendix C

Analytical structure of $\sigma_{++}(s)$

In this Appendix we study analytic properties of $\sigma_{++}(s)$ in order to calculate the inverse Laplace transform (3.55). In general, nonanalytic behavior of $\sigma_{++}(s)$ is determined by two poles, one of which is at $s_1 = 0$, and a cut, see Fig. 3.3. The locations of the other pole and of the cut as well as the contributions of all the mentioned singularities in $\sigma_{++}(s)$ to the integral (3.55), depend on the ratio of $\Gamma_{\rm in}\tau$.

In the fast relaxation regime ($\Gamma_{\rm in}\tau \ll 1$), in the vicinity of the s_1 pole, we find

$$\sigma_{++}(s) = \frac{e^{-E_J/T}}{1+e^{-E_J/T}}\frac{1}{s}. \tag{C.1}$$

The second pole s_2 is the solution of Eq. (3.56) at small $s \sim \Gamma_{\rm in}$:

$$s_2 \;=\; -\left(\langle\gamma_+\rangle + \langle\gamma_-\rangle\right). \tag{C.2}$$

In the vicinity of this pole, $\sigma_{++}(s)$ is given by

$$\sigma_{++}(s) = \left(\frac{1}{1+e^{-E_J/T}} - Z(0)\right)\frac{1}{s-s_2}, \tag{C.3}$$

where $Z(0)$ is defined in Eq. (3.58).

In addition to the poles discussed above, nonanalyticity of $\sigma_{++}(s)$ comes from the singularities of $Z(s)$. The function $Z(s)$ is nonanalytic along the cut

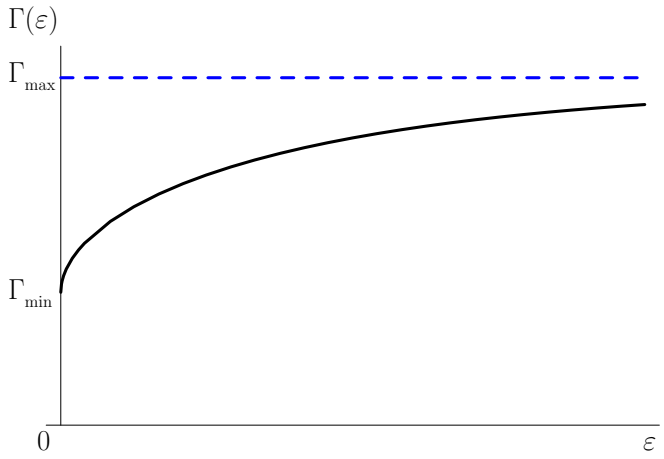

Figure C.1: Dependence of $\Gamma(\varepsilon)$, defined in Eq. (3.34), on quasiparticle energy $\varepsilon = E_p - \Delta$.

$s \in [s_{\min}, s_{\max}]$, where

$$s_{\min} = -\frac{1}{\tau} - \max\left[\Gamma(E_p)\right] \text{ and } s_{\max} = -\frac{1}{\tau} - \min\left[\Gamma(E_p)\right].$$

Here $\Gamma(E_p)$ is defined in Eq. (3.34). The proper contribution to Eq. (3.55) can be calculated by integrating along the contour enclosing the cut

$$I_{\text{cut}} = \frac{-1}{2\pi i}\int_{s_{\min}}^{s_{\max}} ds e^{st}\left(\sigma_{++}(s+i\epsilon) - \sigma_{++}(s-i\epsilon)\right). \tag{C.4}$$

The discontinuity of the imaginary part of $\sigma_{++}(s)$ at the cut is

$$\sigma_{++}(s+i\epsilon) - \sigma_{++}(s-i\epsilon) = \frac{-2i\tau(\tau s+1)\text{Im}Z(s+i\epsilon)}{[\tau s+\text{Re}Z(s)(1+e^{-E_J/T})]^2+[\text{Im}Z(s+i\epsilon)(1+e^{-E_J/T})]^2}. \tag{C.5}$$

In the limit $\Gamma_{\text{in}}\tau \ll 1$ we find

$$\sigma_{++}(s+i\epsilon) - \sigma_{++}(s-i\epsilon) \approx \frac{-2i\tau(\tau\Gamma_{\text{in}})\text{Im}Z(s+i\epsilon)}{[-1+\text{Re}Z(s)]^2+[\text{Im}Z(s+i\epsilon)]^2}, \tag{C.6}$$

which yields a negligible contribution to Eq. (3.55), $I_{\text{cut}} \propto \Gamma_{\text{in}}\tau \ll 1$. Finally, after summing up two relevant contributions, one obtains the result for $\sigma_{++}(t)$ given in Eq. (3.46).

In the opposite limit of slow relaxation ($\Gamma_{\rm in}\tau \gg 1$), the first pole $s_1 = 0$ is the same as in the previous case, see Eq. (C.1). The other pole s_2 is found from Eq. (3.56) assuming $\Gamma_{\rm in}\tau \gg 1$:

$$s_2 \;=\; -\frac{Z(0)}{\tau}\left(1+e^{-E_J/T}\right), \tag{C.7}$$

where $Z(0)$ is defined in Eq. (3.58). In the vicinity of the second pole, $\sigma_{++}(s)$ is given by

$$\sigma_{++}(s) = \left(\frac{1}{1+e^{-E_J/T}} - Z(0)\right)\frac{1}{s-s_2}. \tag{C.8}$$

The contribution from the cut in the limit $\Gamma_{\rm in}\tau \gg 1$ can be evaluated from Eq. (C.5). The discontinuity of the function $\sigma_{++}(s)$ is

$$\sigma_{++}(s+i\epsilon) - \sigma_{++}(s-i\epsilon) \approx -\frac{2i}{s}{\rm Im}Z(s+i\epsilon). \tag{C.9}$$

Hence, the contribution to Eq. (3.55) from the cut is

$$\begin{aligned} I_{\rm cut} \;&=\; -2\int_\Delta^\infty \frac{dE_p}{\delta_r}\nu(E_p)\gamma_+(E_p)\rho_{\rm odd}(E_p)\int_{s_{\min}}^{s_{\max}} ds\frac{e^{st}}{s}\delta(s+\Gamma(E_p)) \\ &=\; 2\int_\Delta^\infty \frac{dE_p}{\delta_r}\nu(E_p)\frac{\gamma_+(E_p)\rho_{\rm odd}(E_p)}{\Gamma(E_p)}\exp\left(-\Gamma(E_p)t\right). \end{aligned} \tag{C.10}$$

Finally, combining proper terms one finds the inverse Laplace transform of Eq. (3.59).

Appendix D

Power spectrum of charge noise

In this Appendix we derive a general expression for the noise power spectrum $S_Q(\omega)$. Combining Eqs. (4.73), (4.76) and (4.77) one finds

$$S_Q(\omega)=\frac{4e^2\left(\sum_k \frac{(\omega^2+\frac{1}{\tau^2})\Gamma_{\rm out}(E_k)f(E_k-\delta E)\bar{\sigma}_{\rm e}+\Gamma_{\rm out}(E_k)^2\rho^b_{\rm odd}(E_k)\frac{\bar{\sigma}_{\rm o}}{\tau}}{(\omega^2+(\Gamma_{\rm out}(E_k)+1/\tau)^2)}+\frac{\bar{\sigma}_{\rm o}}{\tau}\left|\sum_k \frac{\Gamma_{\rm out}(E_k)\rho^b_{\rm odd}(E_k)}{-i\omega+\Gamma_{\rm out}(E_k)+\frac{1}{\tau}}\right|^2\right)}{\mathcal{L}(\omega)\mathcal{L}(-\omega)}. \tag{D.1}$$

Here the product $\mathcal{L}(\omega)\mathcal{L}(-\omega)$ is given by

$$\begin{aligned}\mathcal{L}(\omega)\mathcal{L}(-\omega)=&\omega^2\left(1-\frac{1}{\tau}\sum_k\frac{\rho^b_{\rm odd}(E_k)\Gamma_{\rm out}(E_k)}{\omega^2+\left(\Gamma_{\rm out}(E_k)+1/\tau\right)^2}+\sum_k\frac{f(E_k-\delta E)\Gamma_{\rm out}(E_k)^2}{\omega^2+\left(\Gamma_{\rm out}(E_k)+1/\tau\right)^2}\right)^2\\ &+\left(\frac{1}{\tau}\sum_k\frac{\rho^b_{\rm odd}(E_k)\Gamma_{\rm out}(E_k)(\Gamma_{\rm out}(E_k)+1/\tau)}{\omega^2+\left(\Gamma_{\rm out}(E_k)+1/\tau\right)^2}+\sum_k\frac{f(E_k-\delta E)\Gamma_{\rm out}(E_k)(\omega^2+1/\tau^2+\Gamma_{\rm out}(E_k)/\tau)}{\omega^2+\left(\Gamma_{\rm out}(E_k)+1/\tau\right)^2}\right)^2.\end{aligned} \tag{D.2}$$

Equation (D.1) can be simplified in the thermodynamic limit ($T \gg \delta_b$) by introducing functions $Z_1(\omega)$ and $Z_2(\omega)$:

$$Z_1(\omega) = \frac{\Gamma_{\rm out}}{D}\sum_k\frac{\rho^b_{\rm odd}(E_k)\Gamma_{\rm out}(E_k)}{\omega^2+\left(\Gamma_{\rm out}(E_k)+1/\tau\right)^2}, \tag{D.3}$$

and

$$Z_2(\omega) = \frac{1}{D}\sum_k\frac{\rho^b_{\rm odd}(E_k)\Gamma_{\rm out}(E_k)^2}{\omega^2+\left(\Gamma_{\rm out}(E_k)+1/\tau\right)^2}. \tag{D.4}$$

Here C and D are given by Eq. (4.81). Substituting Eqs. (D.2) - (D.4) into Eq. (D.1), one obtains the general expression for $S_Q(\omega)$:

$$S_Q(\omega)=\frac{4e^2}{\Gamma_{\rm out}}\frac{\left[\left(\frac{\omega}{\Gamma_{\rm out}}\right)^2+\left(\frac{1}{\tau\Gamma_{\rm out}}\right)^2\right]CZ_1(\omega)\bar{\sigma}_{\rm e}+Z_2(\omega)\frac{\bar{\sigma}_{\rm o}D}{\tau\Gamma_{\rm out}}-\frac{\bar{\sigma}_{\rm o}D^2}{\tau\Gamma_{\rm out}}\left[\left(\frac{Z_1(\omega)}{\tau\Gamma_{\rm out}}+Z_2(\omega)\right)^2+Z_2^2(\omega)\left(\frac{\omega}{\Gamma_{\rm out}}\right)^2\right]}{\left(\frac{\omega}{\Gamma_{\rm out}}\right)^2\left[1-\frac{D}{\tau\Gamma_{\rm out}}Z_1(\omega)+CZ_2(\omega)\right]^2+\left[\frac{D+C}{\tau\Gamma_{\rm out}}Z_2(\omega)+\left(C\left(\frac{\omega}{\Gamma_{\rm out}}\right)^2+\frac{C+D}{(\tau\Gamma_{\rm out})^2}\right)Z_1(\omega)\right]^2}. \tag{D.5}$$

The functions $Z_1(\omega)$ and $Z_2(\omega)$ can be written in the form of the dimensionless integrals:

$$Z_1(\omega)=\frac{\Gamma_{\rm out}}{\nu(\delta E)}\int_0^\infty dz\frac{e^{-z}\nu(z)\Gamma_{\rm out}(z)}{\omega^2+\left(\Gamma_{\rm out}(z)+1/\tau\right)^2}, \tag{D.6}$$

and

$$Z_2(\omega)=\frac{1}{\nu(\delta E)}\int_0^\infty dz\frac{e^{-z}\nu(z)\Gamma_{\rm out}^2(z)}{\omega^2+\left(\Gamma_{\rm out}(z)+1/\tau\right)^2}. \tag{D.7}$$

The dimensionless variable z here is defined in Eq. (4.48). Assuming that at low temperature the main contribution to the integrals (D.6) and (D.7) comes from the small z region, $z\ll\delta E/2T$, one can simplify $Z_1(\omega)$ and $Z_2(\omega)$ using Eq. (4.53) to obtain

$$Z_1(\omega)\approx\int_0^\infty dz\frac{e^{-z}\sqrt{z}}{(\omega/\Gamma_{\rm out})^2z+\left(1+\sqrt{z}/\tau\Gamma_{\rm out}\right)^2},$$

and

$$Z_2(\omega)\approx\int_0^\infty dz\frac{e^{-z}}{(\omega/\Gamma_{\rm out})^2z+\left(1+\sqrt{z}/\tau\Gamma_{\rm out}\right)^2}.$$

In the slow relaxation case $\tau\Gamma_{\rm out}\gg1$, the functions $Z_1(\omega)$ and $Z_2(\omega)$ are approximately given by Eq. (4.84).

Finally, by taking the appropriate limits in Eq. (D.5) one can recover Eq. (4.19) for "deep" and Eqs. (4.80) and (4.83) for "shallow" traps, respectively.

Bibliography

[1] M. A. Nielsen and I. L. Chuang, *Quantum Computation and Quantum Information* (Cambridge University Press, Cambridge, 2000).

[2] A. Caldera and A. Leggett, Ann. Phys. (N.Y.) **149**, 374 (1983).

[3] J. Martinis, M. Devoret, and J. Clarke, Phys. Rev. Lett. **55**, 1543 (1985).

[4] J. Clarke, A. Cleland, M. Devoret, D. Esteve, and J. Martinis, Science **239**, 992 (1988).

[5] R. Voss and R. Webb, Phys. Rev. Lett. **47**, 265 (1981).

[6] Y. Nakamura, Y. A. Pashkin, and J. S. Tsai, Nature **398**, 786 (1999).

[7] J. Mooij, T. Orlando, L. Levitov, L. Tian, C. van der Wal, and S. Lloyd, Science **285**, 1036 (1999).

[8] C. van der Wal, A. ter Haar, F. Wilhelm, R. Schouten, C. Harmans, T. Orlando, S. Lloyd, and J. Mooij, Science **293**, 773 (2000).

[9] J. Friedman, V. Patel, W. Chen, S. Tolpygo, and J. Lukens, Nature **406**, 43 (2000).

[10] D. Vion, A. Aassime, A. Cottet, P. Joyez, H. Pothier, C. Urbina, D. Esteve, and M. Devoret, Science **296**, 286 (2002).

[11] Y. Yu, S. Han, X. Chu, S. Chu, and Z. Wang, Science **296**, 889 (2002).

[12] A. Wallraff, D. I. Schuster, A. Blais, L. Frunzio, R.-S. Huang, J. Majer, S. Kumar, S. M. Girvin, and R. J. Schoelkopf, Nature **431**, 162 (2004).

[13] D. DiVincenzo, Fortschr. Phys. **48**, 771 (2000).

[14] T. Yamamoto, Y. Pashkin, O. Astafiev, Y. Nakamura, and J. Tsai, Nature **425**, 941 (2003).

[15] A. J. Berkley, H. Xu, R. C. Ramos, M. A. Gubrud, F. W. Strauch, P. R. Johnson, J. R. Anderson, A. J. Dragt, C. J. Lobb, and F. C. Wellstood, Science **300**, 1548 (2003).

[16] M. Steffen, M. Ansmann, R. C. Bialczak, N. Katz, E. Lucero, R. McDermott, M. Neeley, E. M. Weig, A. N. Cleland, and J. M. Martinis, Science **313**, 1423 (2006).

[17] A. Lupascu, S. Saito, T. Picot, P. C. de Groot, C. J. P. M. Harmans, and J. E. Mooij, Nature Physics **3**, 119 (2007).

[18] M. H. Devoret, A. Wallraff, and J. M. Martinis, cond-mat/0411174 .

[19] J. You and F. Nori, Physics Today **58**, 42 (2005).

[20] Y. Makhlin, G. Schön, and A. Shnirman, Rev. Mod. Phys. **73**, 357 (2001).

[21] G. Wendin and V. S. Shumeiko, *Handbook of Theoretical and Computational Nanotechnology, edited by M. Rieth and W. Schommers* (American Scientific Publishers, Stevenson Ranch, CA, 2006).

[22] M. T. Tuominen, J. M. Hergenrother, T. S. Tighe, and M. Tinkham, Phys. Rev. Lett. **69**, 1997 (1992).

[23] D. V. Averin and Y. V. Nazarov, Phys. Rev. Lett. **69**, 1993 (1992).

[24] K. A. Matveev, M. Gisselfält, L. I. Glazman, M. Jonson, and R. I. Shekhter, Phys. Rev. Lett. **70**, 2940 (1993).

[25] P. Lafarge, P. Joyez, D. Esteve, C. Urbina, and M. Devoret, Phys. Rev. Lett. **70**, 994 (1993).

[26] G. Schön, J. Siewert, and A. D. Zaikin, Physica B **203**, 340 (1993).

[27] A. Amar, D. Song, C. Lobb, and F. Wellstood, Phys. Rev. Lett. **72**, 3234 (1994).

[28] P. Joyez, P. Lafarge, A. Filipe, D. Esteve, and M. H. Devoret, Phys. Rev. Lett. **72**, 2458 (1994).

[29] K. Matveev, L. Glazman, and R. Shekhter, Mod. Phys. Lett. B **8**, 1007 (1994).

[30] T. M. Eiles and J. M. Martinis, Phys. Rev. B **50**, 627 (1994).

[31] J. Aumentado, M. W. Keller, J. M. Martinis, and M. H. Devoret, Phys. Rev. Lett. **92**, 66802 (2004).

[32] B. A. Turek, K. W. Lehnert, A. Clerk, D. Gunnarsson, K. Bladh, P. Delsing, and R. J. Schoelkopf, Phys. Rev. B **71**, 193304 (2005).

[33] A. Guillaume, J. F. Schneiderman, P. Delsing, H. M. Bozler, and P. M. Echternach, Phys. Rev. B **69**, 132504 (2004).

[34] K. W. Lehnert, B. A. Turek, K. Bladh, L. F. Spietz, D. Gunnarsson, P. Delsing, and R. J. Schoelkopf, Phys. Rev. Lett. **91**, 106801 (2003).

[35] J. Männik and J. E. Lukens, Phys. Rev. Lett. **92**, 057004 (2004).

[36] J. Schneiderman, P. Delsing, G. Johansson, M. Shaw, H. Bozler, and P. Echternach, unpublished .

[37] O. Naaman and J. Aumentado, Phys. Rev. B **73**, 172504 (2006).

[38] A. J. Ferguson, N. A. Court, F. E. Hudson, and R. G. Clark, Phys. Rev. Lett. **97**, 106603 (2006).

[39] T. Yamamoto, Y. Nakamura, Y. Pashkin, O. Astafiev, and J. Tsai, Appl. Phys. Lett. **88**, 212509 (2006).

[40] J. Könemann, H. Zangerle, B. Mackrodt, R. Dolata, and A. Zorin, arXiv:cond-mat/0701144 .

[41] J. Schrieffer, *Theory of Superconductivity* (Advanced Book Program, Perseus, Oxford, 1999).

[42] M. Tinkham, *Introduction to Superconductivity* (McGraw-Hill, New York, 1999).

[43] V. Bouchiat, D. Vion, P. Joyez, D. Esteve, and M. H. Devoret, Physica Scripta 165 (1998).

[44] R. M. Lutchyn, L. I. Glazman, and A. I. Larkin, Phys. Rev. B **72**, 014517 (2005).

[45] Y. Blanter, V. Vinokur, and L. Glazman, Phys. Rev. B **73**, 165322 (2006).

[46] S. B. Kaplan, C. C. Chi, D. N. Langenberg, J. J. Chang, S. Jafarey, and D. J. Scalapino, Phys. Rev. B **14**, 4854 (1976).

[47] C. Chi and J. Clarke, Phys. Rev. B **19**, 4495 (1979).

[48] D. Zubarev, V. Morozov, and G. Röpke, *Statistical Mechanics of Nonequilibrium Processes* (Akademie Verlag, Berlin, 1996).

[49] M. Esposito and P. Gaspard, Phys. Rev. E **68**, 66112 (2003).

[50] L. B. Ioffe, V. B. Geshkenbein, C. Helm, and G. Blatter, Phys. Rev. Lett. **93**, 57001 (2004).

[51] C. M. Wilson and D. E. Prober, Phys. Rev. B **69**, 094524 (2004).

[52] W. Lu, Z. Ji, L. Pfeiffer, K. W. West, and A. J. Rimberg, Nature **423**, 422 (2003).

[53] O. Naaman and J. Aumentado, APS March Meeting 2005 (X16.00002) **74**, 064515 (2006).

[54] O. Naaman and J. Aumentado, private communication .

[55] S. Machlup, J. Appl. Phys. **25**, 341 (1954).

[56] P. Santhanam and D. E. Prober, Phys. Rev. B **29**, 3733 (1984).

[57] M. Uren, M. Kirton, and S. Collins, Phys. Rev. B **37**, 8346 (1988).

[58] M. Lax and P. Mengert, J. Phys. Chem. Solids **14**, 248 (1960).

[59] R. M. Lutchyn, L. I. Glazman, and A. I. Larkin, Phys. Rev. B **74**, 064515 (2006).

[60] M. Abramovitz and A. Stegun, *Handbook of Mathematical Functions* (Dover, New York, 1965).

[61] S. Kogan, *Electronic Noise and Fluctuations in Solids* (Cambridge University Press, Cambridge, 1996).

[62] S. M. Kogan and A. Y. Shul'man, Sov. Phys. JETP **29**, 467 (1969).

[63] M. Lax, Rev. Mod. Phys. **32**, 25 (1960).

[64] M. Bixon and R. Zwanzig, Phys. Rev. **187**, 267 (1969).

[65] P. Joyez, V. Bouchiat, D. Esteve, C. Urbina, and M. H. Devoret, Phys. Rev. Lett. **79**, 1349 (1997).

[66] M. Thalakulam, Z. Ji, and A. J. Rimberg, Phys. Rev. Lett. **93**, 066804 (2004).

[67] T. Duty, G. Johansson, K. Bladh, D. Gunnarsson, C. Wilson, and P. Delsing, Phys. Rev. Lett. **95**, 206807 (2005).

[68] M. A. Sillanpää, T. Lehtinen, A. Paila, Y. Makhlin, L. Roschier, and P. J. Hakonen, Phys. Rev. Lett. **95**, 206806 (2005).

[69] K. A. Matveev and L. I. Glazman, Phys. Rev. Lett. **81**, 3739 (1998).

[70] M. Houzet, D. A. Pesin, A. V. Andreev, and L. I. Glazman, Phys. Rev. B **72**, 104507 (2005).

[71] P. M. Ostrovsky, M. A. Skvortsov, and M. V. Feigel'man, Phys. Rev. Lett. **92**, 176805 (2004).

[72] R. Lutchyn and L. Glazman, Phys. Rev. B **75**, 184520 (2007).

[73] V. Ambegaokar, U. Eckern, and G. Schön, Phys. Rev. Lett. **48**, 1745 (1982).

[74] A. I. Larkin and Y. N. Ovchinnikov, Phys. Rev. B **28**, 6281 (1983).

[75] U. Eckern, V. Ambegaokar, and G. Schön, Phys. Rev. B **30**, 6419 (1984).

[76] G. Schön and A. D. Zaikin, Phys. Rep. **237**, 585 (1990).

[77] F. Guinea and G. Schön, Europhys. Lett. **1**, 585 (1986).

[78] A. Kamenev, J. Zhang, A. I. Larkin, and B. I. Shklovskii, Physica A **359**, 129 (2006).

[79] K. K. Likharev and A. B. Zorin, J. Low Temp. Phys. **59**, 347 (1985).

[80] E. M. Lifshitz and L. P. Pitaevskii, *Statistical Physics 2* (Nauka, Moscow, 1978), Chap. 6.

[81] A. Cottet, *PhD thesis* (University of Paris 6, Paris, 2002), Chap. 1.

[82] D. Gunnarsson, T. Duty, K. Bladh, and P. Delsing, Phys. Rev. B **70**, 224523 (2004).

[83] E. Prada and F. Sols, Eur. Phys. J. B **40**, 379 (2004).

[84] F. W. J. Hekking and Y. V. Nazarov, Phys. Rev. B **49**, 6847 (1994).

[85] H. Pothier, S. Gueron, D. Esteve, and M. Devoret, Physica B **35**, 226 (1994).

[86] I. L. Aleiner, P. W. Brouwer, and L. I. Glazman, Physics Reports **358**, 309 (2002).

[87] D. V. Averin and Y. V. Nazarov, Phys. Rev. Lett. **65**, 2446 (1990).

[88] J. Koch, T. M. Yu, J. Gambetta, A. A. Houck, D. I. Schuster, J. Majer, A. Blais, M. H. Devoret, S. M. Girvin, and R. J. Schoelkopf, arXiv:cond-mat/0703002 .